



NOISE ANALYZER--BAND-PASS FILTER OF
VARIABLE WIDTH AND MEAN FREQUENCY

By
Charles M. Edwards
and
Charles T. Goddard

Submitted in Partial Fulfillment of the
Requirements for the Degrees of

BACHELOR OF SCIENCE
and
MASTER OF SCIENCE

From The
Massachusetts Institute of Technology
1941

Signatures of Authors
.....
Department of Electrical Engineering, May 22, 1941
Signature of Professor
in Charge of Research
Signature of Chairman of Department
Committee on Graduate Students

✓

Acknowledgments

The partners of this thesis owe a debt of gratitude to Professor E. A. Guillemin for his suggestions and assistance with filter theory, to Professor C. E. Tucker for his advice and aid in securing material and to Professor R. D. Fay for his encouragement of the project. We also wish to give special thanks to Mr. L. D. Hansen of Fanwood, New Jersey, for his help in securing material.

CHAPTER I
INTRODUCTION

In the design of acoustical equipment, noise filters for machinery and the analyzation of machinery noise to find the sources of disturbance, it is desirable to have a knowledge of the distribution and magnitude of the frequency components which must be considered in the audible spectrum. For such purposes a number of noise analyzers have been developed and a few are sold on the market. Some of these are purely electrical in nature, some combine electrical and mechanical principles, others are entirely mechanical in operation. A brief discussion of some of the developments will give a good history of noise analyzers.

One of the first analyzers was developed as late as 1931, by Sivian, Dunn and White¹ of the Bell Telephone Laboratories. The instrument used a series of fixed band-pass filters, which provided a discontinuous range of about 30 to 10,000 cycles.

In the same year, L. P. Delsasso² at the California Institute of Technology developed a highly selective mechanical resonator which was tunable from 0 to 500 cycles. It was to be used in the analysis of airplane noise. Because it was continuously variable, this mechanical unit had a decided

-
1. "Absolute Amplitudes and Spectra of Certain Musical Instruments and Orchestras", Sivian, Dunn and White, Journal Acoustical Society of America, Vol. 2; Jan., 1931; p.330
 2. "A New Acoustic Analyzer--Determination of the Sound Spectra Produced by Aircraft in Flight", Delsasso; Journal Acoustical Society of America, Vol. 3; July, 1931; p.167

advantage over the Laboratories' electrical device within the range of 0 to 500 cycles.

A noise analyzer developed by Mead and Berry of the General Electric Company in 1934³, used an electrical oscillator, an electro-mechanical modulator, a mechanical filter and mechano-electric coupling between filter and output indicator. From these components it is evident that the apparatus operated on the well known hetrodyne principle. During the next year, H. H. Hall⁴ of Harvard announced a recording analyzer which incorporated a series of electrical and electro-mechanical units; it was also based on the hetrodyne principle of separating frequencies. In both of these developments mechanical components were used to secure high selectivity while passing a narrow band of frequencies.

The General Radio Company has done a lot of work on the development of a suitable noise analyzer. Their 736A Wave Analyzer is a very popular instrument which uses the hetrodyne principle but is entirely electrical in operation. It has a continuous range of 0 to 15,000 cycles and is selective to within 4 cycles. In 1938, H. H. Scott of this company announced the development of a selective amplifier circuit⁵. It employed a special negative feedback network which prevented all

3. "A Portable Frequency Analyzer; Developments in Noise Measurements", Mead and Berry; General Electric Review, Vol. 37, No. 8; August, 1934; p. 378

4. "A Recording Analyzer for the Audible Frequency Range", H. H. Hall; Journal Acoustical Society of America, Vol. 8; October, 1936; pl33

5. "A New Type of Selective Circuit and Some Applications", H. H. Scott; Proc. of I.R.E., Vol. 26, Feb., 1938; p. 226

frequencies except those in a specific band from passing through the amplifier. By providing an adjustment for the feedback network, an analyzer was designed having a continuous range over the audible spectrum. As the discussion which follows will show, it is important that the feedback circuit was so designed that the width of the band passed by the amplifier was approximately proportional to frequency.

In an attempt to design an analyzer with variable selectivity, W. R. Burrall conducted a thesis project here at the Institute-- "Investigation of the Use of a Positive Feedback Network, such as a Regenerative Circuit, as a Band-Pass Filter, the Width of Band Passed to be Adjustable at Will"⁶. The results which he obtained were very unsatisfactory.

All of these developments fall short of giving the instrument which is ideal for noise analyzation. E. J. Abott has presented a fairly complete picture of what the ideal analyzer should be capable of accomplishing. In his article "The Role of Acoustical Measurements in Machinery Quieting"⁷, he points out that frequency analysis seems to be the only reliable method of determining the causes of noise; that such analysis involves three essential characteristics of the components of noise: (1) magnitude; (2) frequency; (3) variation with time. Most of the noise analyzers developed are capable of measuring the magnitude and frequency of a component when it is not varying

6. "Investigation of the Use of a Positive Feedback Network, such as a Regenerative Circuit, as a Band-Pass Filter, the Width of Band Passed to be Adjustable at Will", William F. Burrall; M.I.T. E.E. Thesis, 1938.

7. "The Role of Acoustical Measurements in Machinery Quieting", Ernest J. Abbott; Journal Acoustical Society of America, Vol. 8, No. 2, October, 1936; pp 133-142.

with time, because this requires a relatively simple selective circuit or mechanical resonator. It is the variation of noise components with time that causes the most difficulty in the design of a satisfactory analyzer, for it requires that the instrument be capable of passing not one frequency, but a given band of frequencies. Some of the analyzers do pass such a band of frequencies but for the most part this band is fixed for all of the spectrum. Depending on the magnitude of the variation with time, the ideal analyzer should provide a means of selecting not only the band of frequencies to be passed but also the width of that band. Abbott suggests that a band width of half an octave throughout the audio spectrum would be desirable. He further states that with regard to magnitude, readings should be repeatable to 0.1 db.

So far as the partners of this thesis know only one investigation has resulted in an instrument which approximates the ideal one. Mr. L. P. Reitz, Jr., submitted an M.I.T. M.S. Thesis⁸ in 1940, which provides a "Variable Band-Pass Audio Power Level Meter". Using a system of electric modulators, variable carriers and filters, Mr. Reitz obtained results which showed the practicability of such a system, but his results were limited by the cut-off rates of his filters.

Although fundamentally the system announced with this thesis is similar to Reitz's, the idea was arrived at independently by Mr. Goddard. It will be seen from the following

8. "A Variable Band-Pass Audio Power Level Meter",
L. P. Reitz, Jr.; M.I.T. E.E. Thesis, 1940 (M.S.).

chapter that the beauty of the system used here is that the two filters which determine the selectivity of the device are identical low-pass filters. By using molybdenum-permalloy dust, toroidal cores and complex-m filter theory, a low-pass filter was built which will theoretically allow the analyzer to be selective to within 100 cycles from 0 to 5,000 cycles with a discrimination of 25 db.--a discrimination of 40 db. can be obtained for bands of 200 cycles.

CHAPTER II

NOISE ANALYZER DESIGN AND OPERATION

Note: This chapter will be divided into three parts. The first section will indicate the general use of the system. The second will treat the general composition of the system and its operation. The third will be concerned with the component parts of the system and will indicate their requirements.

GENERAL USE OF THE SYSTEM.

In many respects the system to be described in this chapter meets all of the requirements of a variable bandpass filter. It is capable of selecting any desired band of frequencies in the audible spectrum at the exclusion of all others. The width of the pass-band is independent of the mean frequency and is limited only by the cut-off frequency of the fixed filters used. This limitation merely means that it is impossible to pass bands which are wider than the pass-band range of the low pass filters and it is impossible to select bands which are narrower than the slope of the attenuation curve of the filters will permit. As will be indicated later, this limitation is very small since it is possible to pass any band in the range from zero to five thousand cycles per second, of any width from one hundred to five thousand cycles.

The apparatus differs from a true bandpass filter only in

that the band selected does not reappear at the output of the system in its correct frequency position. If it is desired to select a band of frequencies from 275 to 1275 cycles per second for study it is possible to do so but the band which appears at the output of the system will occupy the position from 4000 to 5000 cycles per second. This is not a serious difficulty in the study of noise spectra as is pointed out in another section of this paper but it does indicate that the apparatus as it is now planned is not suitable for audible observation of signals if the frequency allocation of these signals is important. For all studies wherein observations are made by means of a meter or other optical instrument the present design will be found useful. For other problems an additional piece of equipment would be necessary to transpose the output band of frequencies to their correct position in the audible spectrum.

OPERATION OF THE SYSTEM AS A UNIT.

Figure 1 of this chapter is a block diagram of the component parts of the system. The system consists of two fixed lowpass filters, two modulating systems composed of two modulating units apiece, three sources of carrier supply voltage and additional equipment for measurements.

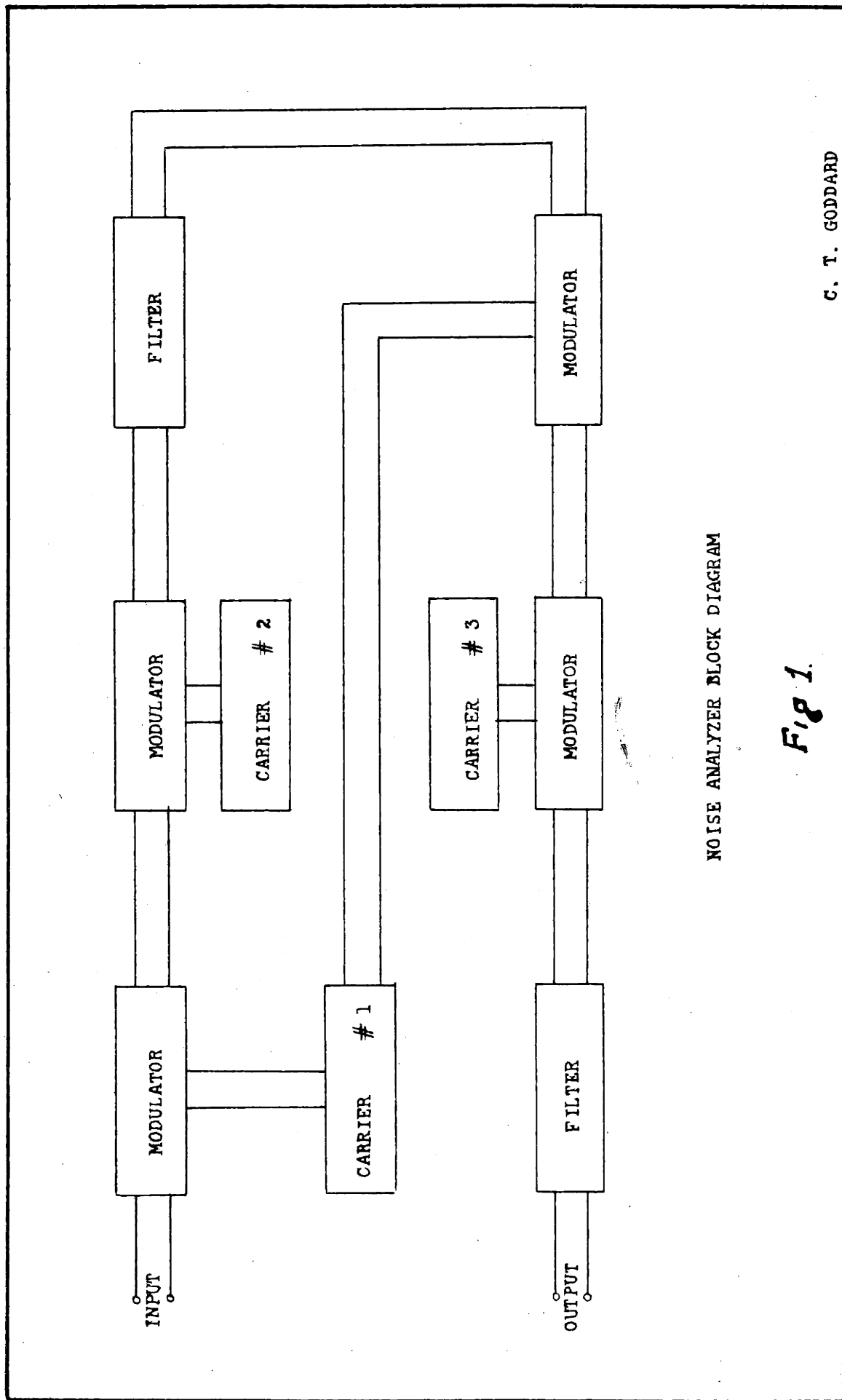
The connections between the various units of the system are indicated in figure 1. And the functional operation of the units is indicated in figure 2.

Figure 2 indicates the equipment encountered by a signal as it progresses through the system and indicates the manner in which the signal is transformed and altered by each of the units. In order to show these operations with a little more clarity, a signal will be traced through the system by means of figure 2.

The signal to be analyzed is assumed to occupy a band of frequencies from zero to five thousand cycles per second. From this section it is desired to select a band of frequencies in the range between "X" and "Y" as indicated in step 1 at the upper left of figure 2.

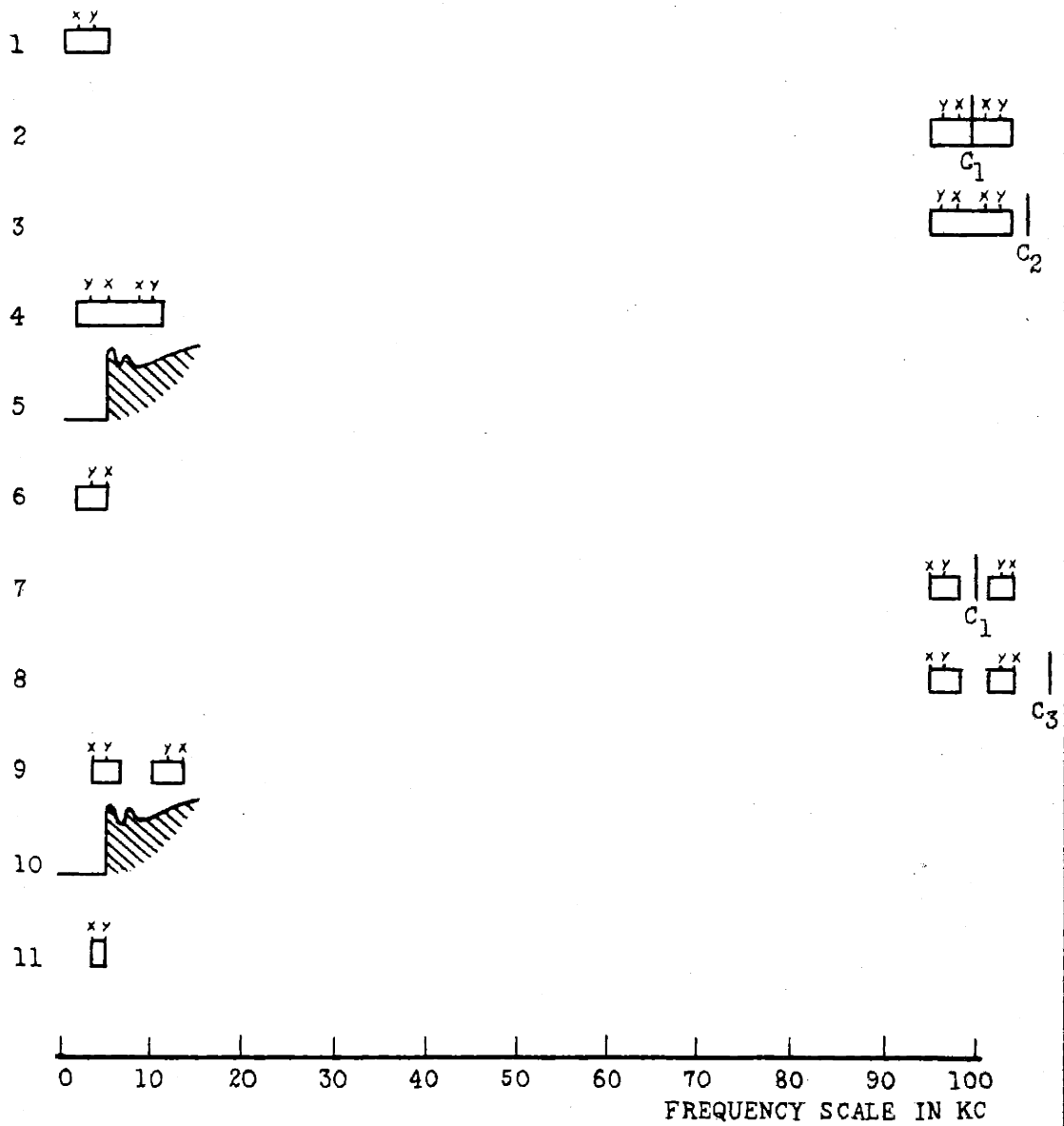
The first step in the process is to modulate the original signal with a carrier frequency of 100 kilocycles per second. The carrier "C₁" is indicated in step 2 and by the frequency scale at the bottom of the figure. The results of this first modulation process are indicated in step 2. The signal at this point is composed of the two side-bands as shown but the carrier signal has been suppressed. The carrier is shown in this step merely to indicate that it is the "cause" of the new location of the band of frequencies to be studied. Note that the two frequency limits previously denoted by "X" and "Y" hold normal and inverted positions as shown.

As is indicated in step 3, the signal is next modulated



NOISE ANALYZER BLOCK DIAGRAM

Fig 1.



OPERATION OF NOISE ANALYZER

- C_1 Fixed 100 kc carrier
- C_2 Variable carrier
- C_3 Variable carrier

Fig 2.

by a carrier designated " C_2 " whose frequency is adjusted to place the point "X" of the original signal at the cutoff frequency of the fixed lowpass filter shown in step 5. In the modulation step indicated in step 3 and step 4, only the "difference frequency" components of the output of the modulator are shown. This is done for convenience and simplicity since any other components except distortion components below 5000 cycles per second would be eliminated from the signal at the filter shown in step 5.

The signal after being modulated in steps 3 and 4 is passed through the fixed lowpass filter as shown in steps 5 and 6. Note that the choice of carrier frequency C_2 was made so that the limit "X" would fall at the filter cutoff. In step 6, the signal is inverted with respect to its original location as shown in step 1 and contains no components which previously existed between zero and the "X" frequency location shown in step 1.

Proceeding through the system in a manner quite similar to steps 2, 3, 4 and 5, the signal is again modulated by a signal of frequency " C_1 " and by a signal of frequency C_3 which will place the point "Y" of the twice-inverted signal at the cutoff frequency of the second lowpass filter. This filter is effective in removing all components of the signal in the range above the point "Y". Again, none of the modulation products except those due to distortion terms in the modulator characteristics will appear in the signal.

after it has passed through the second lowpass filter in step 16.

The final step indicated in figure 2 shows that the signal upon leaving the second lowpass filter is composed only of those frequencies of the original signal between "X" and "Y". As was stated previously, although the resulting signal now occupies a new position in the audible spectrum, it is now in suitable condition for tests by non-audible methods.

There are many advantages to the system as assembled here. Of great importance is the duplicity of similar parts. The two filters are identical as are also the two double modulators. Thus one design for a filter and a double modulator serves for the entire system. So also in the case of the carrier supplies. The three carriers, C_1 , C_2 and C_3 all operate in the range between 100 and 105 kilocycles per second and thus a single design will suffice for all supplies.

Another feature of the system is seen in its operation. The setting of carrier frequency C_2 determines the cutoff at point "X" independent of the setting of carrier frequency C_3 and the same is true of the point "Y" with respect to the setting of carrier frequency C_2 .

As has been stated previously, the use of the system as a true bandpass filter of variable width would require the design of additional equipment to transform the final signal to its original location in the spectrum but since the

apparatus is satisfactory for the analysis of noise spectra, the means of making this transformation has not been included in this work. Although it may be possible to design such a frequency transforming device, the method is not immediately discernable since interfering signals which were so easily removed by the lowpass filters in the present design would play an important part in the problem. It is apparent that another double modulation step would not suffice since the procedure would again invert the signal which is now in its correct orientation with respect to zero frequency.

REQUIREMENTS OF THE COMPONENT PARTS OF THE PRESENT SYSTEM

The modulator problem is more severe than it may at first appear. Many requirements which are not at first apparent have been solved by rather ingenious methods. The first solution of the modulator problem is the choice of the basic system circuit. By the use of lowpass filters as shown, it is possible to remove many of the usual forms of undesired signal before that signal can cause any trouble. Thus it is quite apparent that any components of the modulation products of the form

$$\sin (n c \pm v)$$

$$n = 2, 3, 4, \dots$$

are completely removed from the signal at the lowpass

filters before they can react with similar components of comparable frequencies to give signals in the audible range.

It is apparent that the original signal shown in step 1 must be removed before the modulation by C_2 takes place. If this were not done, the original signal would become hopelessly scrambled with the audio frequency signal from this modulator. Thus a modulator which is capable of suppressing the original signal in its output circuit would be desirable. The same argument holds for the signal as it passes through the third modulating unit in step 7.

Another requirement placed on the modulators is that the carrier shall not appear in the output of the individual units. If this were allowed, the carrier " C_1 " would react with the second modulator to cause a beat note which would interfere with the signal in the audible range. This difficulty can not be removed by the use of filters since the carrier and signal frequencies in steps 2 and 7 are very close together.

Except for the requirements that there shall be no original carrier or original signal appearing in the output of the modulators, there are not many restrictions on the type that can be used. Of course, no great amount of original ~~frequency distortion~~ signal can be tolerated, but it has already been stated that harmonics of the carrier signal will cause no harm.

The filters as units in the system as a whole would be required to have as steep a cutoff characteristic as

possible so as to permit the use of the system for selecting narrow bands of noise for analysis. They would be required to have a high attenuation for all signals beyond the cutoff so as to remove all undesired signals including those of multiples of the carrier frequency. In the pass band the filters should be reasonably constant in attenuation to prevent amplitude distortion of the signal being analyzed.

The sources of carrier voltage for the modulators would be required to maintain a reasonable degree of stability with regard to frequency drift but this requirement would not be too severe. For commercial use, it would probably be desirable to use one fixed source of signal for the carrier C_1 and to obtain the signals C_2 and C_3 by beating a separate source with C_1 . The variations in system fidelity would then depend on the beat oscillators used for C_2 and C_3 and since these could be in the range of audio frequencies, the stability could be easily maintained. Variations in the frequency of C_1 would have little effect on the operation of the system by this method.

The wave-form of the carrier generators would not have to be very pure as was noted previously.

As a conclusion to this chapter, it should be stated that the final form of noise analyzer as pictured in the block diagram of figure 2 of this chapter was the result of many hours of experimenting on paper to obtain the relative simplicity and the resulting duplication of the components. The major feature of the final design is probably the manner in which the main requirements of the system are distributed among the various components so that no one unit is made to share an unnecessary part of the burden of requirements.

CHAPTER III

Part B

Constant-k Type

As pointed out in Chapter II, the practicability of this system for a noise analyzer is almost entirely determined by how sharp a cut-off characteristic can be realized in the two low-pass filters. Thus, in considering the basis for designing these filters the attenuation characteristic is of primary importance. Unfortunately most of the literature on filters using coils and condensers is primarily concerned with impedance rather than with attenuation. Therefore, an investigation was made of the constant-k types of filters to discover how sharp a cut-off characteristic could be obtained using coils with "Q's" of the order of 50 to 200.

In the m-derived constant-k type of filter the rate of cut-off is determined by the value of "m" and the "Q" of the coils--"m" fixes the position of the "infinite peak" with respect to the cut-off frequency and the "Q" of the coils limit the value of this peak. Professor E. A. Guillemin has derived some approximate relations¹ showing the effect of dissipation on the attenuation characteristic of an m-derived section of a constant-k filter at critical places in the function; i.e., at cut-off, at the "infinite peak" point and in the pass region. Appendix B presents a brief derivation of these relations which are as follows:

1. From personal notes by Professor Guillemin.

(1) Attenuation at cut-off: (f_c)

$$\gamma_{ic}^* = \frac{1}{m} \sqrt{\frac{2}{Q_1}} \quad (\text{NAPIERS})$$

$$\text{WHERE: } Q_1 = \frac{\omega_c L}{R}$$

(2) Attenuation at peak: (f_∞)

$$\gamma_{i\infty}^* = \ln \left[4Q_\infty \left(\frac{\omega_\infty^2}{\omega_1^2} - 1 \right) \right] \quad (\text{NAPIERS})$$

$$\text{WHERE: } Q_\infty = \frac{\omega L}{R} \quad \text{AT } \omega_\infty$$

$$\frac{\omega_\infty^2}{\omega_1^2} = a^2 ; \quad a = \frac{1}{\sqrt{1-m^2}}$$

(3) Attenuation in pass-band: $0 < \omega < \omega_c$

$$\gamma_i^* = \frac{1}{Q_1} \times \frac{m}{\sqrt{1-x^2} \left(1 - \frac{\omega^2}{\omega_\infty^2} \right)} \quad (\text{NAPIERS})$$

$$\text{WHERE: } x = \frac{\omega}{\omega_c}$$

$$Q_1 = \frac{\omega_c L}{R}$$

Using these relations and the fact that at other points in the characteristic the attenuation is approximately equal to ideal values*, computations were made and a set of graphs composed to present the findings in a correlated form. There are four graphs, 1882, 1883, 1884 and 1885, representing coils with "Q's" of 50, 100, 150 and 200 respectively. Each graph has curves for the following values of "m": 0.14 (a = 1.01),

$$* \quad \gamma = \ln \left(\frac{\gamma_k + m}{\gamma_k - m} \right)$$

$$\text{WHERE: } \gamma_k = \sqrt{1 - \frac{1}{x^2}}$$

0.197 (a = 1.02), 0.274 (a = 1.04), 0.377 (a = 1.08), 0.507 (a = 1.16) and 0.600 (a = 1.25).

When considering these graphs it becomes apparent that coils with "Q's" of the order of 200 are required to obtain a reasonable amount of sharpness at cut-off using such low values of "m" as 0.14 and 0.197. With a "Q" of 200 and an "m" of 0.14, a cut-off rate of about 22 db. in 2% can be realized and with the same "Q" and an "m" of 0.197, the rate of cut-off is 28 db. in 3%.

Although these rates are sufficiently sharp for most applications, it was felt that a much sharper one would be necessary to show the practicability of the system used in this project. At first it was hoped that double-m-derived constant-k filters would give a better attenuation function than single-m-derived. However, upon investigation it was found that the attenuation function for the double-m filters is the same as that for the single-m. In the double-m case the formula for attenuation is ideally:

$$\gamma = \ln \left(\frac{\gamma_k + m \cdot m_2}{\gamma_k - m \cdot m_2} \right) \quad \text{WHERE:} \quad \gamma_k = \sqrt{1 - \frac{1}{k^2}}$$

This is the same as that for the single-m section if $m, m_2 = m$. It follows, also, that dissipation will limit the peak attenuation points in the double-m cases in the same manner as in the single-m.

Complex-m Derivation

When presented with the problem, Professor Guillemin suggested that a study be made of complex-m filter theory. He was of the opinion that a section of filter designed on this basis would give a much sharper cut-off than any real-m-derived type.

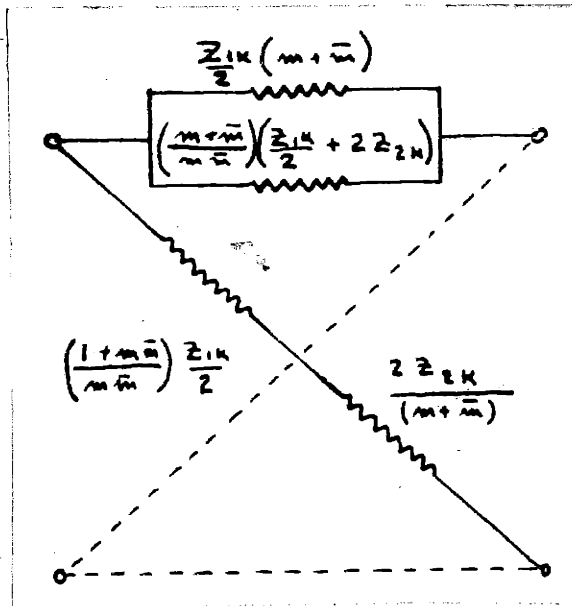
Theoretically a complex-m filter will give a point of infinite attenuation because of dissipation. For a constant-k m-derived filter the attenuation is given by:

$$\delta = \ln \left(\frac{\gamma + m}{\gamma - m} \right)$$

$$\text{Where: } \gamma = \sqrt{\frac{\gamma_1}{\gamma_2}} \text{ (on the lattice basis)}$$

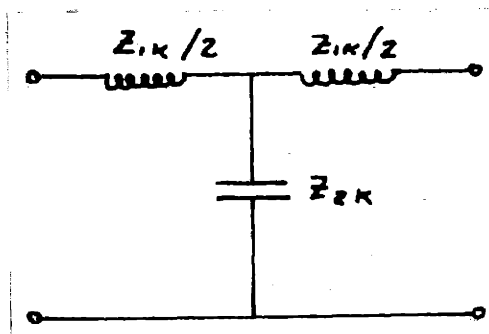
If the coils contain dissipation γ will be a complex expression. Therefore, to make δ infinite in the above expression, "m" must also be complex and equal to γ at the point of infinite attenuation.

Part I of Appendix C contains the mid-series derivation of the complex-m-type lattice structure which gives a point of infinite attenuation at cut-off and is physically realizable as follows:



Where: $m = \frac{1 - j}{\sqrt{2} Q_c}$; $\bar{m} = \frac{1 + j}{\sqrt{2} Q_c}$
 $Q_c = \frac{\omega_c L}{R}$ (AT CUT-OFF)

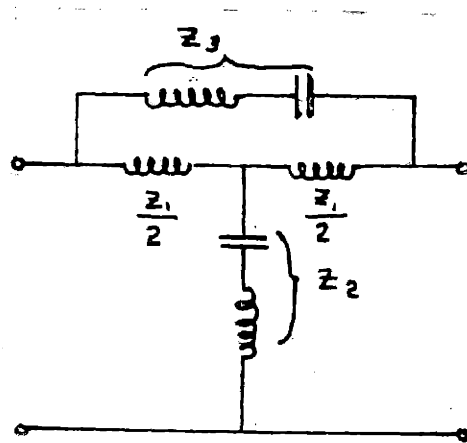
And Z_{1K} and Z_{2K} are the elements in the constant-k proto-type section, as follows:



Part II of Appendix C gives the derivation of the approximate attenuation characteristic of such a complex-m-type structure and graph 1886 presents a plot of the attenuation in the proximity of cut-off. It will be noted that with coils having "Q's" as low as 50, a cut-off rate of "infinity" in 4% can be obtained. As in the case of the real-m structures with

low values of "m", the attenuation beyond cut-off drops off very rapidly.

Theoretically the lattice structure is a convenient form of filter to use, but in practice unbalanced types are much less expensive and easier to build. Therefore, an effort was made to change this lattice complex-m structure into some unbalanced form. In his Volume II of Communication Networks,* Professor Guillemin gives a bridged-T structure which is equivalent to the complex-m lattice in Figure :



$$\text{Where: } \frac{Z_1}{2} = \frac{(m + \bar{m}) Z_{1K}}{2}$$

$$\frac{Z_3}{2} = \frac{(m + \bar{m})}{(m \bar{m})} \left(\frac{Z_{1K}}{2} + 2 Z_{2K} \right)$$

$$2 Z_2 = \frac{2 Z_{2K}}{(m + \bar{m})} + \left\{ \frac{(1 + m \bar{m})}{(m + \bar{m})} - (m + \bar{m}) \right\} \frac{Z_{1K}}{2}$$

The structure in Figure is physically realizable if $\left(\frac{1 + m \bar{m}}{m + \bar{m}} \right) \geq (m + \bar{m})$. If we write $m = m_1 + j m_2$, this condition reduces to: $m_1 \leq \sqrt{\frac{1 + m_2^2}{3}}$

* See pages 439-440.

For the case where the infinite peak is at cut-off:

$$m = \frac{1-\epsilon}{\sqrt{2Q_c}} \quad ; \text{ or } m_1 = \sqrt{\frac{1}{2Q_c}} \quad \text{and} \quad m_2 = -\sqrt{\frac{1}{2Q_c}} \quad . \quad \text{Substituting}$$

and solving:

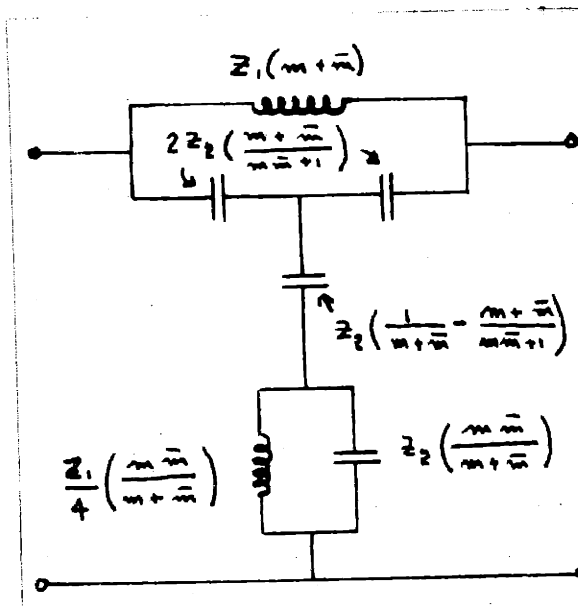
$$\sqrt{\frac{1}{2Q_c}} \leq \sqrt{\frac{1}{3} + \frac{1}{6Q_c}}$$

$$\frac{1}{2Q_c} \leq \frac{1}{3} + \frac{1}{6Q_c}$$

$$\frac{2Q_c}{3} \geq \frac{2}{3}$$

Therefore, $Q_c \geq 1$ is the condition which must be satisfied to make the structure in Figure physically realizable.

Whereas the lattice in Figure requires 6 coils and 4 condensers, Figure calls for 4 coils and 2 condensers. In an attempt to further reduce the number of coils needed to build a network having an attenuation function equivalent to the lattice in Figure, the derivation of a bridged-T structure on the mid-shunt-derived basis was considered. By inspection such a filter should have only 2 coils and 4 condensers, since it is the reciprocal of the bridged-T in Figure. Appendix C, Part III, gives the derivation of this structure, which is as follows:



This structure is physically realizable if $\frac{1}{m + \bar{m}} \geq \frac{m + \bar{m}}{m\bar{m} + 1}$, which is the same condition that had to be fulfilled for the structure in Figure . As in that case the condition is met if the coils have a "Q" greater than 1.

Since it is on the mid-shunt-derived basis, the structure in Figure has the same characteristic impedance as the mid-shunt prototype structure. Therefore, it can be used in cascade with mid-shunt m-derived and prototype sections in a composite filter.

CHAPTER IV

Design and Construction of Filter on M-Derived Basis

From the investigations made in Chapter III, it is evident that the complex-m filter section should give the sharpest cut-off characteristic. Theoretically the Cauer, Bode and single-m-derived types will give as sharp a characteristic as might be desired, but in practice dissipation limits the sharpness. Therefore, it was decided to use a section of complex-m in cascade with as many sections of m-derived and constant-k prototype as would be required to give the desired cut-off characteristic and minimum attenuation beyond cut-off.

Since "Q" is an important factor in designing coils for use in filters, an investigation was made to determine what form of coil would be best suited to the needs in this case; namely, high "Q" with stability and linearity. Professor C. E. Tucker suggested that toroidal coils using permalloy-dust cores would meet the requirements. He informed us that he had a limited number of such cores and that more could be obtained through the Western Electric Company.

Substantiating Professor Tucker's views, some interesting data on powered permalloy was found in an article by Shackelton and Barber¹ of the Bell System. The average permeability of cores made of powered permalloy is 75*; the permeability is

1. "Compressed Powered Permalloy Manufacture and Magnetic Properties", W.J. Shackelton and I.G. Barber; A.I.E.E. Transactions, Vol. 47, No. 2; April, 1928.

substantially constant for saturations upto about 100 Gaussses and does not vary more than 10% for saturations upto 4,000 Gaussses; the eddy-current and hysteresis losses are negligible at audio frequencies. In favor of these cores it should also be mentioned that coils using them do not require shielding since all the flux is confined to the core--a big factor when high "Q's" are required.

An order was placed with the Western Electric Company for a number of these permalloy-dust cores, but they had discontinued manufacture of the ones ordered. To replace them they are manufacturing a series of newly developed cores made of molybdenum permalloy dust. These cores have even better characteristics than the permalloy-dust ones and have higher permeabilities, with the average being 125. These new cores are recommended for use with frequencies up to 12,000 c.p.s. For anyone who might be interested in cores at higher frequencies there is a series of permalloy-dust cores with a permeability of about 26 recommended for use upto 60,000 c.p.s.

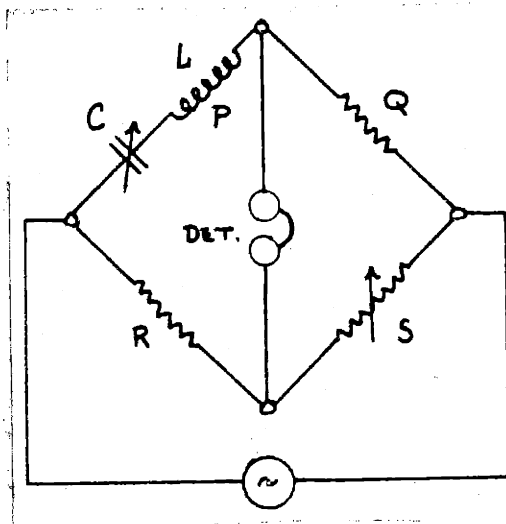
Three different cores were used in the filter for this thesis project. Designating them by their Western Electric piece-part number they have the following specifications:

Permeability = 125 ± 10 for frequencies upto 12,000 c.p.s.

Core Number	Outside Dia. (inches)	Inside Dia. (inches)	Axial Height (inches)
P-468109	2.25	1.4	0.55
P-469715	2.00	1.25	0.53
P-467585	1.35	0.92	0.35

Using these cores and the proper size wire, coils with "Q's" of 65 to 224 were obtained at 5,000 cycles.

Before discussing building the coils and the various sections of the filter, it would be well to show briefly how accurate measurements were made of inductance and "Q" and of capacity. Many bridges are recommended for measuring self-inductance² but few can be used to measure the effective resistance of a coil and thereby obtain a measure of its "Q". Although it depends on frequency, Gruneisen and Giebe's bridge method of series resonance seems to be the simplest and most accurate if a reliable frequency source is available. Also this method gives a measure of both the inductance and the effective resistance, in one setting of the bridge. The circuit and balance conditions for the bridge are as follows:



$$L = \frac{1}{\omega^2 C} \quad (\text{HENRIES})$$
$$P = \frac{QR}{S} \quad (\text{OHMS})$$

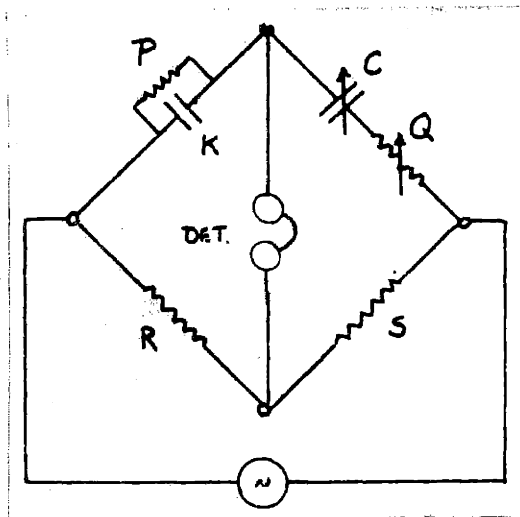
(C IS IN FARADS)

For an accurate frequency reference the communications laboratory standard of 1000 c.p.s. was used--the frequency of

2. A. Campbell and E. C. Childs, The Measurement of Inductance, Capacitance and Frequency; New York, 1935.

this standard is good to a few parts in a million. Lissajou figures on the screen of a cathode-ray oscilloscope served to check the frequency of the oscillator used as a source against the 1000 cycle standard.

For measuring capacity Wien's series-resistance method³ was used as follows:



EXACTLY :

$$K = \frac{S}{R} \times \frac{C}{1 + \omega^2 C^2 Q^2} \quad (\text{FARADS})$$

$$P = \frac{R}{S} = \frac{1 + \omega^2 C^2 Q^2}{\omega^2 C^2 Q} \quad (\text{OHMS})$$

USUALLY :

$$\cos \phi = \frac{1}{\omega K P} \quad \text{IS SMALL}$$

THEN APPROX :

$$K = \frac{CS}{R} \quad (\text{FARADS})$$

(C IN FARADS)

Although the bridge in Figure does not depend on frequency for measuring capacity when P is large and low loss standard condensers are used, all measurements were made with the source being checked against the 1000 cycle standard. Standard condenser C was composed of precision Leeds and Northrup decade boxes and a General Radio air condenser.

In constructing the coils, the approximate number of turns needed for a given inductance on a given core was calculated from the following formula:

3. Ibid. p.347

For toroidal coils of uniform cross-section:

$$L = 2 \mu b N^2 \ln \left(\frac{r_2}{r_1} \right) \text{ (HENRIES)}$$

WHERE: μ = PERMEABILITY IN AEMU UNITS TIMES 10^{-7}

b = AXIAL HEIGHT IN METERS

N = NUMBER OF TURNS

r_2 = OUTSIDE RADIUS

r_1 = INSIDE RADIUS

A sample calculation using the above formula is given in Appendix D. With this number of turns the coil was measured on the General Radio impedance bridge and the proper number of turns removed to give the required inductance within the accuracy of this bridge. Then using the bridge in Figure , the inductance was made as accurate as possible to within removing or adding one turn.

To make certain that the cores would not be saturated beyond about 100 Gauss by the currents which would be encountered by the coils in this filter, rough calculations were made for several coils to determine the flux concentration on the basis of 1 milliwatt input to 600 ohms. These calculations were made using the following formula for flux density in a toroidal coil of uniform cross-section:

$$B = \frac{4\pi N I \mu}{10 l}$$

WHERE: I = CURRENT IN AMPERES

l = MEAN CIRCUMFERENCE IN CM.

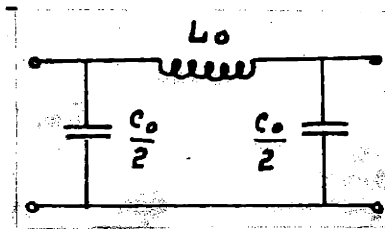
μ = PERMEABILITY IN AEMU UNITS

N = NUMBER OF TURNS

A sample calculation using the above formula is given in Appendix D.

Before any part of the filter could be designed, the cut-off frequency, impedance level and type of internal termination had to be chosen. For no particular reason a cut-off frequency of 5,000 c.p.s. was selected--however, it was felt that one set of filters should be able to take care of at least half of the audible spectrum, that is, up to 5,000 cycles. Then too, from the results obtained at this medium frequency, it would be easy to predict what results could be obtained at frequencies in the low or high portion of the audible spectrum. The impedance level of 600 ohms was selected for two reasons: one is that this level is common practice in telephone work and the other is that "reasonable" values of inductance would be needed--lower levels would make it impractical to design the coils in the complex-m section and higher levels would make it impractical to design the coils in the prototype section. The mid-shunt type of internal termination was decided upon because of two factors: (1) the mid-shunt-derived complex-m section has only two coils;(2) the mid-shunt terminated mid-shunt-m-derived sections have only one coil. Then, too, when building up a filter section by section, it is desirable to have only capacitances at the terminals of sections.

Since all sections are derived from the prototype, the value of the elements for it will be given first as follows:



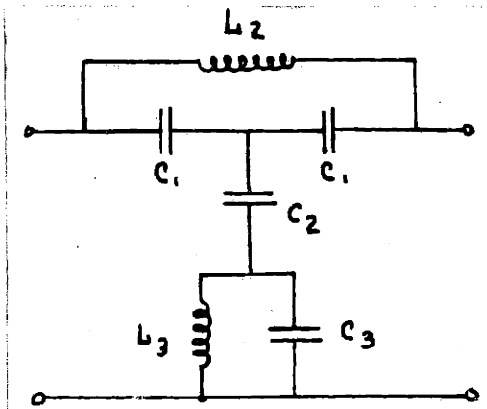
$$L_0 = \frac{Z_0}{\pi f_c} = \frac{600}{\pi(5000)} = 38.2 \text{ mh}$$

$$C_0 = \frac{1}{Z_0 \pi f_c} = \frac{1}{(600)\pi(5000)} = 0.1062 \text{ mh}$$

WHERE: $Z_0 = \text{NOMINAL IMPEDANCE} = 600^{\omega}$
 $f_c = \text{CUT-OFF FREQUENCY} = 5000 \text{ C.P.S.}$

Complex-m Section

When designing the complex-m section a "Q" had to be chosen in view of being able to obtain such a value with the inductances required. On the basis of a trial coil it was certain that 50 would be satisfactory; also, such a value would give the steepness of cut-off desired. Using the relations given in Figure of Chapter III and in Appendix C, Part III, the elements for the complex-m section are derived from the prototype as follows:



$$C_1 = \frac{C_0 (m\bar{m} + 1)}{2(m + \bar{m})} = 0.271 \text{ mfd.}$$

$$C_2 = C_0 \frac{1}{\left\{ \frac{1}{(m + \bar{m})} - \frac{1}{(m\bar{m} + 1)} \right\}} = .0222 \text{ mfd.}$$

$$C_3 = \frac{C_0 (m + \bar{m})}{m\bar{m}} = 1.062 \text{ mfd.}$$

$$L_2 = L_0 (m\bar{m}) = 7.64 \text{ mh.}$$

$$L_3 = \frac{L_0 (m\bar{m})}{4(m + \bar{m})} = 0.956 \text{ mh.}$$

WHERE: $f_c = f_{\omega} = 5000 \text{ C.P.S.}$

$$Q_c = \frac{\omega_c L}{R}$$

$$m = \frac{1 + \frac{1}{Q_c}}{\sqrt{2Q_c}} = \frac{11.7}{10}$$

$$\bar{m} = \frac{1 - \frac{1}{Q_c}}{\sqrt{2Q_c}} = \frac{1 - 1}{10}$$

For L_3 in Figure , core P-467585 and #24 enameled wire were used. From the formula on page and a permeability of 115 it was calculated that about 106 turns would be required to give 0.956 mh. By measurement at 5000 cycles, 111 turns gave 0.959 mh. which was as near 0.956 as could be obtained-- that is, within 0.5% of the required value. The effective resistance for this coil was measured as 0.459 ohms which by calculation made the "Q" 65.6. In order to make this "Q" equal 50.0, resistance wire was added in series with the coil.

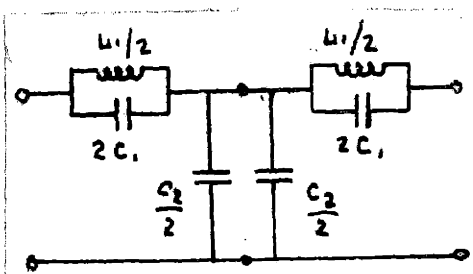
For L_2 in Figure , core P-469715 and #24 enameled wire were used. On the basis of a permeability of 115, the formula on page gave 235 as the number of turns which would be required to give an inductance of 7.64 mh. By measurement at 5000 cycles 227 turns gave an inductance of 7.66 mh., which differs by less than 0.5% from the required value. The effective resistance for this coil was measured as 1.813 ohms, which by calculation gives a "Q" of 132. As in the case of L_3 , resistance was added to this coil to give a "Q" of 50.0.

Using these coils and decade condenser boxes a temporary complex-m section was composed and tested while terminated in its nominal impedance of 600 ohms. A General Radio 713-B oscillator calibrated against the 1000 cycle standard was used as the frequency source and a General Radio 736-A wave analyzer was used to measure the attenuation in db. directly. The results of the test are shown on graph 1887. It was assumed that the big difference between the measured and predicted

curves was due to reflection losses because of mismatching between the characteristic impedance of the complex-m section-- this is the same as the characteristic impedance of the mid-shunt-terminated-prototype constant-k section--and the terminal impedances of 600 ohms. This assumption was later found to be correct when this complex-m section was placed in cascade with terminal sections using "m" equals 0.6--the results are given on sheet 1889. From this graph it may be concluded that the complex-m section constructed agrees very closely with the theoretical predictions based on the approximations made in Chapter III and Appendix C.

Terminal Half-sections

To give the composite filter a fairly constant characteristic impedance over the pass band, two half shunt-m-derived sections mid-series terminated were designed. For the coils required #24 wire was used on P-469715 cores. The resulting coils had "Q's" of about 156 at 5000 c.p.s., and inductance as shown in the following figure of the two sections in cascade:



$$L_1 = L_0 m = 22.92 \text{ mh.} ; \frac{L_1}{2} = 11.46 \text{ mh.}$$

$$C_1 = C_0 \frac{(1-m^2)}{4m} = .0283 \text{ mfd}$$

$$2C_1 = .0566 \text{ mfd.}$$

$$C_2 = C_0 m = .06372 ; \frac{C_2}{2} = .03186 \text{ mfd.}$$

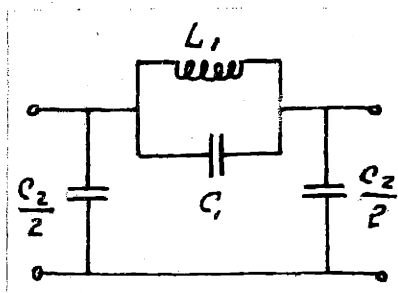
$$m = 0.6$$

Graph 1888 shows the measured attenuation of these two half sections in cascade compared with the theoretical. The difference in the two curves is undoubtedly due to reflection effects, since for a terminal section there is a maximum reflection loss at the peak frequency. (See page 355 of Guillemin, Volume 2)

Two M-Derived Sections

For "filling in" the attenuation characteristic between the complex-m section peak and the $m \neq 0.6$ terminal sections peak, two m-derived sections were required. From the results of the previous coils, it was certain that "Q's" of 150 would be obtained for the coils in these two sections. Therefore, the curves on Sheet 1884 were used to determine what "m" values should be chosen to give peaks at the correct points for giving a minimum attenuation of about 40 db. or higher.

The first section was designed and built to give a peak at 5050 cycles on the basis of $m = 0.14$. Core P-469715 and #20 wire were used to give the inductance of 5.35 mh. required. At 5000 c.p.s. the inductance was measured as 5.35 mh. and the "Q" of this coil was measured and calculated as 192. The section was composed as follows:



$$L_1 = L_0 m = 5.35 \text{ mh.}$$

$$C_2 = C_0 m = .01473 ; \frac{C_2}{2} = .00736 \text{ mfd.}$$

$$C_1 = \frac{C_0(1 - m^2)}{4m} = 0.186 \text{ mfd}$$

$$m = 0.14$$

Before adding this section to the two previously constructed, the standard decade boxes were eliminated as capacitance elements. Western Electric multi-capacitance type condensers were wired to give the proper values of capacitance required in the sections as measured with the bridge in Figure . These condensers together with the coils and the resistance elements of the complex-m section were attached to a board in true "bread-board" style.

The effect of adding the $m = 0.14$ section is shown on graph 1890. The boost in attenuation near cut-off is quite appreciable.

Using $m = 0.274$ a second "m" section was designed to give a peak at 5200 cycles. Core P-468109 and 250 turns of #20 wire were used to give the coil of 10.47 mh. required. At 5000 c.p.s. this coil had a "Q" of 224. Referring to figure , the values of the elements are:

$$L_1 = 10.47 \text{ mh.}$$

$$C_1 = 0.0895 \text{ mfd.}$$

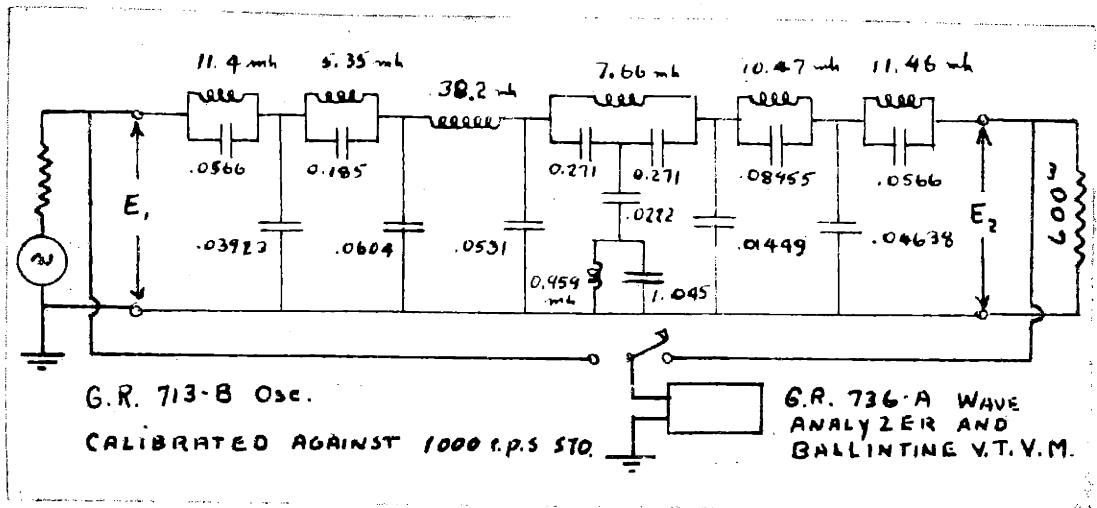
$$\frac{C_2}{2} = 0.0145 \text{ mfd.}$$

Graph 1890 shows the effect of adding this section as a part of the composite filter. The resulting two minimum points of attenuation are nearly equal and are above 40 db.

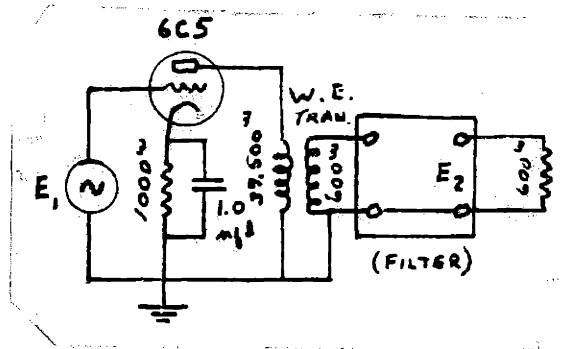
Prototype Section

A sketch of the prototype section is given in Figure . The coil for it was wound on a P-468109 core of #24 wire to give an inductance of 38.2 mh. with a "Q" of 134 at 5000 c.p.s.

With this section added as a part of the composite filter, the resulting attenuation near cut-off is as shown on graph 1890. The attenuation characteristic of the composite filter over the range from 100 to 40,000 c.p.s. is given on graph 1891. These two graphs show that: the minimum attenuation beyond cut-off (5,000 cycles) is 44 db.; upto 3,000 cycles the attenuation is practically zero; from 3,000 to 4,800 cycles it only increases to 2.5 db.; at 4900 cycles it is 8 db.; and at cutoff it is of the order of 60 db. If the rate of cut-off is considered from 4,800 cycles and the minimum attenuation is taken as 44 db., then the cut-off rate is approximately 41.5 db. in 200 cycles or in 4%. If the cut-off rate is considered from 4,900 cycles, then it is 36 db. in 100 cycles or in 2%. Figure gives the composite filter with the values of the elements and the circuit used to test it:

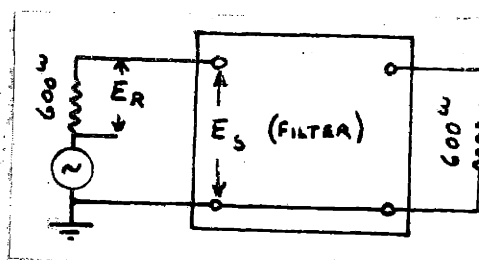


Since this filter will be used on the output of a vacuum tube amplifier for the system in this project, a characteristic under this condition was taken using the following circuit:



As shown on graph 1892, if a reference of -2.5 db. is taken the attenuation is essentially the same for this circuit as that given on graph 1891 for the filter itself. In the vicinity of 10,000 c.p.s. there is a deviation, but the lower attenuation for the circuit with the vacuum tube is undoubtedly due to a peak in the output transformer about this point. Such a difficulty can be overcome by a properly designed matching transformer or circuit from tube to filter.

As a matter of interest the characteristic impedance of the filter was measured by using the following circuit:



$$Z_I = \frac{E_S}{E_R} (600) \text{ OHMS}$$

The results obtained appear on graph 1893. Except for the irregularity just before cut-off, and the fact that the impedance does not go to zero at cut-off, these results agree fairly well with predictions for a filter terminated in mid-series of mid-shunt derived half-sections having $m = 0.6$. These variations from theoretical predictions are undoubtedly due to dissipation.

The photograph included at the end of this chapter serves to give an indication of the physical size of the filter constructed. In practice the coils should be "potted", then the entire filter could be mounted in much less space.

As for cost, these cores can be purchased for about one dollar on the average from Western Electric. The wire itself is not an expensive item. For a permanent filter good quality paper condensers or mica condensers should be used.

CHAPTER V

MODULATORS

GENERAL

The design of a proper modulator to meet the requirements stated in chapter 2 was a time consuming problem. In all, three distinct modulator systems made up of two modulator units each were designed, constructed and tested. These units will be described in some detail in this chapter but for the sake of simplicity and clarity, much of the analytical studies have been consolidated and listed in appendix E. Many of the design problems encountered in one unit were also encountered in the others. For this reason such studies will be found in the appendix and repeated references will be made to that section.

The modulating devices used in this research were,

1. The 6L7 vacuum tube which is a relatively new device designed primarily for use as a modulator or "mixer" in superheterodyne circuits in radio receivers.
2. The copper-oxide rectifier unit which is a device used as a modulator for carrier telephone systems.
3. The 6H6 vacuum tube which is a device comprising two high-vacuum diodes

mounted in a single envelope.

THE 6L7 VACUUM TUBE AS A MODULATOR.

The 6L7 is a multi-grid tube designed for service where it is desired to have dual control of the current in the plate circuit. The dynamic characteristics of the tube when used in the type of circuit used for the modulator in these studies are shown in figure 1 of this chapter. As is noted in the circuit diagram accompanying figure 1, the tube has two control grids which are effectively shielded from each other by the screen grid as shown. The two control grids have independant control over the space current flowing between the cathode and the plate of the tube. In operation the tube behaves somewhat like the "Co-planner Grid" tube¹ which was investigated several years ago in a thesis research at M. I. T..

The graphs of figure 1 indicate that the transfer conductance of the circuit shown may be made to vary linearly with the voltage applied to the number three grid of the tube. The characteristics may be classified as belonging to the type of modulator indicated in figure 4 of appendix E. In a discussion of this type of modulator in the appendix it was noted that the original or voice frequency signal appears in the output in addition

1. See Bibliography.

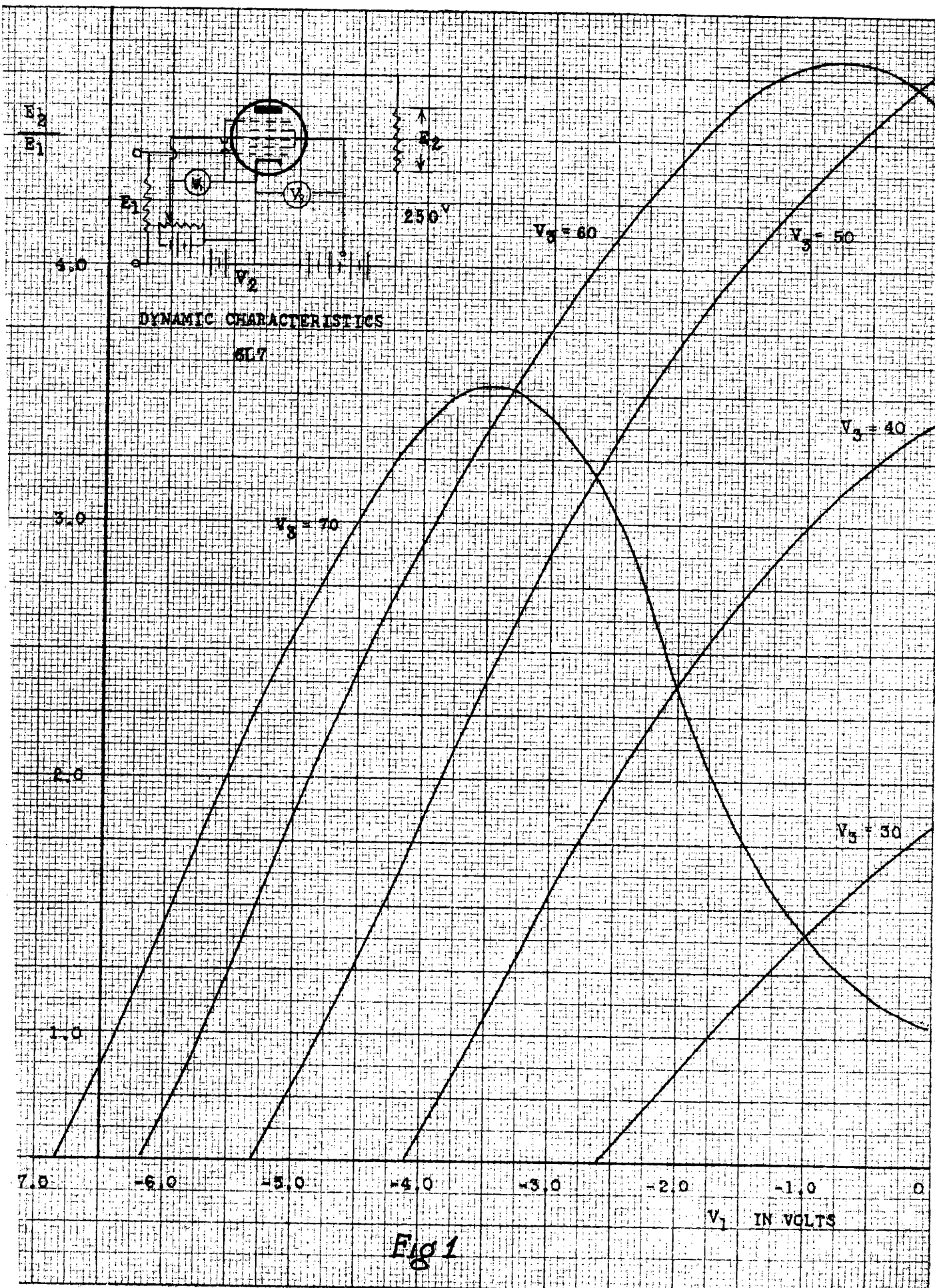


Fig 1

to the desired modulation products. Furthermore, it was noted that the ratio of side-band amplitude to original signal appearing in the output of such a device is 1:2. The use of two such modulator circuits in tandem would result in a ratio of 1:4 unless some means were devised to remove the undesired original signal after the first modulation. This problem in itself does not present great difficulties but in combination with the problem of balance with respect to the carrier signal appearing in the load circuit, many difficulties were encountered.

The circuit used in each modulating unit was similar to that shown in figure 1 of this chapter except that two tubes were used in an attempt to remove the carrier signal from the output by maintaining electrical balance in the circuit. The original voice signal was applied to the two number one grids connected in push-pull and the carrier was applied to the two number three grids in parallel. This circuit is the usual form used in modulator circuits of this nature for obtaining a balance.

As is stated in Appendix E, The amplitude of the carrier signal was about twenty decibels stronger than the applied voice frequency signal in order to cause the circuit to function as stated in the appendix. When used as a single modulating device it was possible to maintain a fairly good carrier balance by means of a center-tapped resistor in the plate circuit. The addition of a special condenser

to adjust for a balance in the interelectrode capacitances of the tubes and the associated wiring helped to secure a better balance and the unit appeared quite satisfactory as a modulator.

In order to use two modulators of this type in tandem in the noise analyzer circuit it was necessary to remove the original voice frequency signal from the output of the modulator. This required the addition of a filter between the two modulators but this was found to be impractical. The use of a balanced filter complicated the type of unbalance which had to be corrected to such an extent that it was found impossible to decrease the carrier signal in the output of the first modulator to the desired extent. The use of an unbalanced filter would have necessitated the addition of circuit elements to connect as buffers between the balanced and unbalanced sections and this was found to be unfeasible because of the unbalance which such a circuit contributed to the modulators as a whole.

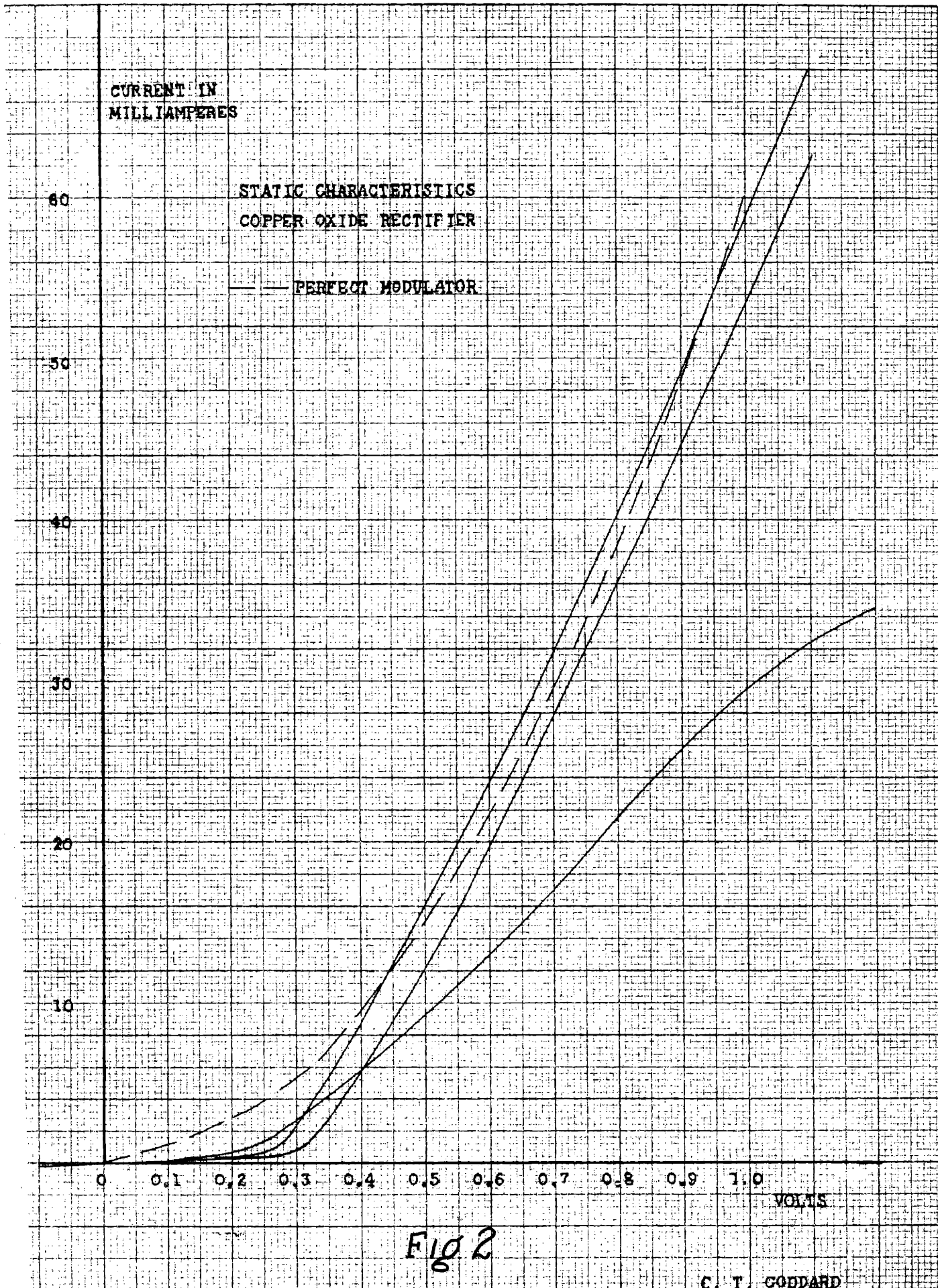
Because of the relatively high impedance levels at which a modulator of this type must be operated, the interelectrode capacitance and unsymmetrical wiring of the units caused phase unbalances which were impossible to predict. In time it was decided that the best solution to the problem would be to try a circuit which could be made to operate favorably at low impedance levels in order to alleviate the phase balance problem.

THE COPPER OXIDE RECTIFIER AS A MODULATOR.

Copper-oxide units are used extensively as modulators in carrier telephone installations for long-distance transmission. As is indicated in Appendix E, they may be operated in circuits of low impedance level and thus the inter-element capacitance does not have as much control of unbalances as in the multi-grid vacuum tube circuits which must be operated at high impedance levels. The circuit used in the experimental work involving these units as modulators is indicated in figure 7 of Appendix E. A complete discussion of the function of such a rectifier circuit is given in the appendix and it is seen that the original voice frequency signal and the carrier are absent in the output circuit provided the circuits are in perfect balance.

Figure 2 of this chapter indicates the static characteristics of one of the units which was available for this part of the study of modulator circuits. Each unit was made up of four copperoxide elements which were wired to form a lattice as shown in figure 7 of Appendix E. The static characteristics shown are representative of the average of the units available although some of the units were more nearly identical than is indicated in figure 3.

The final circuit used in the tests of copperoxide units was of a form similar to that shown in figure 4 of



this chapter. A more detailed discussion of the modulator circuit will be given when discussing the merits of the 6H6 vacuum tube as a modulator.

It was stated on the previous page that the low impedance level at which the copperoxide units can be operated is an aid to obtaining good phase balance. This statement is true if the magnitude of capacitance unbalance is comparative^{Ma} in the two cases. However, the copper-oxide units are made up of metallic discs of about one quarter of an inch diameter and the two discs are in close contact, being separated only by the thickness of the oxide layer on one of the discs. This construction indicates that the inter-element capacitance would be high and such was found to be the case.

It was found to be possible to correct the phase unbalance of the units to a decided extent by shunting the individual elements by fixed condensers of an appropriate value.

With the elements balanced as indicated by external condensers it was found that the amount of carrier and original voice signal appearing in the output of the modulator circuit was still intolerable for use in the noise analyzer circuit developed in chapter II. The reason for this is quite apparent from figure 2 of this chapter. The elements appear to be excellent units for modulators since they are a fair approximation to the square law or "perfect modulator". However, the square law

circuit parameter defeats its own purpose in one respect. Although such a modulator unit will give remarkably pure output if the individual units are found to be in an inherent state of balance, it is almost impossible to correct for a resistive unbalance if one exists. The only useful instrument for correcting for a resistive unbalance is a shunt or series linear resistor connected to the element or elements which cause the unbalance. Of course, the shearing of a characteristic curve of the form shown here by means of a linear resistance can be made to balance the units at a single point on the static curve, but the true problem of correcting the differential resistance over the entire curve can never be accomplished by such a means.

Because of the difficulties of capacitance and resistance balancing which has been discussed on the previous pages, it was decided that the copper-oxide units available were unsuitable for the work at hand. If a larger supply of such units had been available so that a substitution method of selection of units could have been made, a few units suitable for use in the design of the noise analyzer would probably have been found. It must be noted that the operating qualifications of the noise analyzer are more strict than those that are imposed on a modulator in a carrier-telephone system.

THE 6H6 VACUUM TUBE AS A MODULATING ELEMENT.

THE FINAL FORM OF TANDUM DOUBLE-BALANCED MODULATOR.

From the discussion of difficulties encountered in an attempt to use copper-oxide units as modulator elements in a double-balanced circuit, it is apparent that the desired modulating element should be capable of operating between relatively low terminal impedances and should have a nearly linear current-voltage characteristic. In addition, it should have reasonably low interelectrode capacitance and corresponding units should be very nearly alike electrically.

The static characteristics of a 6H6 vacuum tube are indicated in figure 3. It is seen from an inspection of the curves that the diodes of this type are a very near approach to the desired form of modulating element. In addition to the qualifications indicated by figure 3, the diodes have a very low interelectrode capacitance and variations in characteristics due to tube heating ~~were~~ found to be almost identical in diodes in the same tube envelope. This is probably due to the use of a common filament and the tube elements therefore react the same under varying conditions. The fact that the two diodes went through the same exhaust procedure during their manufacture would also be a reason for this equality of drift.

A rigorous discussion of the operation of diodes of this type is to be found in Appendix E. Figures 7 and 8

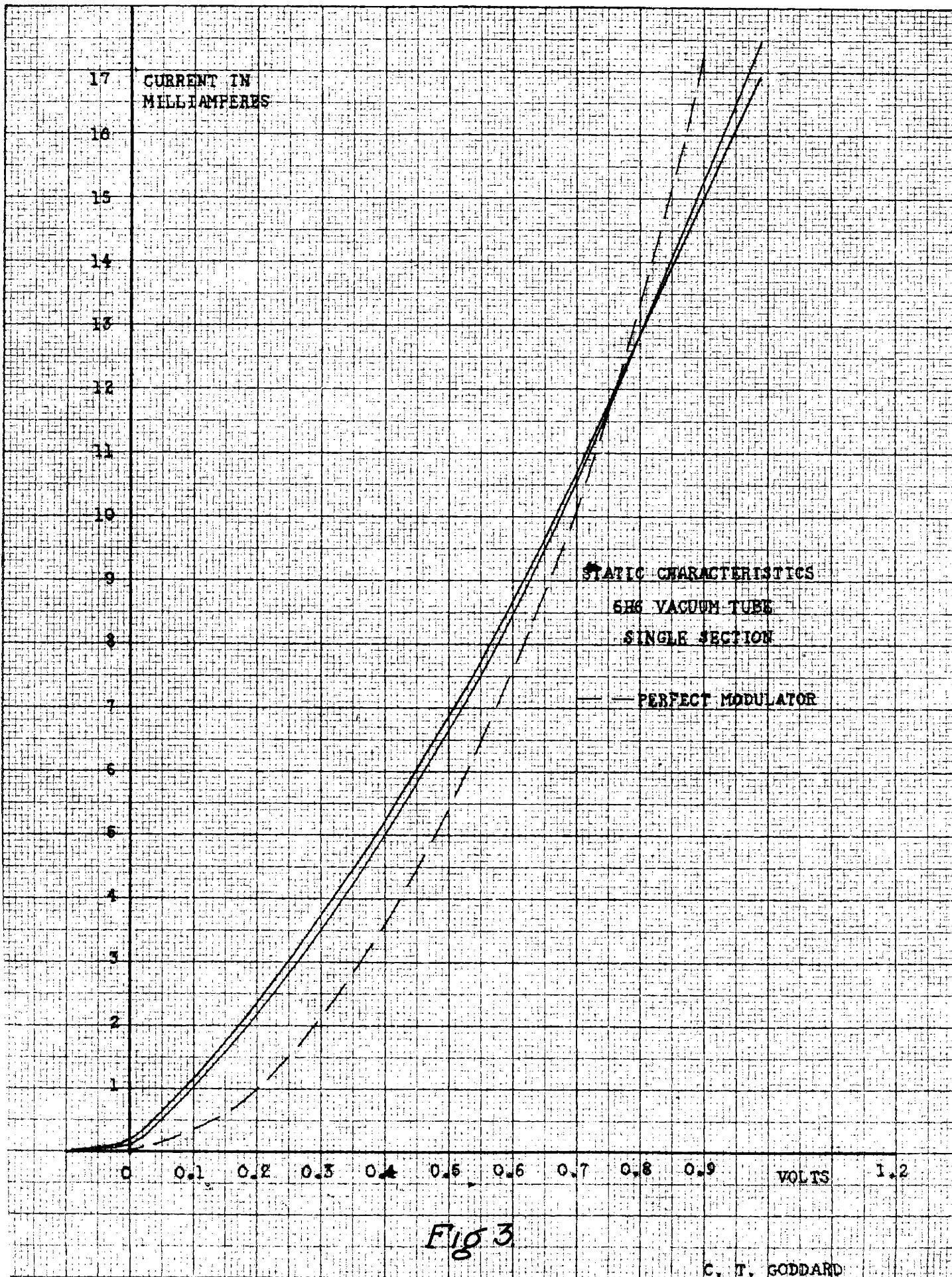
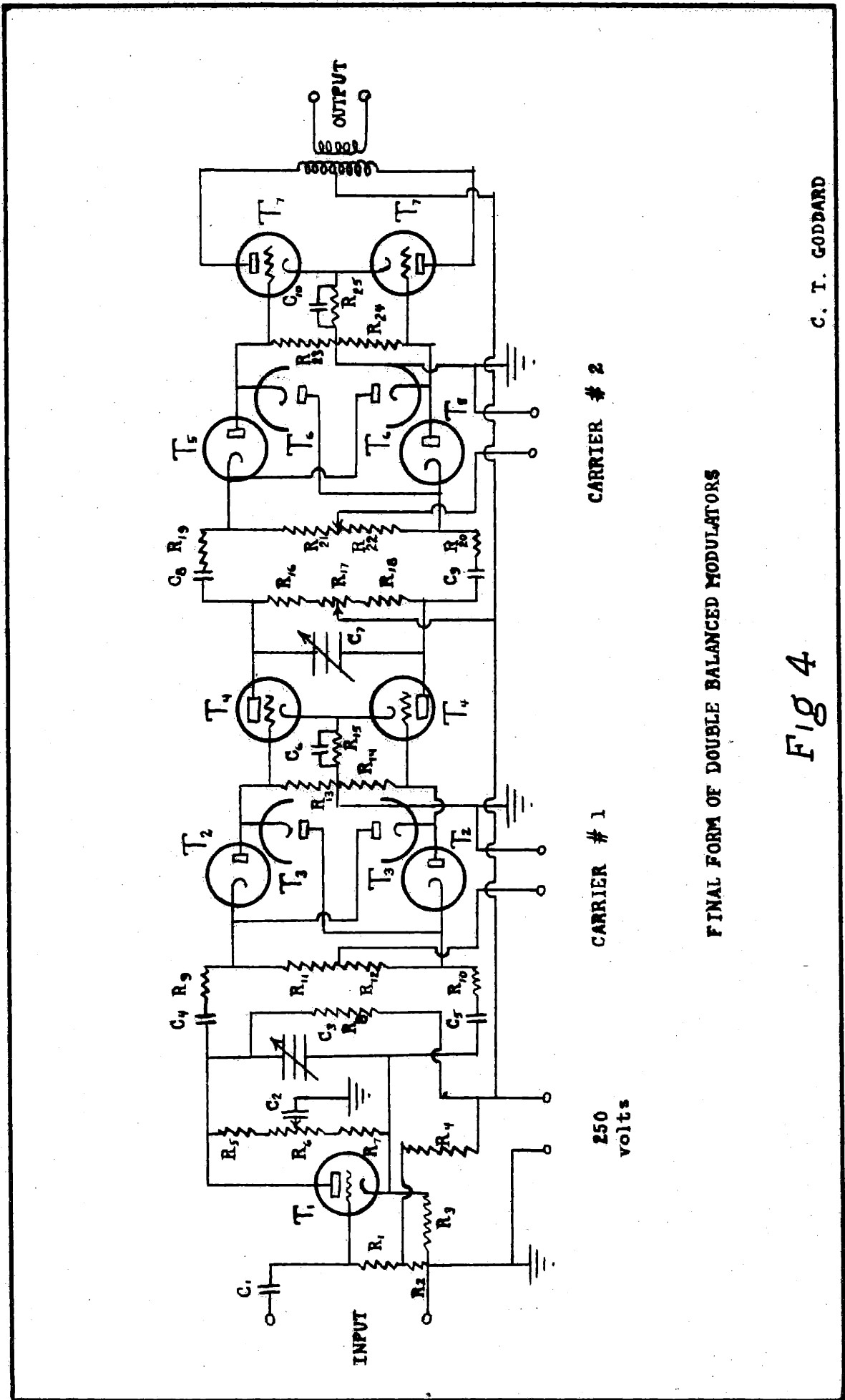


Fig 3

C. T. GODDARD

of this section of the appendix indicate the circuit and output current respectively. From the discussion in the appendix concerning these diagrams, it is shown that the modulation products are of the form that was considered suitable for a modulator for the Noise Analyzer in that they are made up of higher order harmonics of the carrier with the voice signals in superposition but that no original voice or carrier signal appears in the output.

The diagram of figure 4 of this chapter indicates the final form of tandem double-balanced modulator which meets the requirements of the Noise Analyzer as set forth in chapter 2. The two lattice type of double-balanced modulators are indicated with elements of a single 6H6 in the same corresponding arms to insure a good balance for the carrier voltage. The first tube and its associated apparatus is a combination isolating and balancing circuit for the first modulator. The two intermediate triodes are part of an isolating circuit between the two modulators and they again form an easy means of obtaining a balance for the second modulator. The two triodes in the output stage perform the functions of isolating the second modulator from the terminal equipment and of affording a transformation from balanced to unbalanced circuits for connecting to the filters of the Noise Analyzer. The first triode also functions as a phase inverter or element for connecting



FINAL FORM OF DOUBLE BALANCED MODULATORS

Fig 4

C. T. GODDARD

between an unbalanced input source and the balanced modulators without effecting the balance.

With this brief discussion of the elements comprising the entire unit, it would be well to examine the individual parts of the modulator system in more detail.

It is assumed that, in practice, the signal input to the first modulator will be derived from an unbalanced source. The first triode is used to couple from this source to the modulator. The "phase inverting" circuit is of recent design and incorporates a single tube. The balanced output voltage is obtained from this stage from the equal resistors connected between the plate and the direct current plate source and the cathode and the direct current plate source. The return wire from the plate source to a tap on the input resistor provides a neutralization, in part, of the high negative bias which results from the plate current drop through the high cathode resistor. The combination of fixed and variable resistors connected between the plate and cathode and forming a return to ground potential is a means of balancing the modulator circuit. The phase balance for the first modulator is also obtained at this point by means of the special balancing condenser shown. This condenser is constructed in a manner such that the capacitance between the plate and ground or the capacitance between the cathode and ground can be made to predominate to obtain

correct phase balance. The balance is obtained at a high impedance part of the circuit because of the small condenser that can be used at this point. In constructing this part of the unit, a balance was obtained with the modulator alone and the first triode output circuit was then brought into balance with the modulator. The network between the first triode and the modulator serves as an attenuator and matching network between the triode and the modulator proper.

The two triodes which isolate the second modulator from the first is a single tube containing two identical triode units. The balance for the second modulator is obtained in the plate circuit of this stage in a manner similar to that used for the first modulator.

It should be noted that each modulator must be balanced between the plate circuit of the preceding stage and the grid circuit of the following stage and that no other part of the system can effect this balance once it has been obtained.

The output of the entire modulator unit is surprisingly free from undesired modulation products when compared with the experiences which were had with the operation of other modulation circuits which were investigated in this research.

APPENDIX E
MODULATOR THEORY

GENERAL:

Modulators used in electrical communications may be grouped according to many different qualifications but for the problem at hand it is best that they be separated into two classes only. These are the so-called "high-power" and "low-power" classes, depending on whether the output must supply a large or a negligible amount of power to the terminating apparatus. The material to be discussed in this section will be concerned mainly with the "low-power" type of modulators and it will be assumed that all power capabilities of the systems will be obtained through the use of one or ~~more~~ stages of amplification following the apparatus described here.

The general trend in modulator design has been influenced not only by the advancement in vacuum tube design but also by the type of service which the modulator is to provide. Thus if the equipment is to be used solely for laboratory measurements it may be desired that the modulated signal should be extremely pure in that it contains only the desired modulation products. If the application of a modulator

circuit is to be made as one of many units in a carrier telephone system, the choice of system will be made by a judicious weighting of cost and simplicity against the quality of transmission desired.

Many different types of electrical circuit elements are used as modulators and yet the fundamentals of their operation are quite the same. Whether the circuit to be used involves the use of grid or plate modulation in a triode or modulation by some means whereby the transconductance of the circuit element is varied by some external means as in the case of the 6L7 vacuum tube, or modulation by means of the non-linearity of a diode rectifier, the fundamental analysis of the system to be used will follow along in quite the same manner.

The starting point for the method of analysis to be described in this appendix is the decision of the type of signal that is desired in the load impedance of the system.

The most perfect modulator yet devised is one whose output contains only the two side-band signals with the carrier and original voice signal suppressed and no higher order harmonic or distortion terms present. Such an output signal will therefor be assumed as the starting point in this analysis.

THEORY OF THE PERFECT MODULATOR

Assuming that the perfect modulator is one which provides an output signal of the type described on the previous page, we may describe the input and output signals as

$$\begin{aligned} e_1 &= E_1 \cos vt && \text{(input signal)} \\ i_2 &= I_2 [\sin(c+v)t + \sin(c-v)t] && \text{(output signal)} \end{aligned} \quad (1)$$

The apparatus comprising the modulator (which will also be shown later to contain the carrier generating source) may be as shown by the box of figure 1.

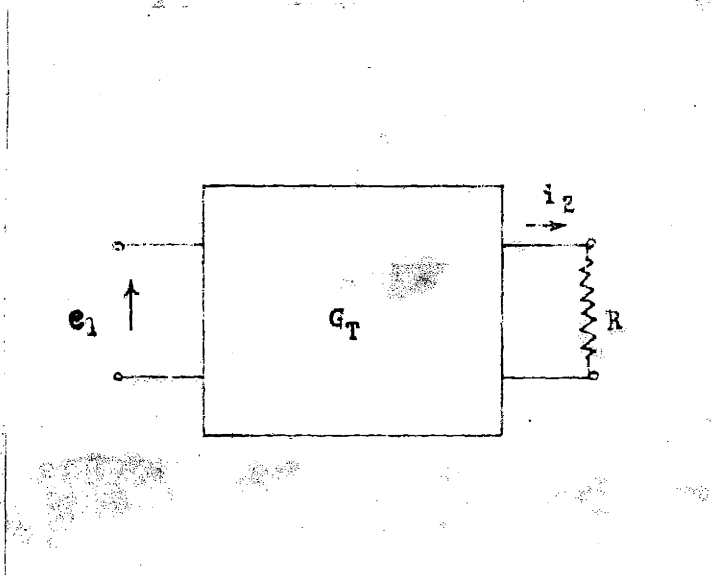


Fig 1

The load resistance "R" may be transferred to the box and assumed to be an integral part of the modulator.

If, now, we define G_T the transfer conductance of the modulator so that,

$$G_T = \frac{i_2}{e_1} \quad (2)$$

$$G_T = \frac{I_2 [\sin (c+v)t + \sin (c-v)t]}{E_1 \cos vt} \quad (3)$$

which shows the desired form of "G_t".

Applying trigonometric formulas of identity to equation (3) results in

$$G_T = \frac{I_2 2 \sin ct \cos vt}{E_1 \cos vt} = \frac{2 I_2}{E_1} \sin ct \quad (4)$$

which is an exact solution for the type of control circuit desired to accomplish "pure" modulation.

In practice it is impossible to accomplish the result shown in equation (4) and a new artifice must be used to obtain the desired results. Thus, let us change the picture of the modulator as shown in figure 2.

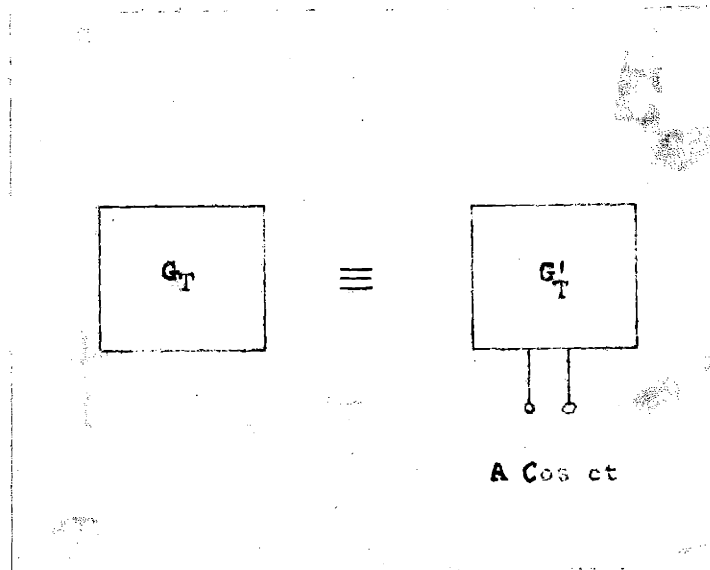


Fig 2

In this manner, the periodic variation of the transconductance is obtained by the application of an alternating carrier signal as shown. The exact equivalence of the two systems as shown must be taken for granted for the time being and an

exact proof of their equivalence will be presented later.

To obtain a perfect modulator it may be seen by an inspection of figure 2. that the new transconductance parameter " G_t " must vary linearly with the applied external signal voltage which will be designated as the "carrier". It must be proportional to the applied carrier voltage and must be capable of assuming both positive and negative values. The desired variation of " G_t " as a function of the applied carrier voltage " E_c " is shown in figure 3.

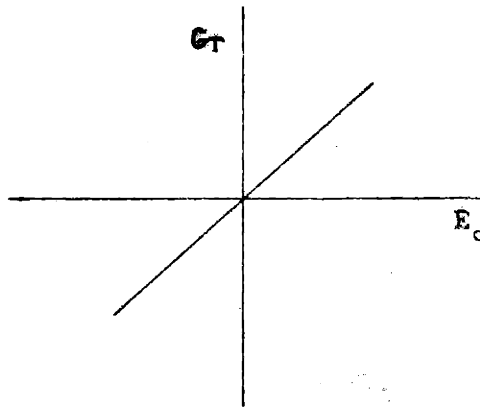


Fig 3

An exact agreement between the derived "perfect modulator" characteristics and an actual modulator will rarely be found. Although it may be possible to approach these characteristics, most applications of modulator circuits will be found suitable if the agreement is held over a part of the characteristic curve.

E - I CHARACTERISTICS OF A PERFECT MODULATOR.

In most modulator designs it is found that the carrier

voltage is from ten to one hundred times as large as the applied signal voltage at the input to the modulator. This is done for obvious reasons. It is desired to cause the transconductance of the modulator to vary at the carrier frequency and at the direct control of the instantaneous carrier voltage as shown in equation (4). The modulator element is under the control of all voltages impressed upon it and thus the signal voltage must be very small if it is to have a negligible control over the transconductance. From this discussion it is seen that the instantaneous carrier voltage determines the operating point on the characteristic and the signal voltage causes minute variations of the transconductance in the immediate vicinity of that point. The transconductance determination of equation 4. may be re-written,

$$G'_T = \frac{di}{de} = Ke \quad ; \quad i = \frac{Ke^2}{2} \quad (5)$$

with the subscripts removed since the slope in question is the slope at the operating point determined by the carrier.

Integration of equation (5) shows that the E - I characteristics for the perfect modulator are as shown in figure 6.

SOLUTION WHEN THE TRANSCONDUCTANCE IS A LINEAR FUNCTION OF THE CARRIER VOLTAGE BUT DISPLACED FROM THE ORIGIN.

In most modulator circuits using grid control of vacuum

tubes in balanced modulator circuits, the transconductance of the system varies in a manner similar to that shown in figure 4. When the modulator voltage varies between the limits shown, the transconductance varies between limits g_{t_a} and g_{t_b} as shown. As the carrier varies sinusoidally, the transconductance varies in a manner given by,

$$G_T = g_0 + (g_b - g_a) \sin ct \quad (6)$$

and since

$$i_2 = e, G_T = [E, \cos vt] [g_0 + (g_b - g_a) \sin ct]$$

then

$$i_2 = g_0 E, \cos vt + \frac{E(g_b - g_a)}{2} \left[\sin(c+v)t + \sin(c-v)t \right] \quad (7)$$

From equation (7) it is seen that even though the lower limit of the carrier swing may cause the transconductance to approach zero, the original signal will appear in the output

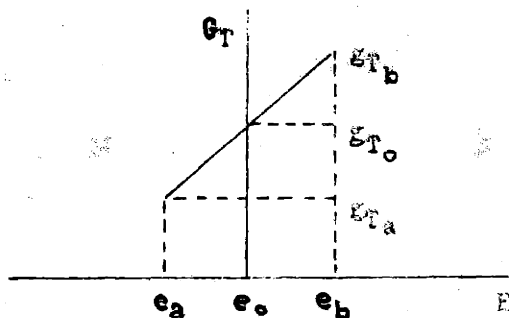


Fig. 4

of the modulator and will be directly proportional to the average value of the transconductance. The carrier voltage

may be suppressed in the modulator circuit but the appearance of the original signal in the output may be undesirable. Figure 5 indicates the appearance of the modulated signal in the output of a modulator having the characteristics described here.

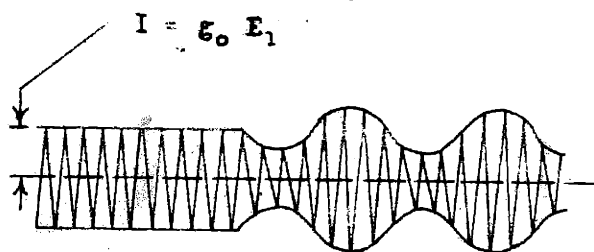


Fig. 5

COMPARITIVE QUALITIES OF THE PERFECT AND ONE FORM OF IMPERFECT MODULATOR

Equation (5) indicates that a modulator element whose $E - I$ characteristics obey a square law will result in perfect modulation. From the form of the equation and from an examination of figure 6 it is seen that the differential resistance of the modulating element of a perfect modulator is nonlinear. Although it was shown that such a device would produced the desired modulated signal, some assumptions were made that are not entirely justifiable under ordinary operating

conditions. One assumption that was made was that the voice frequency signal at the input to the modulator was small enough to have negligible effect on the transconductance of the modulator. This assumption is not met rigorously in

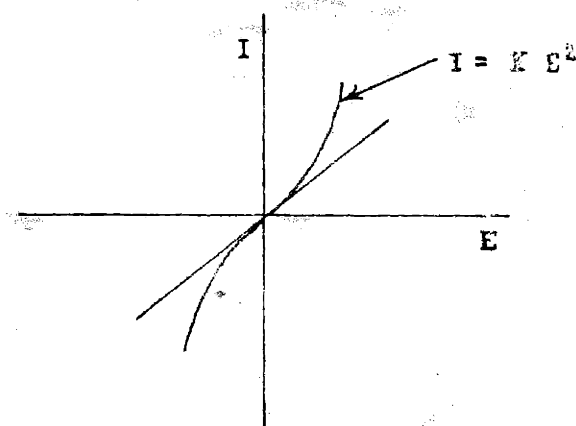


Fig. 6.

practice and the resulting changes in signal variations indicate that the actual transconductance of the modulator is not as simple as has been indicated. Although the changes in transconductance caused by the amplitude of the input signal show a difference between theory and practice, this difference is even more marked if examined in a different manner. Thus, assuming that the modulator characteristics are as shown in figure 6 (square-law curve), it is seen that the variations caused by the voice frequency or input signal will take place around the operation point determined by the instantaneous carrier voltage and these variations, no matter how small, will

take place along a non-linear portion of the curve. The application of this voltage will result in the production of harmonics of the input signal which can not necessarily be balanced to prevent their appearance in the output of the modulator.

Thus, although the square-law modulator will provide a reasonably "pure" modulation as far as the higher harmonics of the output sidebands are concerned, the appearance of harmonics of the input signal may be a source of trouble.

If these difficulties are to be avoided, it may be desirable to use a type of modulator element whose characteristics are of the form shown by the straight-line curve of figure 6. The application of voltages of carrier and voice frequency will not cause distortion of the type mentioned above since the modulator unit is a linear although time-varying device. The expression for the transconductance of a device of this form is,

$$g(t) = \frac{4}{\pi} g (\sin ct + \frac{1}{3} \sin 3ct + \frac{1}{5} \sin 5ct \dots) \quad (8)$$

and the resulting output current of such a modulator is,

$$i_2 = g(t) e_1 = \frac{2gE_1}{\pi} \left[\cos(c+v)t - \cos(c-v)t + \right. \\ \left. + \frac{1}{3} \cos(3c+v)t - \frac{1}{3} \cos(3c-v)t + \right. \\ \left. + \frac{1}{5} \cos(5c+v)t - \frac{1}{5} \cos(5c-v)t \right. \\ \left. + \dots \dots \dots \right] \quad (9)$$

The preceding sections of this appendix shows the basic analysis of the most desirable form of modulator element. For a discussion of the circuits by which the various results pictured there may be obtained, it is best to consider circuit elements which have a constant value of pure resistance to one polarity of applied carrier voltage and an infinite resistance to carrier voltage of opposite polarity - - these values to be held independent of the magnitude of the applied carrier signal. Such a circuit element is closely approximated by most diode rectifier units when biased properly.

THE DOUBLE BALANCED OR "RING BRIDGE" MODULATOR.

The circuit of a typical double balanced modulator is shown in figure 7. The input and output impedances shown may be pure resistances or any arbitrary networks which maintain the circuit in a state of balance. For the sake of simplicity it is best to consider these units to be inductances of negligible resistance and leakage. Thus the carrier currents flowing in these terminations will experience no voltage drops and the carrier voltages may be considered to appear directly across the diodes. Similarly, the signal input and output voltages will appear across the total terminations but will cause a negligible current to flow in the terminations.

During the interval of one half of the carrier cycle

the two lateral diodes will be biased in such a direction that they will be conducting, i.e., they will have assumed a resistance value previously specified.

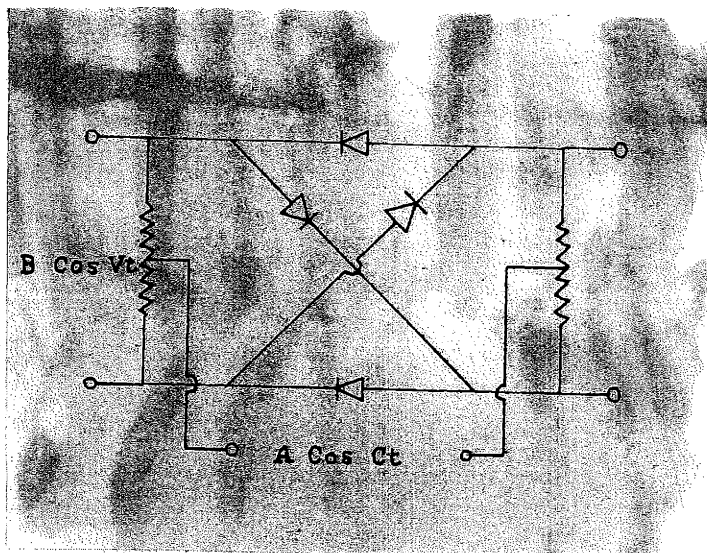


Fig. 7.

The input signal will thus appear across the output terminals and will vary in a positive sense exactly as they appear in the input. During the next half cycle, these two diodes will be non-conducting or will have assumed an infinite resistance value. Now, however, the two cross-over diodes will have become conducting or will have assumed their low values of resistance and the input signal will appear at the output in a negative or reversed sense. The variations in output voltage will thus be in exact accordance with the variations in input voltage but the transconductance will have assumed a negative value.

Due to the "cross-over" or commutation process, this type of modulator is sometimes referred to in the literature as a "commutator modulator".

The appearance of the output signal is indicated in figure 8. Due to the symmetrical form of both the signal envelope and the carrier signal appearing in this diagram it is quite evident that these signals will not appear in the output signal.

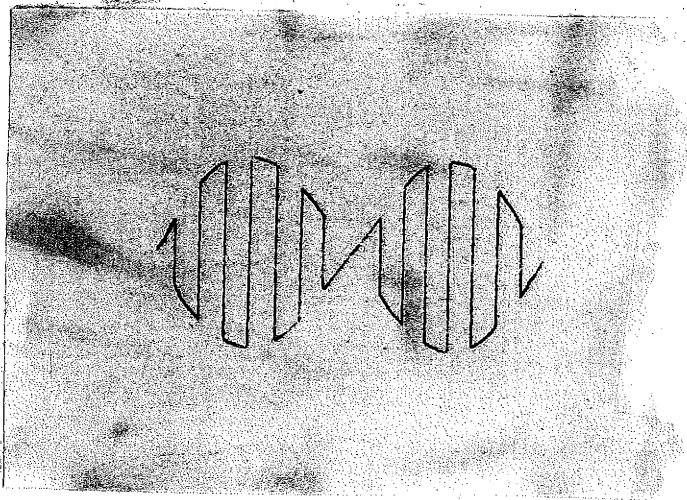


Fig. 8.

For a rigorous proof that the output does not contain signals of the original voice or carrier frequencies, reference should be made to figure 6. The straight line function in this diagram is an exact picture of the E - I characteristics of the double balanced modulator. The positive values of G_t or the first quadrant of the diagram indicate conduction by the two transverse diodes and the negative values of G_t or the third quadrant of the figure indicates conduction by

the two "cross-over" diodes.

THE "SINGLE BALANCED" MODULATOR.

The arrangement of diodes in a modulator of the single balanced type is indicated in figure 9. To simplify the description of the operation of this modulator, it would be well to consider the diodes as having a constant resistance during one half of a carrier cycle and an extremely high value of resistance during the other half of a cycle.

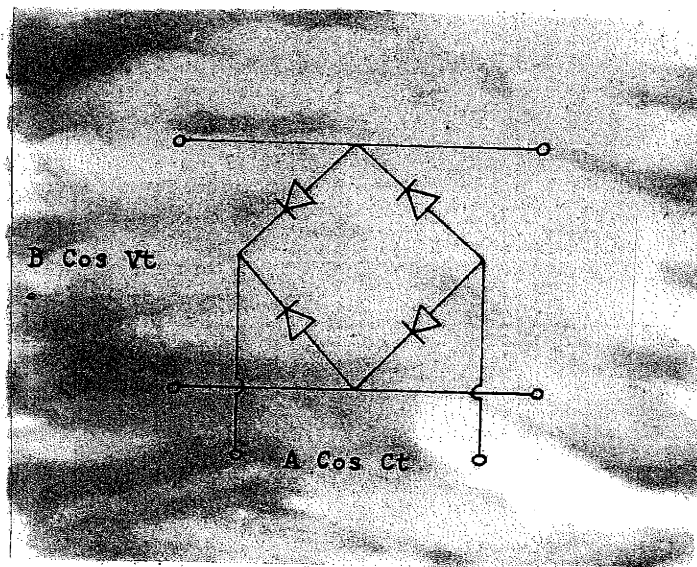


Fig. 9.

In this type of modulator circuit it is customary to use terminating equipment of very high impedance values. Then, during the half cycle when all diodes are conducting there will be an apparent low resistance or short circuit relative to the terminating impedances across the signal circuits. during the other half cycle, none of the diodes will be conducting and the output signal will be an exact replica

of the input signal.

The resulting output voltage function will be of the form shown in figure 10 except that this figure was drawn for the case of a zero resistance shunt or direct short through the diodes during the half cycle when they are conducting.

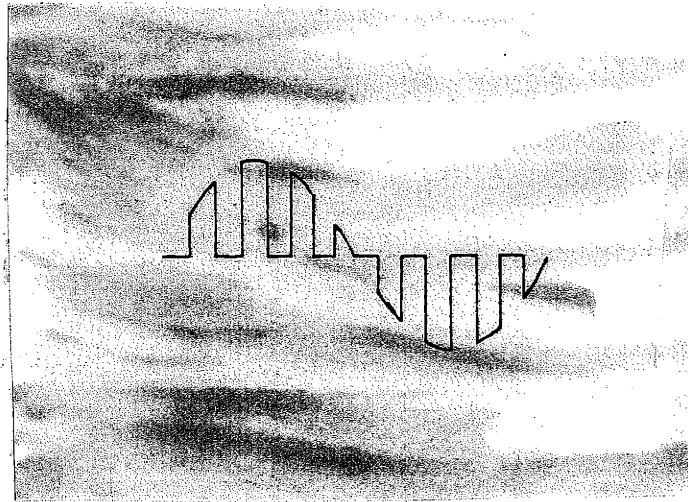


Fig. 10

This type of modulator circuit is somewhat similar to the modulator of figure 4 except that the conductance function of the single balanced modulator as analyzed here is assumed to be a step function rather than a linear sloping function of the carrier voltage. The discussion of the modulator of figure 4 applies to the present case in that the original voice frequency signal will appear in the output of the modulator. This is also quite apparent from figure 10. The balancing effect of the four diodes to changes in the instantaneous values of carrier voltages

prevents the appearance of the carrier signal in the output.

THE PROBLEM OF IMPEDANCE MATCHING.

An interesting simplification of the problem of impedance matching to modulators of the diode type has been advanced by Sigurd Kruse¹ in Ericsson Technics. The assumptions made by Mr. Kruse are that the transfer conductance of the individual elements in the modulator have a constant and relatively high value during one half of the carrier cycle and a constant and relatively low value during the other half cycle.

With these assumptions he also assumes that applying direct current as a carrier source will not change the problem. By means of this artifice, the rules of ordinary network theory may be applied to the modulator and it is found that the image impedance of the modulator is,

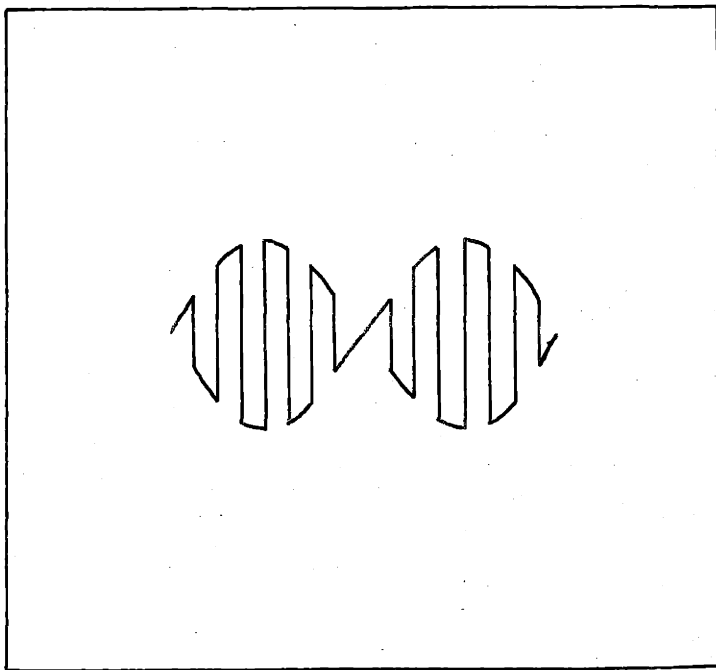
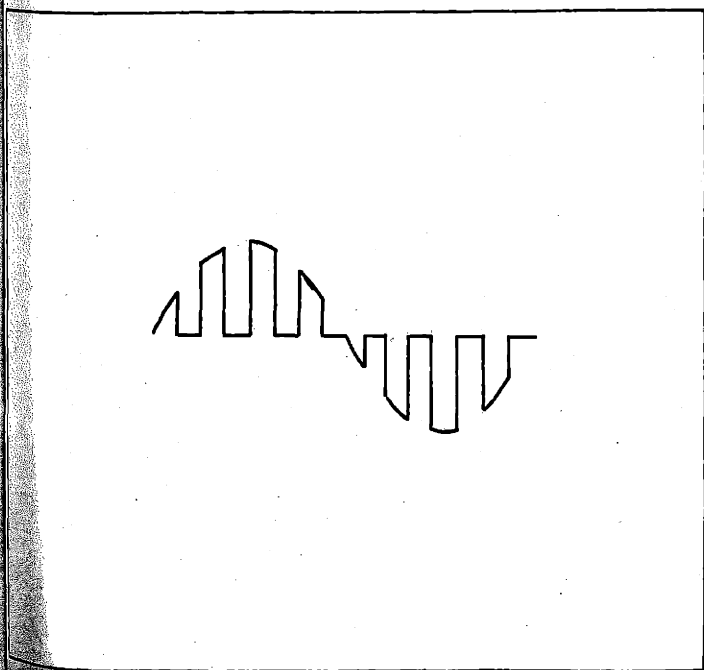
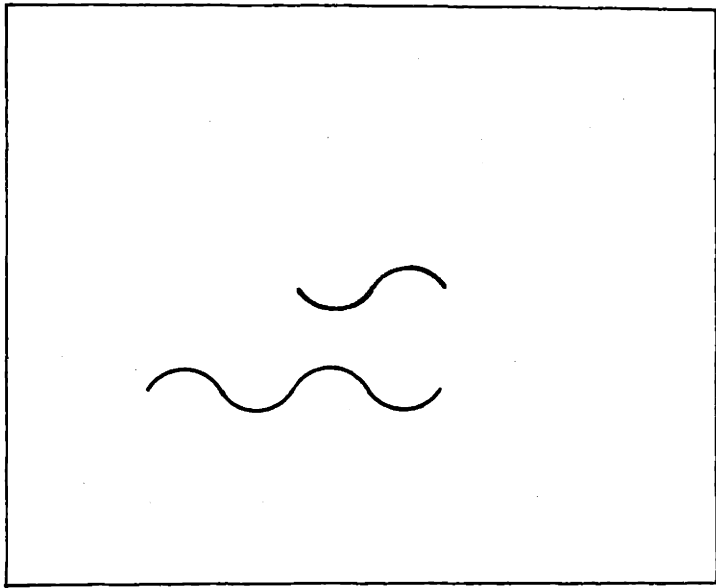
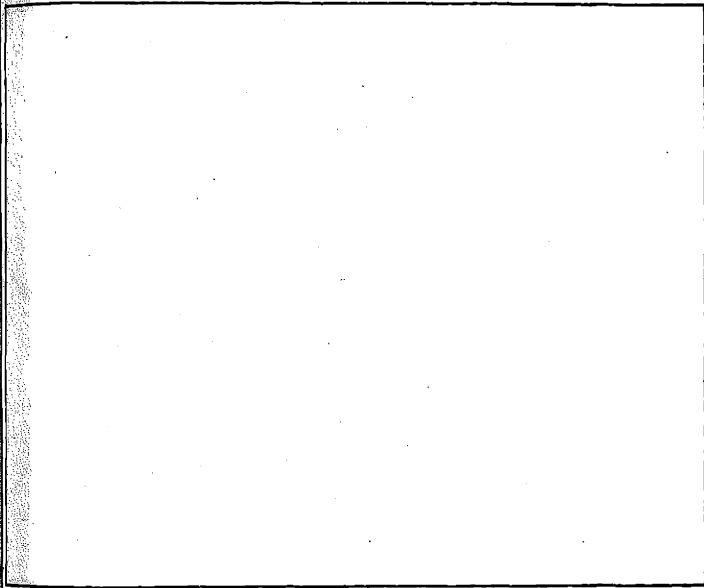
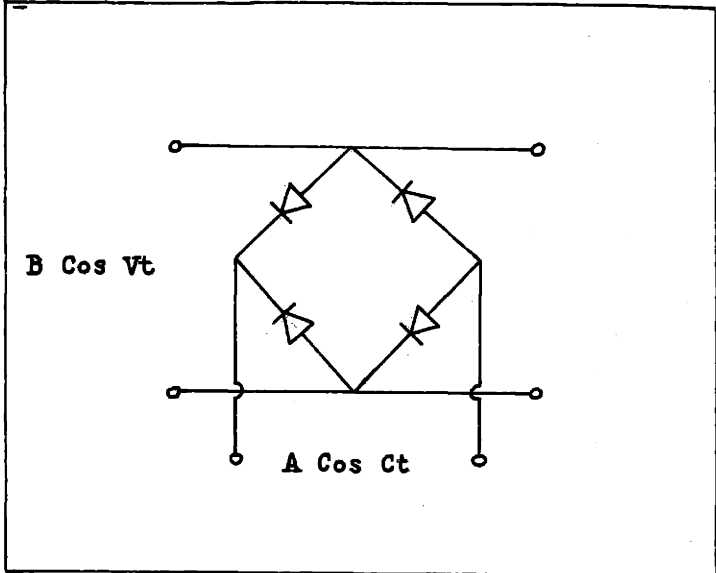
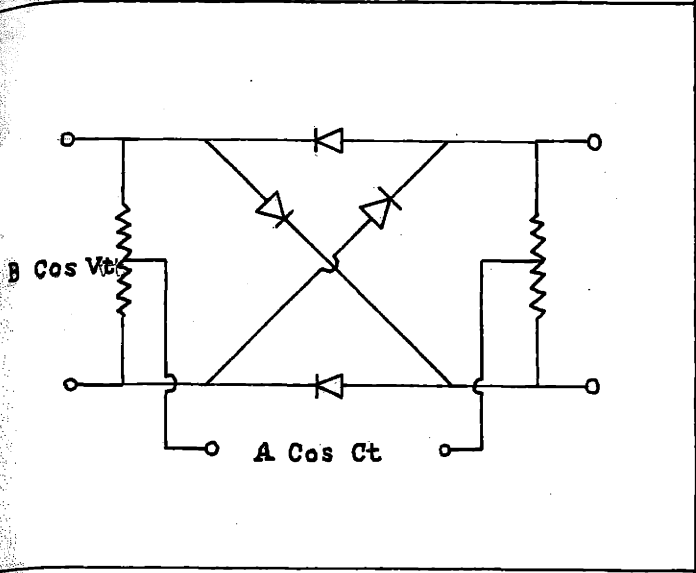
$$Z = \frac{1}{\sqrt{g_1 g_2}} \quad (10)$$

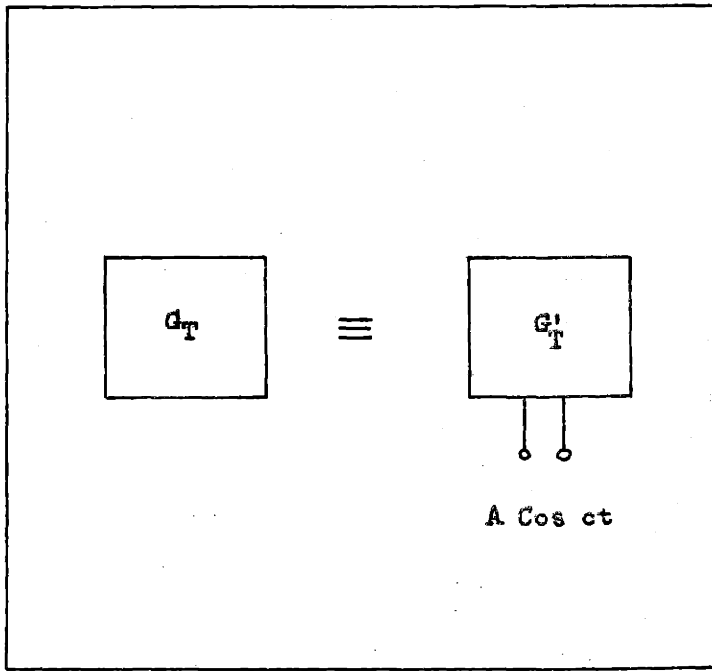
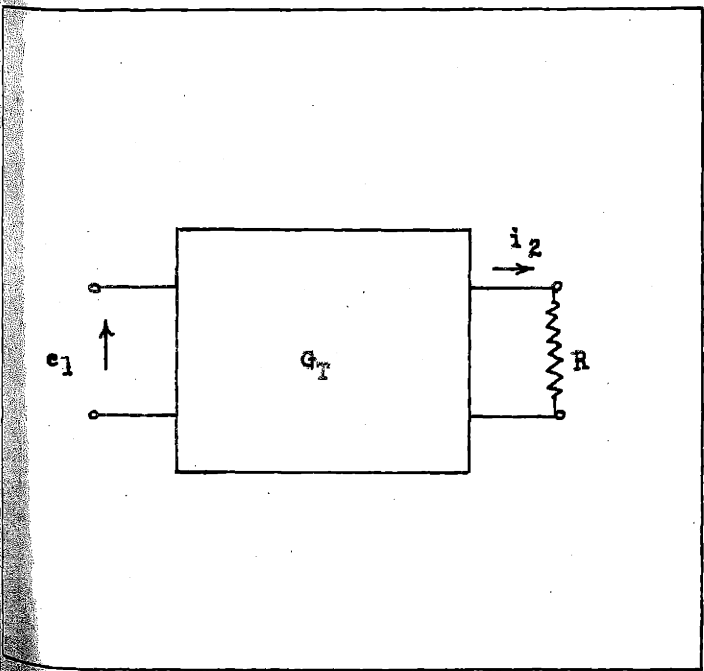
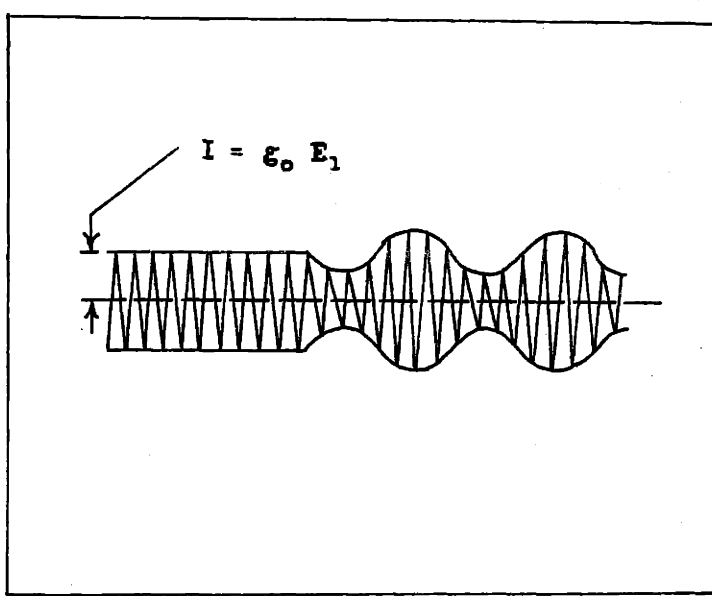
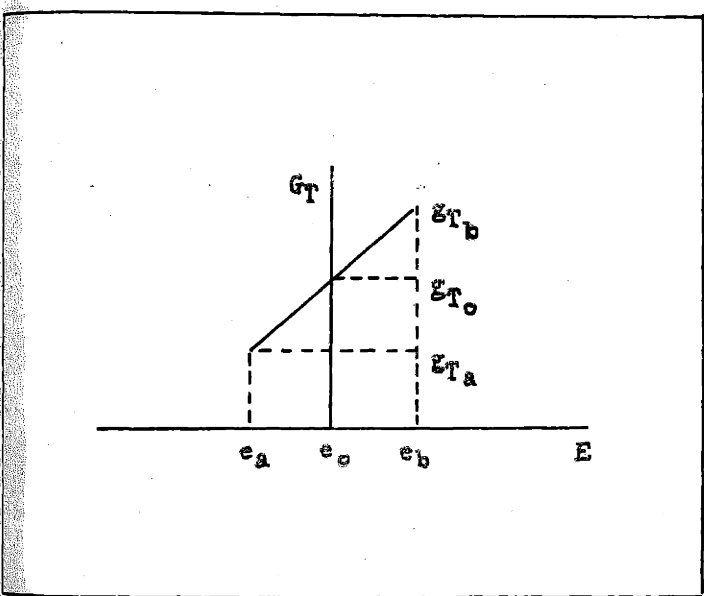
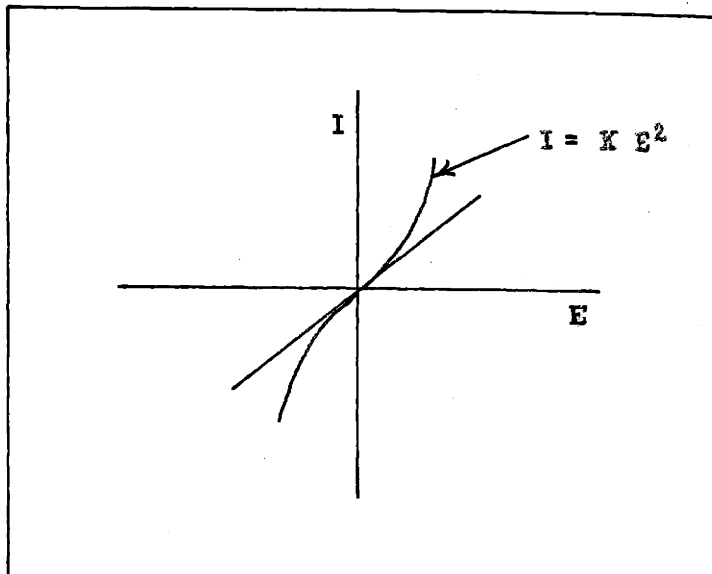
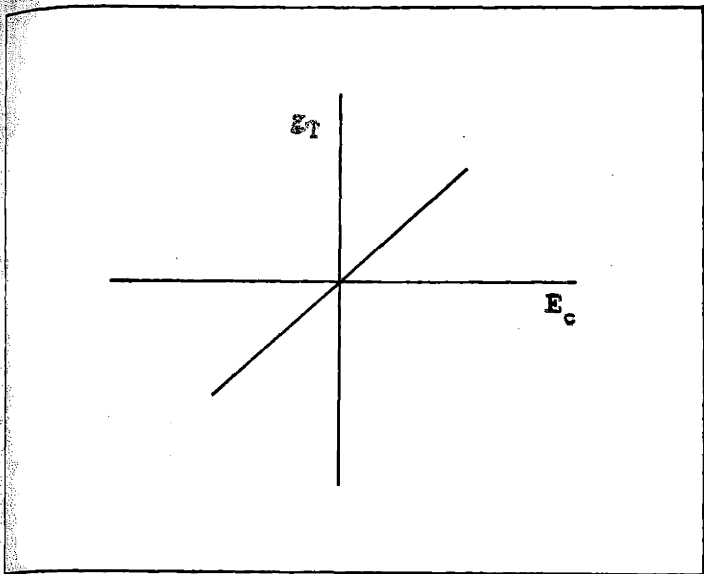
and the image attenuation of the modulator is,

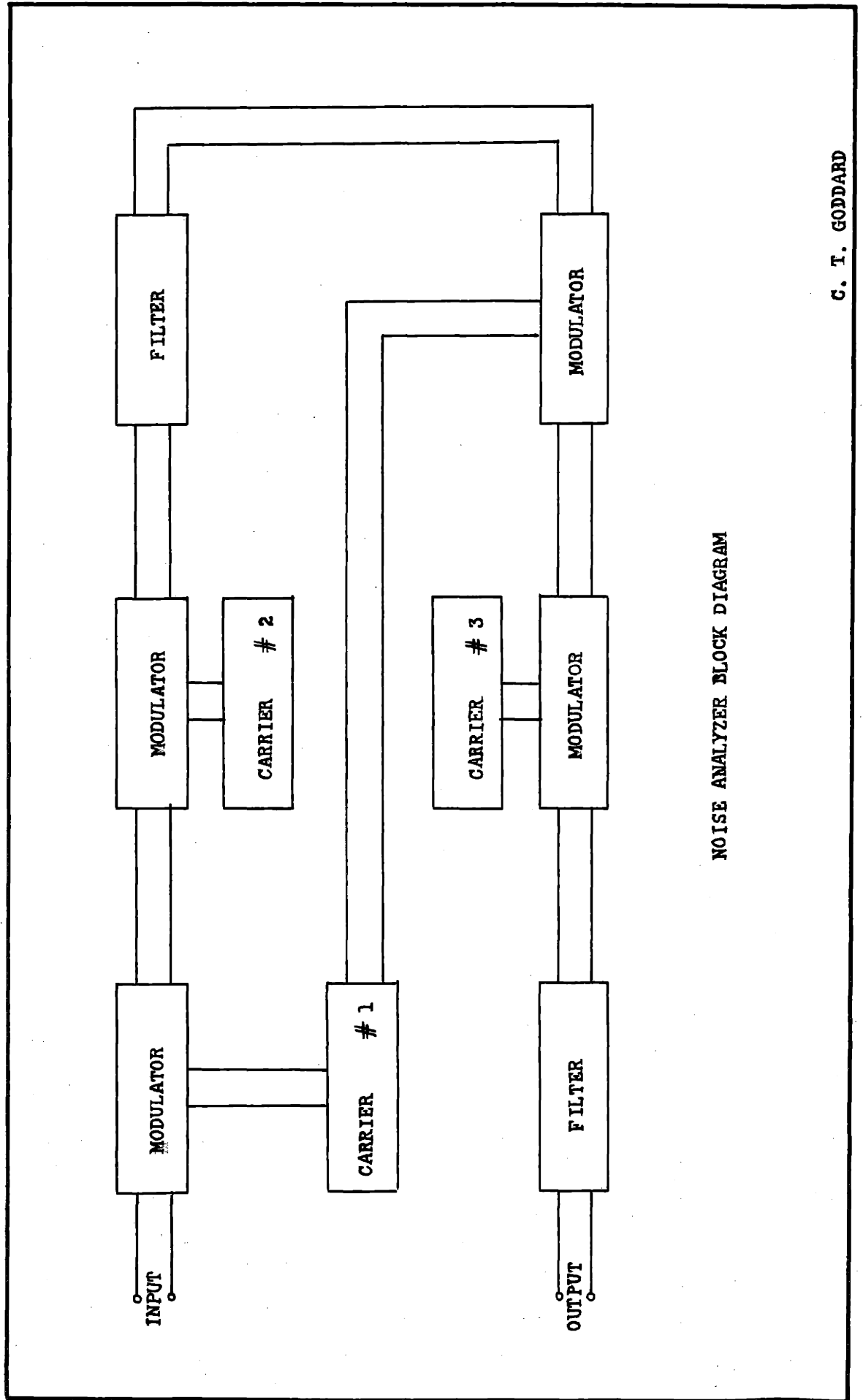
$$\tanh \frac{\beta}{2} = \sqrt{\frac{g_2}{g_1}} \quad (11)$$

Since the ratio of g_2 to g_1 is usually of the order of 10^{-4} it is seen that the attenuation is a small fraction of a decibel.

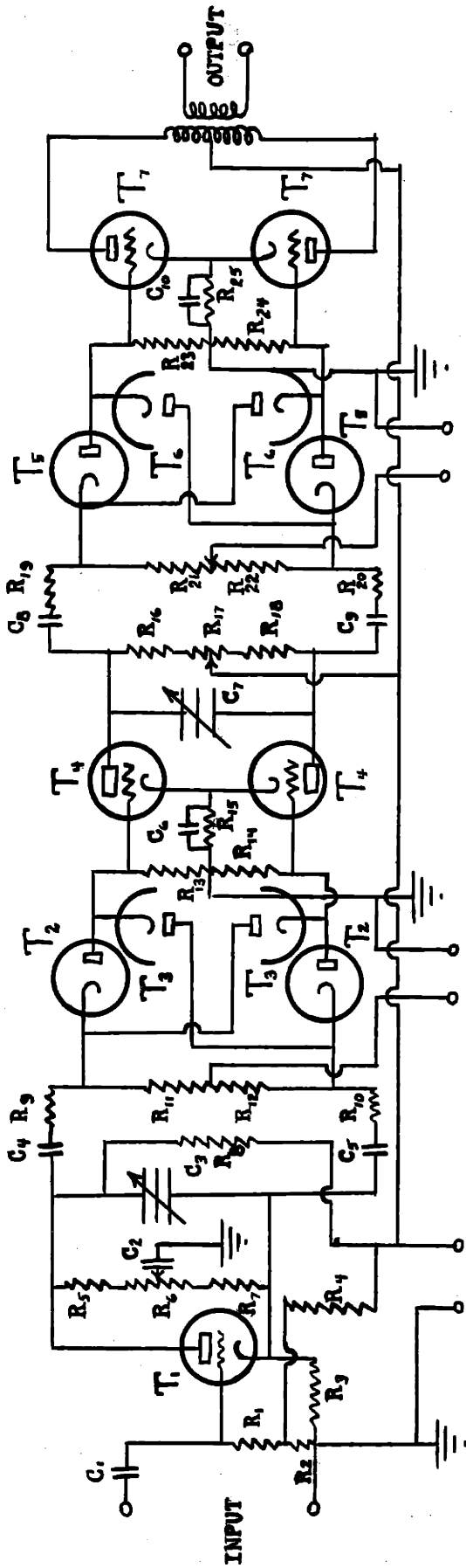
1. See Bibliography.







NOISE ANALYZER BLOCK DIAGRAM



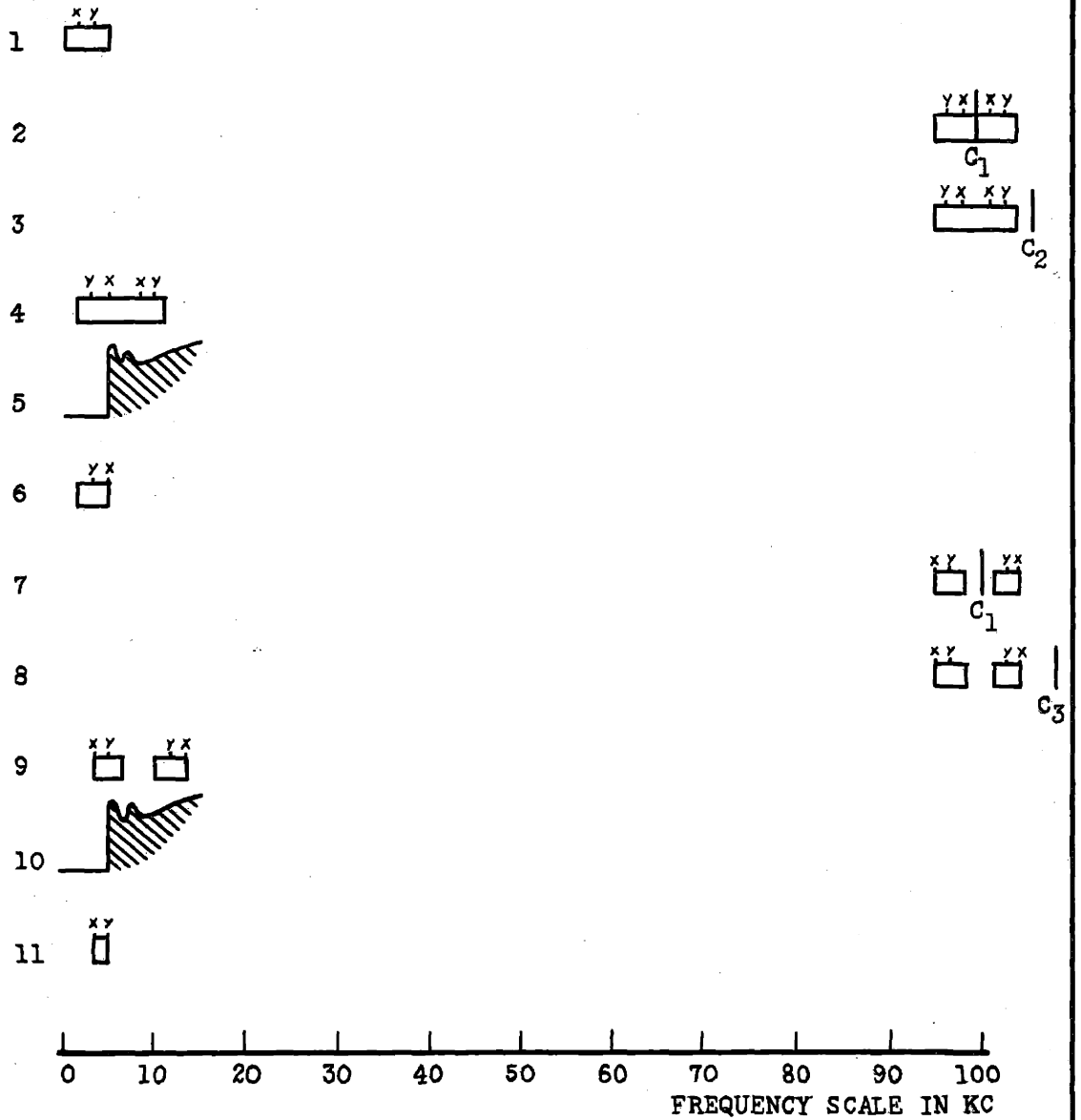
CARRIER # 2

CARRIER # 1

250 volts

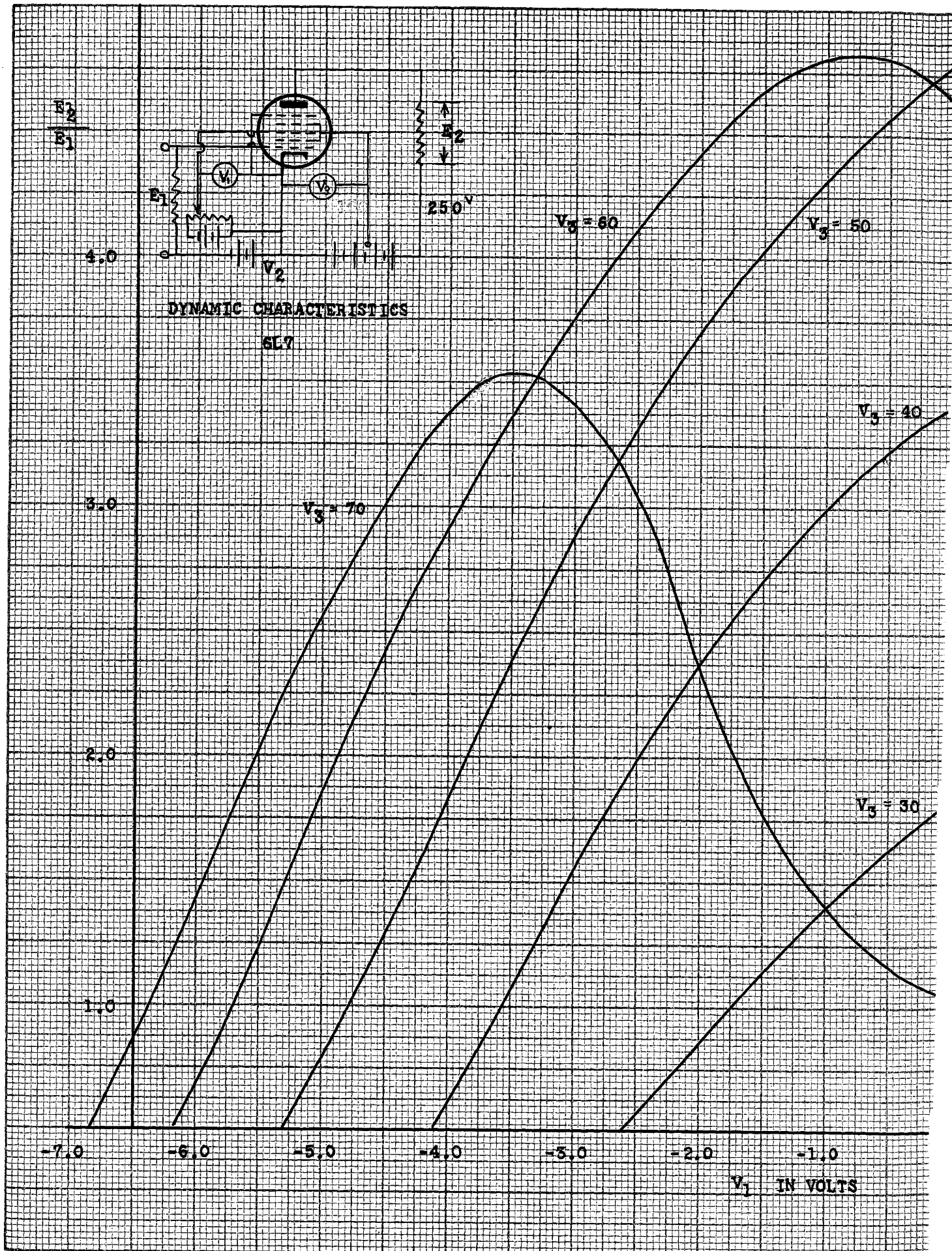
FINAL FORM OF DOUBLE BALANCED MODULATORS

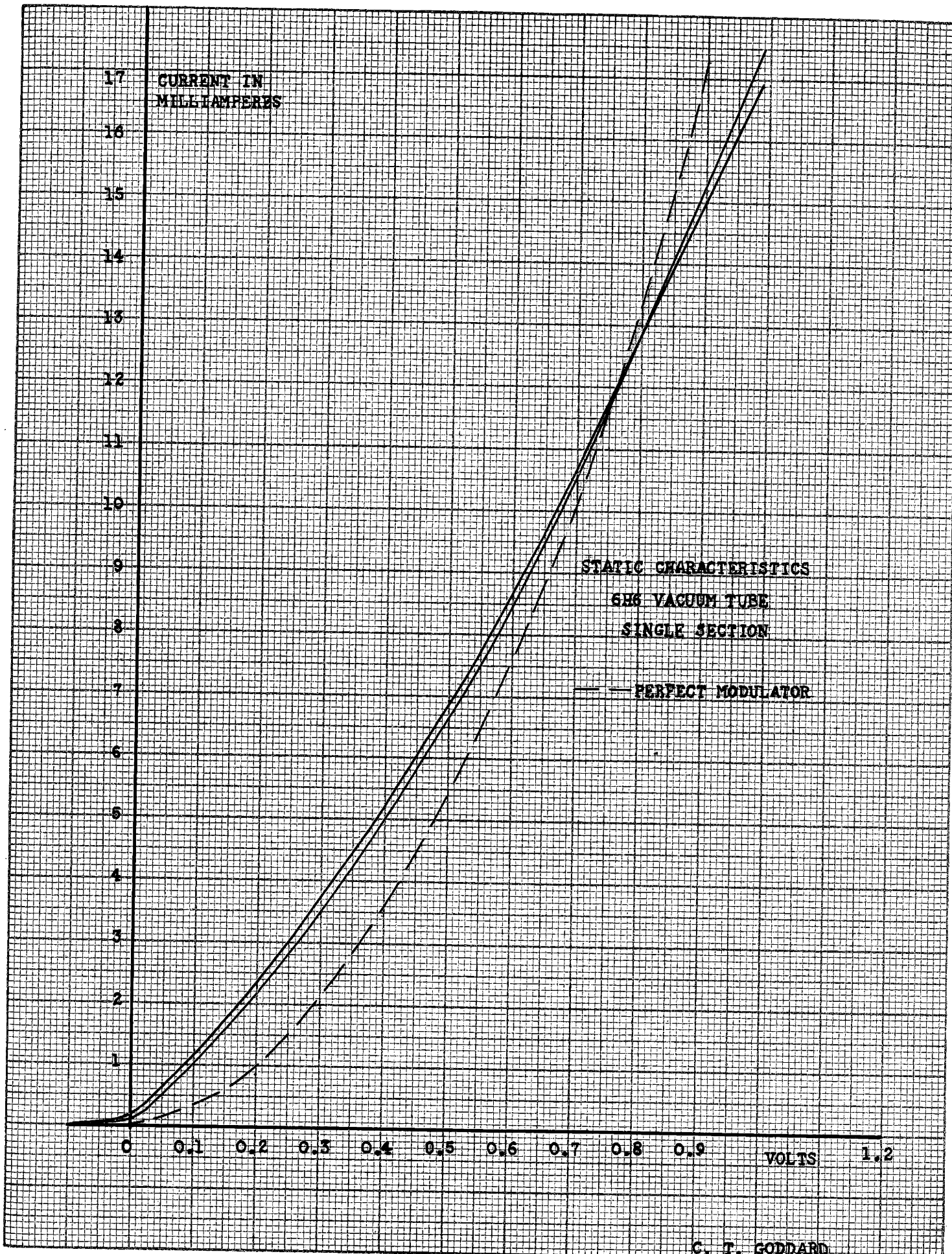
C. T. GODDARD

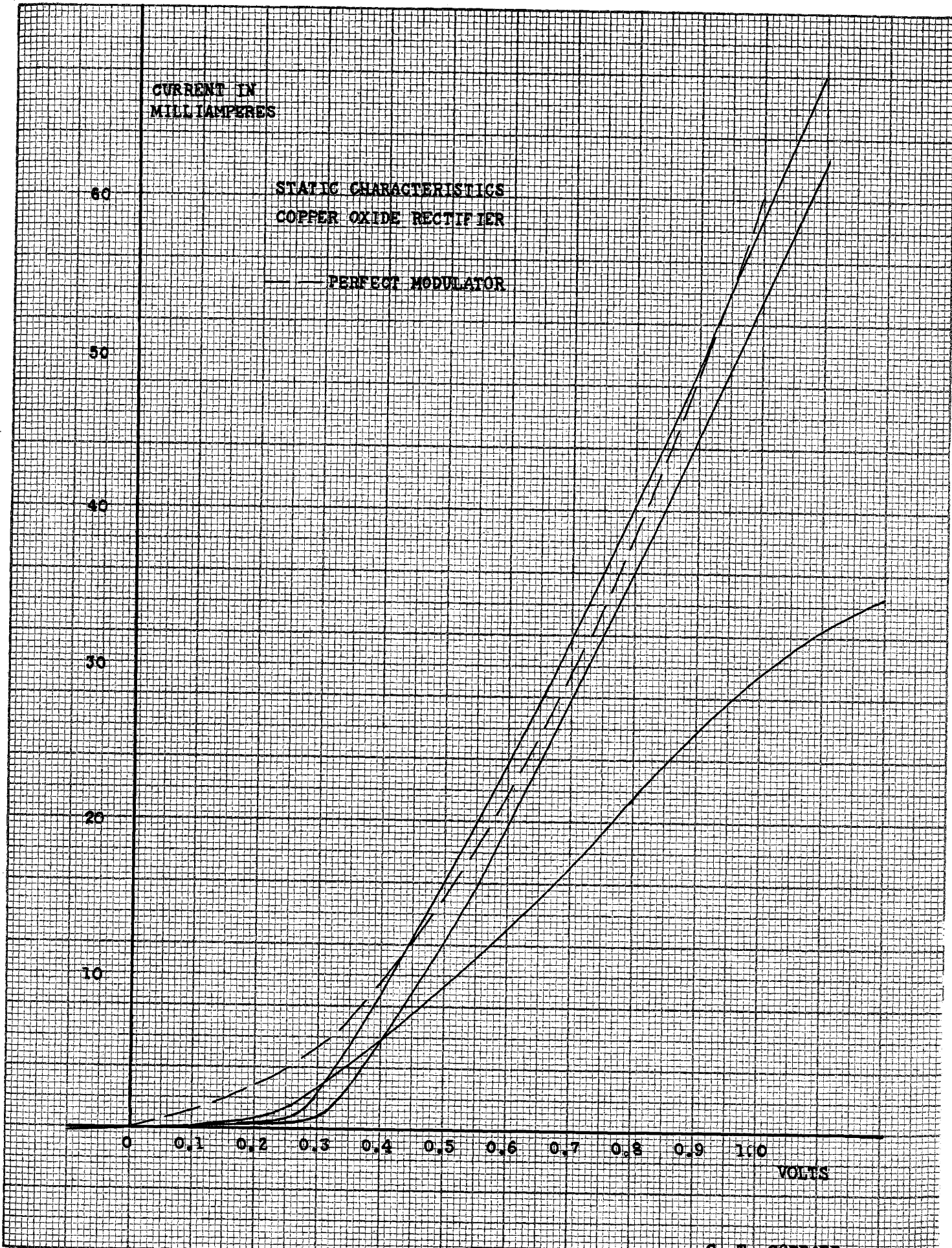


OPERATION OF NOISE ANALYZER

- C_1 Fixed 100 kc carrier
- C_2 Variable carrier
- C_3 Variable carrier







CURRENT IN
MILLIAMPERES

STATIC CHARACTERISTICS
COPPER OXIDE RECTIFIER

— PERFECT MODULATOR

60

50

40

30

20

10

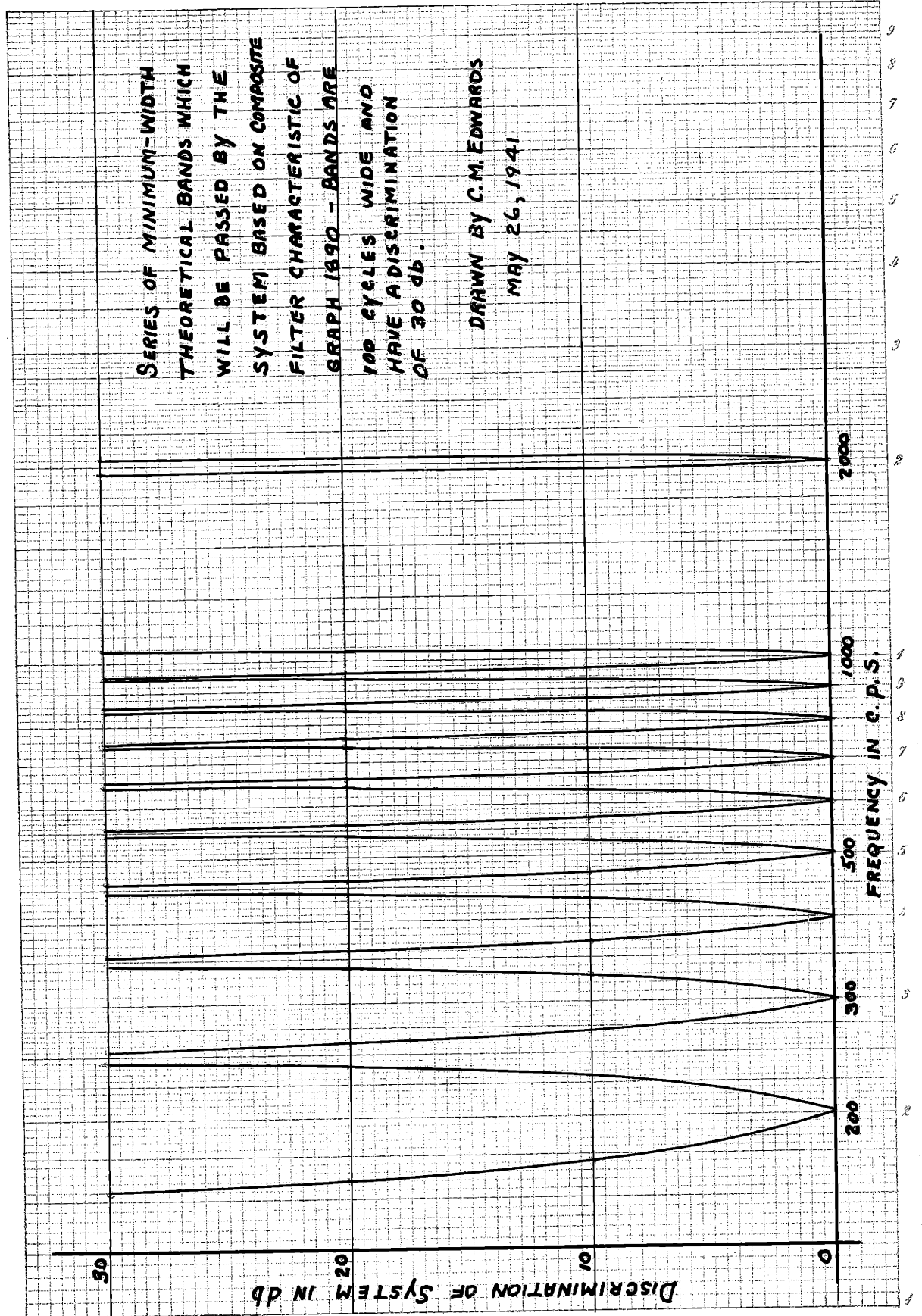
0 0.1 0.2 0.3 0.4 0.5 0.6 0.7 0.8 0.9 1.0

VOLTS

CHAPTER VI
RESULTS FROM THE SYSTEM

Effectively, the modulation processes as described in Chapter II serve the purpose of placing the frequency spectrums at the proper positions for cut-off by the two low-pass filters. Although no actual results were secured to show how the system will perform, from the characteristics of the sharp-cut-off filter, predictions can be made as to what results may be obtained by using two such filters--the modulation processes should have no effect on the attenuation characteristics of the bands passed.

From graph 1890 it may be predicted that on the basis of a discrimination of 30 db. bands as narrow as 100 cycles may be passed by the system. Such a series of pass-bands is shown on graph . Of course, any number of such graphs could be drawn to show other bands passed by the system between 0 and 5,000 cycles. For all bands wider than 100 cycles there will be better discrimination. However, the maximum possible is 44 db.



SERIES OF MINIMUM-WIDTH
THEORETICAL BANDS WHICH
WILL BE PASSED BY THE
SYSTEM BASED ON COMPOSITE
FILTER CHARACTERISTIC OF
GRAPH 1890 - BANDS ARE
100 CYCLES WIDE AND
HAVE DISCRIMINATION
OF 30 db.

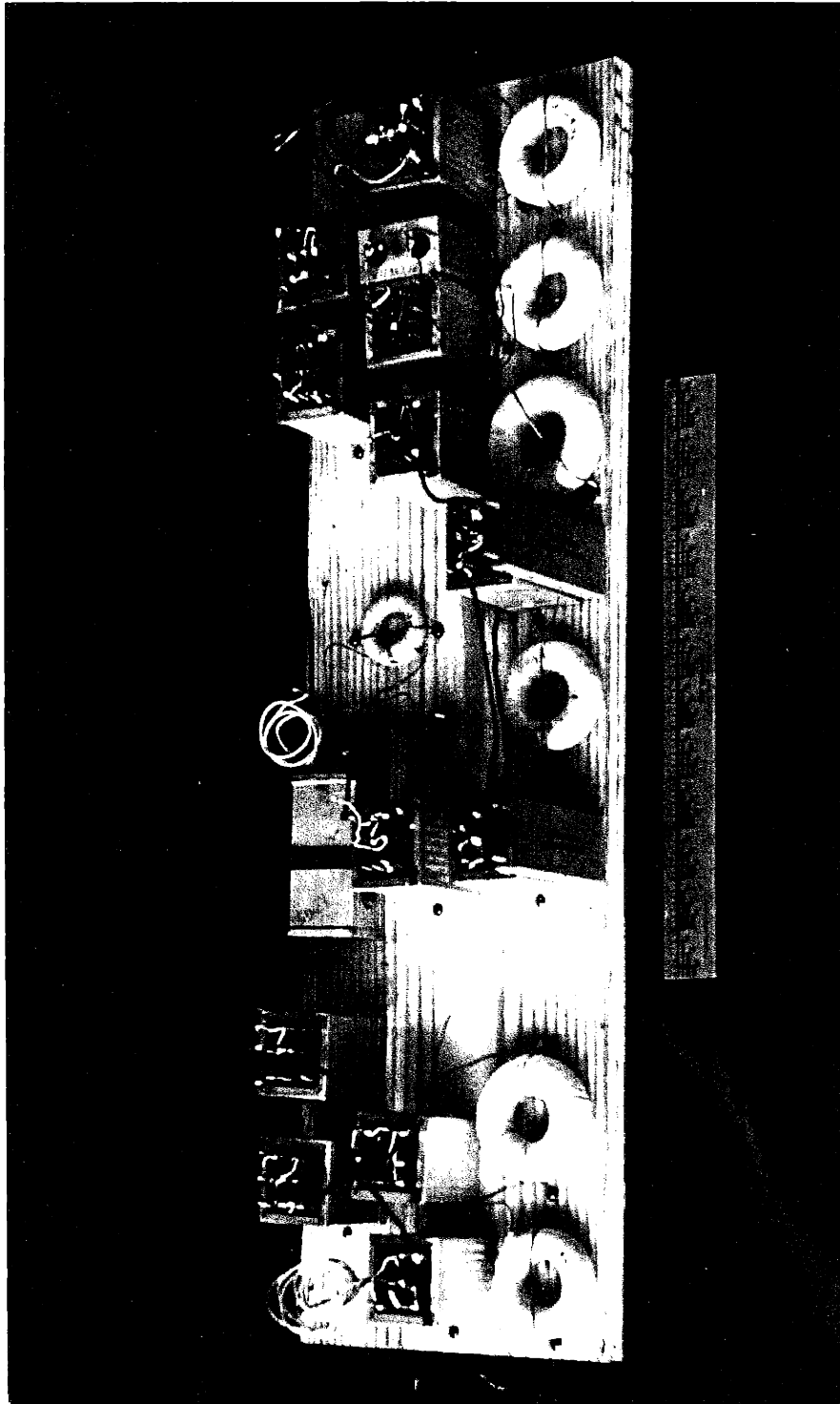
DRAWN BY C.M. EDWARDS
MAY 26, 1941

CHAPTER VII

CONCLUSIONS

There is little doubt in the authors' minds that the system announced here is practicable for a noise analyzer. As shown on graph good selectivity characteristics can be obtained for frequencies of 200 to 5,000 cycles. However, to make such a system effective over the entire audio range--i.e., 00 to 10,000 cycles--two sets of low-pass filters should be built. Off hand, it is suggested that cut-off frequencies of 1000 and 10,000 cycles be used. Provided the two sets of filters had the same percentage rate of cut-off, the 10,000 cycle set would give the same selectivity at 1000 cycles that the 1000 cycle set would give at 100 cycles.

As a suggestion for improving the cut-off rate of the filter designed here, an attempt might be made to use higher "Q" coils in the complex-m section. From graph 1886 it is evident that the rate of cut-off/^{of}a complex-m section improves directly as the "Q" of the coils is increased. At the same time it should be pointed out that as the cut-off rate is improved the attenuation beyond cut-off falls off proportionately more rapidly. Thus a higher rate of cut-off in the complex-m section would probably require the addition of another m-derived section between cut-off and/^{the}terminal sections' peak.



Photograph of Composite Filter on Bread-board

Bibliography

M.I.T. Theses

1. Baryshanski and Burtner, "An Investigation of the Properties of Certain Double-M-Derived Low-Pass Filters"; E. E. Thesis 1931.
2. William F. Burrall, "Investigation of the Use of a Positive Feedback-Network, such as a Regenerative Circuit, as a Band-Pass Filter, the Width of Band Passed to be Adjustable at Will"; E. E. Thesis 1938.
3. Gilman, "Characteristics and Design Formula of Several Lattice Type Wave Filters", E. E. Thesis 1937.
4. L. P. Reitz, Jr., "A Variable Band-Pass Audio Power Level Meter"; E. E. Thesis 1940.

Periodicals

1. "Extentions to the Theory and Design of Electric Wave-Filters", Otto J. Zobel; B.S.T. Journal, Vol. X, April, 1931; pp 284-341.
2. "The Role of Acoustical Measurements in Machinery Quieting", Ernest J. Abbott; J. Acoustical Soc. of America, Vol. 8, No. 2, October, 1936; pp 133 - 142.
3. "A Portable Frequency Analyzer", M. S. Mead and T. M. Berry, General Electric Review, Vol. 37, No. 8, August, 1934; pp 378 - 383.
4. "Compressed Powered Permalloy Manufacture and Magnetic Properties", W. J. Shackelton and I. G. Barber; A.I.E.E. Transactions, Vol. 47, No. 2; April, 1928.

Books

1. A. Campbell and E. C. Childs, The Measurement of Inductance, Capacitance and Frequency; New York, 1935.
2. E. A. Guillemin, Communication Networks, Volume II; New York, 1935.
3. T. E. Shea, Transmission Networks and Wave Filters, New York, 1938.

APPENDIX B

EFFECT OF DISSIPATION ON THE PROPAGATION
FUNCTION OF CONSTANT-K TYPE FILTERS

FROM NOTES BY PROFESSOR E. A. GUILLEMIN

(FOR INTRODUCTION SEE GUILLEMIN'S COMMUNICATION
NETWORKS, VOL. 2; PAGE 445)

LET: γ - BE THE NON-DISSIPATIVE FUNCTION

γ^* - BE THE DISSIPATIVE FUNCTION

$$\gamma = (\alpha + j\beta) \quad \text{WHERE: } \alpha = \frac{R}{2L}; \beta = \frac{G}{2C}$$

$$\text{THEN: } \gamma^* = \gamma - j \left(\frac{d\gamma}{d\omega} \right) \gamma - \frac{1}{2} \left(\frac{d^2\gamma}{d\omega^2} \right) \gamma^2 + \frac{j}{6} \left(\frac{d^3\gamma}{d\omega^3} \right) \gamma^3 + \dots$$

THIS EXPRESSION IS BASED ON THE APPROXIMATION:

$$\frac{1}{2} \left(\frac{R}{2L\omega} - \frac{G}{2C\omega} \right) \ll 1$$

IN THE TRANSMISSION RANGE:

$$\gamma = 0 + j\gamma_2$$

$$\gamma^* = j\gamma_2 + \left(\frac{d\gamma_2}{d\omega} \right) \gamma - \frac{j}{2} \left(\frac{d^2\gamma_2}{d\omega^2} \right) \gamma^2 - \frac{1}{6} \left(\frac{d^3\gamma_2}{d\omega^3} \right) \gamma^3 + \dots$$

THEREFORE -

$$\text{ATTENUATION FUNCTION, } \gamma_1^* = \left(\frac{d\gamma_2}{d\omega} \right) \gamma - \frac{1}{6} \left(\frac{d^3\gamma_2}{d\omega^3} \right) \gamma^3 + \dots$$

$$\text{PHASE FUNCTION, } \delta_2^* = \delta_2 - \frac{1}{2} \left(\frac{d^2 \delta_2}{d\omega^2} \right) \delta^2 + \dots$$

IN ATTENUATION RANGE : (EXCEPT IN VICINITY OF ω_∞ 's)

$$\delta = \delta_1 + j k \pi ; \text{ SO THAT,}$$

$$\delta^* = \delta_1 + j k \pi - j \left(\frac{d\delta_1}{d\omega} \right) \delta - \frac{1}{2} \left(\frac{d^2 \delta_1}{d\omega^2} \right) \delta^2 + \dots$$

OR —

$$\begin{cases} \delta_1^* = \delta_1 - \frac{1}{2} \left(\frac{d^2 \delta_1}{d\omega^2} \right) \delta^2 + \dots \\ \delta^* = k\pi - \left(\frac{d\delta_1}{d\omega} \right) \delta + \frac{1}{6} \left(\frac{d^3 \delta_1}{d\omega^3} \right) \delta^3 + \dots \end{cases}$$

$$\text{SINCE — } \delta = \ln \left(\frac{\gamma+1}{\gamma-1} \right) ; \quad \frac{d\delta}{d\omega} = \frac{2}{(1-\gamma^2)} \cdot \frac{d\gamma}{d\omega}$$

$$\frac{d^2 \delta}{d\omega^2} = \frac{2}{(1-\gamma^2)} \left\{ \frac{d^2 \gamma}{d\omega^2} + \frac{2\gamma}{(1-\gamma^2)} \left(\frac{d\gamma}{d\omega} \right)^2 \right\}$$

$$\text{WHERE: } \gamma = \frac{\sqrt{\omega^2 - \omega_c^2}}{\omega}$$

$$\text{THEN — } \frac{d\delta}{d\omega} = \frac{2}{\sqrt{\omega^2 - \omega_c^2}} ; \quad \frac{d^2 \delta}{d\omega^2} = \frac{-2\omega}{(\omega^2 - \omega_c^2)^{3/2}}$$

$$\text{AND, } \delta^* = -j \frac{2(\alpha + \beta)}{\sqrt{\omega^2 - \omega_c^2}} + \delta + \frac{(\alpha + \beta)^2 \omega}{(\omega^2 - \omega_c^2)^{3/2}} + \dots$$

IN TRANSMISSION RANGE : $0 < \omega < \omega_c$

$$\begin{cases} \delta_1^* \approx \frac{2(\alpha + \beta)}{\sqrt{\omega_c^2 - \omega^2}} = \left(\frac{R}{L\omega_c} + \frac{G}{C\omega_c} \right) \cdot \left(1 - \frac{\omega^2}{\omega_c^2} \right)^{-1/2} \\ \delta_2^* \approx \delta_2 - \frac{(\alpha + \beta)^2 \omega}{(\omega_c^2 - \omega^2)^{3/2}} = \delta_2 - \frac{1}{4} \left(\frac{R}{L\omega_c} + \frac{G}{C\omega_c} \right)^2 \cdot \frac{\omega}{\omega_c} \cdot \left(1 - \frac{\omega^2}{\omega_c^2} \right)^{-3/2} \end{cases}$$

IN ATTENUATION RANGE : $w_1 < w < \infty$

$$\begin{cases} \gamma_1^* \approx \gamma_1 + \frac{(\alpha + \beta)^2 w}{(w^2 - w_1^2)^{3/2}} = \gamma_1 + \frac{1}{4} \left(\frac{R}{Lw_1} + \frac{G}{Cw_1} \right)^2 \cdot \frac{w}{w_1} \cdot \left(\frac{w^2}{w_1^2} - 1 \right)^{-3/2} \\ \gamma_2^* \approx \pi - \frac{2(\alpha + \beta)}{\sqrt{w^2 - w_1^2}} = \pi - \left(\frac{R}{Lw_1} + \frac{G}{Cw_1} \right) \cdot \left(\frac{w^2}{w_1^2} - 1 \right)^{-1/2} \end{cases}$$

M-DERIVED TYPE OF PROPAGATION FUNCTION

FOR M-DERIVED FILTERS : $y = h \frac{\sqrt{w^2 - w_1^2}}{w}$; $h = \frac{w_{\infty}}{\sqrt{w_{\infty}^2 - w_1^2}}$

THUS : $\frac{d\gamma}{dw} = \frac{2}{\sqrt{w^2 - w_1^2}} \times \frac{\sqrt{1 - \frac{w_1^2}{w_{\infty}^2}}}{\left(1 - \frac{w^2}{w_{\infty}^2}\right)}$

$$\frac{d^2\gamma}{dw^2} = \frac{-2w}{(w^2 - w_1^2)^{3/2}} \times \frac{\sqrt{1 - \frac{w_1^2}{w_{\infty}^2}} \left\{ 1 + 2\left(\frac{w_1}{w_{\infty}}\right)^2 - 3\left(\frac{w}{w_{\infty}}\right)^2 \right\}}{\left(1 - \frac{w^2}{w_{\infty}^2}\right)^2}$$

IN TRANSMISSION RANGE : $0 < w < w_1$

$$\begin{cases} \gamma_1^* \approx \frac{2(\alpha + \beta)}{\sqrt{w_1^2 - w^2}} \times \sqrt{1 - \frac{w_1^2}{w_{\infty}^2}} = \left(\frac{R}{Lw_1} + \frac{G}{Cw_1} \right) \times \frac{\sqrt{1 - \frac{w_1^2}{w_{\infty}^2}}}{\sqrt{1 - \frac{w^2}{w_1^2}} \left(1 - \frac{w^2}{w_{\infty}^2}\right)} \\ \gamma_2^* \approx \gamma_2 - \frac{(\alpha + \beta)^2 w}{(w_1^2 - w^2)^{3/2}} \times \frac{\sqrt{1 - \frac{w_1^2}{w_{\infty}^2}} \left\{ 1 + 2\left(\frac{w_1}{w_{\infty}}\right)^2 - 3\left(\frac{w}{w_{\infty}}\right)^2 \right\}}{\left(1 - \frac{w^2}{w_{\infty}^2}\right)^2} \end{cases}$$

IN ATTENUATION RANGE : $\omega_1 < \omega < \infty$ (EXCEPT IN VICINITY OF ω_0)

$$\left\{ \begin{aligned} \gamma_1^* &\approx \gamma_1 + \frac{1}{4} \left(\frac{R}{L\omega_1} + \frac{G}{C\omega_1} \right)^2 \frac{\left(\frac{\omega}{\omega_1} \right)}{\left(\frac{\omega^2}{\omega_1^2} - 1 \right)^{3/2}} \times \frac{\sqrt{1 - \frac{\omega_1^2}{\omega^2}} \left\{ 1 + 2 \left(\frac{\omega_1^2}{\omega^2} \right) - 3 \left(\frac{\omega_1^2}{\omega^2} \right) \right\}}{\left(1 - \frac{\omega_1^2}{\omega^2} \right)^2} \\ \gamma_2^* &\approx \pi - \frac{2(\alpha + \beta)}{\sqrt{\omega^2 - \omega_1^2}} \times \frac{\sqrt{1 - \frac{\omega_1^2}{\omega^2}}}{\left(1 - \frac{\omega_1^2}{\omega^2} \right)} \end{aligned} \right.$$

ATTENUATION AT THE ω_0 'S

HERE USE :- $y^* = y - f \left(\frac{dy}{d\omega} \right) \delta + \dots$

BUT IN THE VICINITY OF ω_0 : $y = 1 + \frac{dy}{d\omega} (\omega - \omega_0)$

SO WE HAVE : $y^* = 1 + \left\{ (\omega - \omega_0) - f(\alpha + \beta) \right\} \left(\frac{dy}{d\omega} \right)_{\omega = \omega_0}$

AND SO LONG AS :- $\left| (\omega - \omega_0) - f(\alpha + \beta) \right| \left(\frac{dy}{d\omega} \right)_{\omega = \omega_0} \ll 2$

OR, $\gamma_1^* \gg 0$

WE HAVE : $\gamma^* \approx \ln \left\{ \frac{2}{\left[(\omega - \omega_0) - f(\alpha + \beta) \right] \left(\frac{dy}{d\omega} \right)_{\omega = \omega_0}} \right\}$

FOR $y = \frac{h \sqrt{\omega^2 - \omega_1^2}}{\omega} = \frac{\omega_0}{\omega} \times \frac{\sqrt{\omega^2 - \omega_1^2}}{\sqrt{\omega_0^2 - \omega_1^2}}$

$\left(\frac{dy}{d\omega} \right)_{\omega = \omega_0} = \frac{1}{\omega_0} \cdot \frac{1}{\left(\frac{\omega_0^2}{\omega_1^2} - 1 \right)}$

HENCE, OVER A RANGE FOR WHICH,

$$\frac{(w - w_{\infty}) - \gamma(\alpha + \beta)}{w_{\infty} \left(\frac{w_{\infty}^2}{w_1^2} - 1 \right)} \ll 2 \quad \text{or FOR } w = w_{\infty}, \text{ IF}$$

$$\frac{1}{4} \left(\frac{R}{Lw_{\infty}} + \frac{G}{Cw_{\infty}} \right) \ll \left(\frac{w_{\infty}^2}{w_1^2} - 1 \right)$$

WE HAVE APPROXIMATELY :

$$\gamma_1^* = \ln \left\{ \frac{2w_{\infty} \left(\frac{w_{\infty}^2}{w_1^2} - 1 \right)}{(w - w_{\infty}) - \gamma(\alpha + \beta)} \right\}$$

WITHOUT THIS CONDITION FULFILLED, WE HAVE :

$$\gamma_1^* = \ln \left\{ 1 + \frac{2w_{\infty} \left(\frac{w_{\infty}^2}{w_1^2} - 1 \right)}{(w - w_{\infty}) - \gamma(\alpha + \beta)} \right\}$$

AT $w = w_{\infty}$:

$$\gamma_1^* = \ln \left| 1 + \frac{2w_{\infty} \left(\frac{w_{\infty}^2}{w_1^2} - 1 \right)}{(\alpha + \beta)} \right| \cong$$

$$\cong \ln \left\{ \frac{\left(\frac{w_{\infty}^2}{w_1^2} - 1 \right)}{\frac{1}{4} \left(\frac{R}{Lw_{\infty}} + \frac{G}{Cw_{\infty}} \right)} \right\}$$

$$\text{LET : } \left(\frac{R}{Lw_{\infty}} + \frac{G}{Cw_{\infty}} \right) = \frac{1}{Q_{\infty}}$$

$$\text{THEN : } \boxed{\gamma_1^* \cong \ln \left[4Q_{\infty} \left(\frac{w_{\infty}^2}{w_1^2} - 1 \right) \right]} \quad (\text{NAPIERS})$$

ATTENUATION AT CUT-OFF

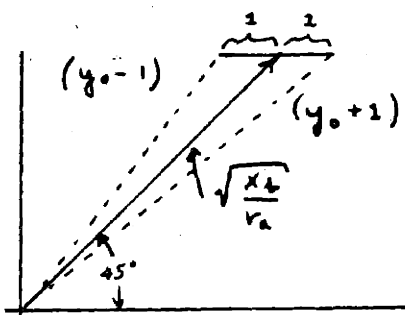
LET US SAY THAT THE CUT-OFF IS DUE TO A ZERO IN X_a
(ON THE LATTICE BASIS), THEN:

$$z_a = r_a ; z_b = r_b + jx_b ; y_0 = \sqrt{\frac{r_b + jx_b}{r_a}}$$

$$y_0 \approx \sqrt{\frac{jx_b}{r_a}}$$

FOR THE DETERMINATION OF $\left(\frac{y_{0+1}}{y_{0-1}}\right)$ CONSIDER THE FOLLOWING

FIGURE:



$$|y_{0+1}|^2 \approx \frac{x_b}{r_a} + 2\sqrt{\frac{x_b}{r_a}} \times \frac{1}{\sqrt{2}} = \frac{x_b}{r_a} \left(1 + \sqrt{2} \sqrt{\frac{r_a}{x_b}}\right)$$

$$|y_{0-1}|^2 \approx \frac{x_b}{r_a} - 2\sqrt{\frac{x_b}{r_a}} \times \frac{1}{\sqrt{2}} = \frac{x_b}{r_a} \left(1 - \sqrt{2} \sqrt{\frac{r_a}{x_b}}\right)$$

HENCE:- $\left|\frac{y_{0+1}}{y_{0-1}}\right| \approx 1 + \sqrt{\frac{2r_a}{x_b}}$

AND THUS: $\gamma_{ic}^* = \sqrt{\frac{2r_a}{x_b}}$

FROM WHICH IT FOLLOWS: $\gamma_{ic}^* = \sqrt{\frac{2(\alpha + \beta)}{x_b} \left(\frac{dx_a}{dw}\right)}$

SUPPOSE, $x_b = h_b w$ AND $x_a = h_a \frac{(w^2 - w_1^2)}{w}$

THEN: $\left.\frac{dx_a}{dw}\right|_{w_1} = 2h_a$

$$\begin{aligned}
 \text{AND - } \gamma_{ic}^* &= 2 \sqrt{\frac{h_a}{h_b}} \times \sqrt{\frac{(\alpha + \beta)}{w_1}} \\
 &= 2 \sqrt{\frac{(\alpha + \beta)}{w_1}} \\
 &\quad \frac{1}{\sqrt{1 - \frac{w_1^2}{w_b^2}}} \\
 &= \frac{2 \sqrt{\frac{1}{2Q_1}}}{\sqrt{1 - \frac{w_1^2}{w_b^2}}}
 \end{aligned}$$

$$\gamma_{ic}^* = \boxed{\frac{1}{m} \sqrt{\frac{2}{Q_1}}} \quad (\text{NAPIERS})$$

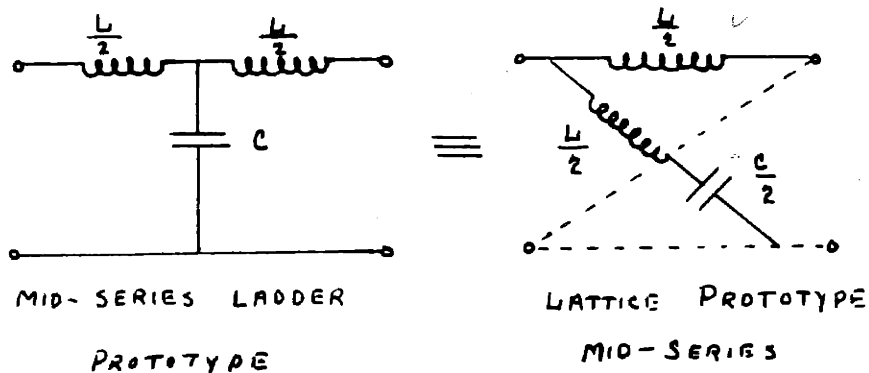
APPENDIX C

PART I

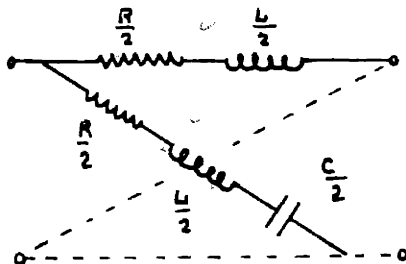
MID-SERIES DERIVATION OF COMPLEX-M FILTER

FROM NOTES BY PROFESSOR E. A. GUILLEMIN

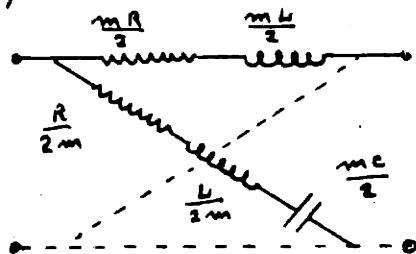
CONSIDER LOW-PASS CONSTANT-K FILTER:-



CONSIDER THE RESISTANCE OF THE COIL:



THE M-DERIVATION YIELDS:



FROM WHICH : $z_a = \frac{m}{2} (R + j\omega L)$

$$z_b = \frac{1}{2m} \left(R + j\omega L + \frac{4}{j\omega C} \right)$$

SINCE, $y = \sqrt{\frac{z_b}{z_a}}$; $y = \frac{1}{m} \sqrt{1 - \frac{4}{LC\omega^2 \left(1 + \frac{R}{j\omega L}\right)}}$

BUT : $\omega_c^2 = \frac{4}{LC}$

HENCE : $y = \frac{1}{m} \sqrt{1 - \frac{1}{X^2 \left(1 + \frac{R}{j\omega L}\right)}}$

WHERE : $X = \frac{\omega}{\omega_c}$

IF WE WANT THE INFINITE PEAK AT $\omega = \omega_c$, THEN $y = 1$

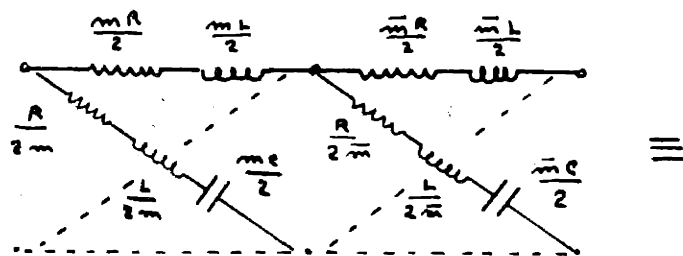
FOR $\omega = \omega_c$, THIS GIVES : $m = \sqrt{\frac{\frac{R}{j\omega_c L}}{1 + \frac{R}{jL\omega_c}}} \approx \sqrt{\frac{R}{jL\omega_c}}$

$$m \approx \sqrt{\frac{R}{2L\omega_c}} (1 - j)$$

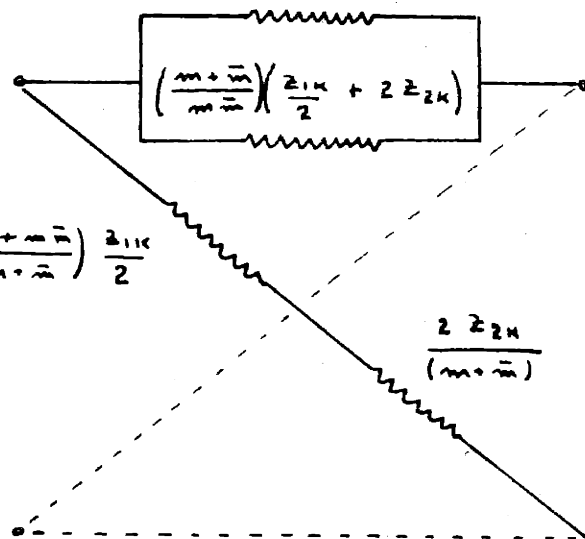
$$m \approx \frac{1 - j}{\sqrt{2Q_c}} = \frac{1}{\sqrt{j}Q_c}$$

IF THIS COMPLEX VALUE FOR "m" WERE USED IN THE ABOVE LATTICE NETWORK, IT WOULD NOT BE PHYSICALLY REALIZABLE. HOWEVER, BY USING TWO SUCH STRUCTURES IN CASCADE, ONE HAVING THE ABOVE VALUE FOR "m", THE OTHER HAVING AN "m" WHICH IS THE

CONJUGATE OF THIS (\bar{m}), THE PEAK OF INFINITE ATTENUATION WILL STILL BE OBTAINED AND A PHYSICALLY REALIZABLE NETWORK WILL RESULT; SINCE :



$$(m + \bar{m}) \frac{Z_{1K}}{2}$$



$$\begin{cases} Z_{1K} = R + j\omega L \\ Z_{2K} = -\frac{1}{j\omega C} \end{cases}$$

(FOR THE DERIVATION OF THE ABOVE EQUIVALENT NETWORKS SEE , E.A. GUINLEMIN'S , COMMUNICATIONS NETWORKS , VOLUME 2 ; PP 437 - 38.)

APPENDIX C

PART II

PROPAGATION FUNCTION OF COMPLEX-M FILTER

SINCE, $y = \frac{1}{m} \sqrt{1 - \frac{1}{x^2(1 + \frac{R}{j\omega})}}$; AND $m = \frac{1}{\sqrt{jQ_c}}$

$$y = \sqrt{jQ_c} \cdot \sqrt{1 - \frac{1}{x^2(1 + \frac{1}{jQ_c})}}$$

LET, $x = 1 + \delta$; $x^2 = (1 + \delta)^2 \cong 1 + 2\delta + \delta^2 \cong 1 + 2\delta$ | $\delta < 1$

THEN: $y \cong \sqrt{jQ_c} \times \sqrt{1 - \frac{1}{(1 + 2\delta)(1 + \frac{1}{jQ_c})}}$

BY FURTHER APPROXIMATIONS :

$$y \cong \sqrt{jQ_c} \times \sqrt{1 - \frac{1}{1 + 2\delta + \frac{1}{jQ_c}}} \quad \left\{ \begin{array}{l} \text{SINCE, } \frac{2\delta}{jQ_c} \ll 1 \\ jQ_c \end{array} \right.$$

$$y \cong \sqrt{jQ_c} \times \sqrt{1 - (1 - 2\delta - \frac{1}{jQ_c})} \quad \left\{ \begin{array}{l} \text{SINCE, } (1 \pm x)^{-1} = \\ 1 \mp x + x^2 \mp x^3 \\ \text{WHERE: } x < 1 \end{array} \right.$$

IN THIS CASE, $(2\delta + \frac{1}{jQ_c}) = x < 1$

THEREFORE: $y \cong \sqrt{jQ_c} \times \sqrt{2\delta + \frac{1}{jQ_c}} = \sqrt{1 + j2\delta Q_c}$

CONSIDER THE TWO CONJUGATE SECTIONS -

$$y_m \approx \sqrt{1 + j2\delta Q_c} \quad \text{AND} \quad y_{\bar{m}} \approx -j \sqrt{1 + 2j\delta Q_c}$$

THEREFORE, THE PROPAGATION FUNCTION FOR THE TWO SECTIONS IN CASCADE IS:

$$\gamma = \ln \left\{ \frac{\sqrt{1 + j2\delta Q_c} + 1}{\sqrt{1 + j2\delta Q_c} - 1} \right\} + \ln \left\{ \frac{\sqrt{1 + j2\delta Q_c} + j}{\sqrt{1 + j2\delta Q_c} - j} \right\}$$

FOR THE RANGE IN WHICH, $\delta Q_c < \frac{1}{2}$, THIS IS APPROX.:

$$\gamma \approx \ln \left(\frac{1 + j\delta Q_c + 1}{1 + j\delta Q_c - 1} \right) + \ln \left(\frac{1 + j\delta Q_c + j}{1 + j\delta Q_c - j} \right)$$

AND,

$$\gamma_1 \approx \ln \left| \frac{2}{\delta Q_c} \right| + \delta Q_c \quad (\text{ATTENUATION FUNCTION})$$

FOR THE RANGE IN WHICH, $\delta Q_c > \frac{1}{2}$, THIS IS APPROX.:

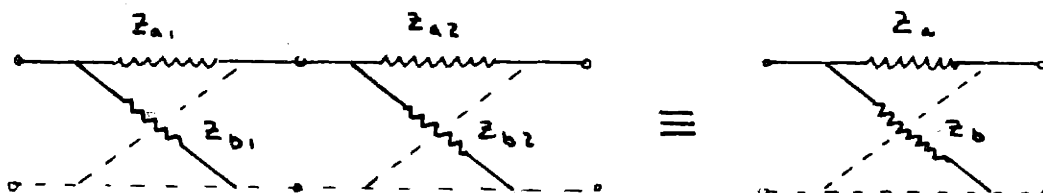
$$\gamma \approx \ln \left(\frac{\sqrt{j2\delta Q_c} + 1}{\sqrt{j2\delta Q_c} - 1} \right) + \ln \left(\frac{\sqrt{j2\delta Q_c} + j}{\sqrt{j2\delta Q_c} - j} \right)$$

$$\gamma \approx \sqrt{\frac{2}{j\delta Q_c}} + j \sqrt{\frac{2}{j\delta Q_c}} \quad \text{AND} \quad \gamma_1 = \frac{1}{\sqrt{\delta Q_c}} \pm \frac{1}{\sqrt{\delta Q_c}}$$

$$\begin{cases} \text{FOR } \delta > 0 & \gamma_1 = \frac{2}{\sqrt{\delta Q_c}} \\ \text{FOR } \delta < 0 & \gamma_1 = 0 \end{cases}$$

APPENDIX C

PART III

CASCADING LATTICE STRUCTURES

CONDITION: ALL THESE STRUCTURES HAVE THE SAME IMAGE

IMPEDANCE; I. E., $Z_a Z_b = Z_{a1} Z_{b1} = Z_{a2} Z_{b2} = Z_0$,
ON CONSTANT-K BASIS.

PROPAGATION FUNCTIONS ARE AS FOLLOWS:

$$\delta_1 = \ln \left(\frac{\sqrt{\frac{Z_{b1}}{Z_{a1}}} + 1}{\sqrt{\frac{Z_{b1}}{Z_{a1}}} - 1} \right); \quad \delta_2 = \ln \left(\frac{\sqrt{\frac{Z_{b2}}{Z_{a2}}} + 1}{\sqrt{\frac{Z_{b2}}{Z_{a2}}} - 1} \right)$$

$$\delta = \delta_1 + \delta_2 = \ln \left(\frac{\sqrt{\frac{Z_b}{Z_a}} + 1}{\sqrt{\frac{Z_b}{Z_a}} - 1} \right)$$

SUBSTITUTING: $y_1 = \sqrt{\frac{Z_{b1}}{Z_{a1}}}$, ETC.

$$\delta = \delta_1 + \delta_2 = \ln \left(\frac{y_1 + 1}{y_1 - 1} \right) = \ln \left(\frac{y_1 + 1}{y_1 - 1} \right) + \ln \left(\frac{y_2 + 1}{y_2 - 1} \right)$$

THEREFORE: $\frac{y + 1}{y - 1} = \left(\frac{y_1 + 1}{y_1 - 1} \right) \times \left(\frac{y_2 + 1}{y_2 - 1} \right) = \frac{(y_1 y_2 + 1) + (y_1 + y_2)}{(y_1 y_2 + 1) - (y_1 + y_2)}$

$$\text{OR, } \frac{y+1}{y-1} = \frac{\left(\frac{y_1 y_2 + 1}{y_1 + y_2}\right) + 1}{\left(\frac{y_1 y_2 + 1}{y_1 + y_2}\right) - 1}$$

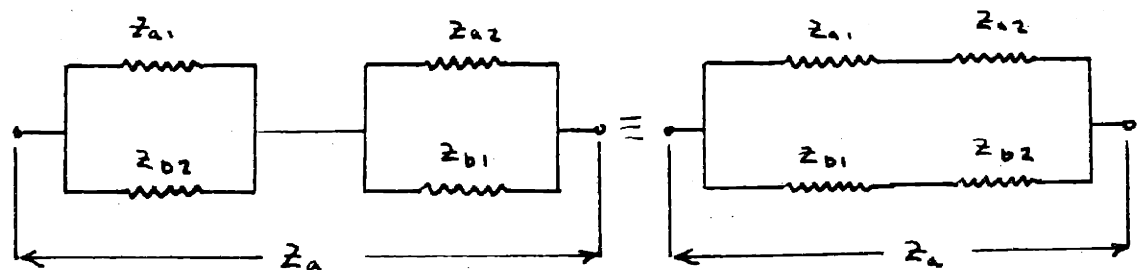
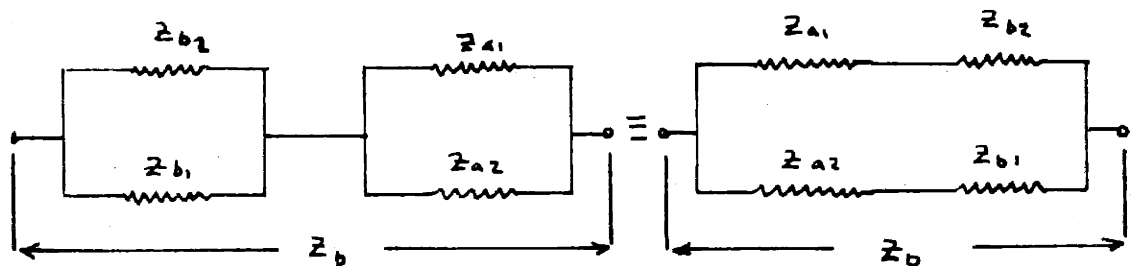
$$\text{FROM WHICH: } y = \frac{y_1 y_2 + 1}{y_1 + y_2} = \frac{y_1 y_2}{y_1 + y_2} + \frac{1}{y_1 + y_2}$$

$$\text{AND } \sqrt{\frac{Z_b}{Z_a}} = \frac{1}{\sqrt{\frac{Z_{a1}}{Z_{b1}} + \frac{Z_{a2}}{Z_{b2}}}} + \frac{1}{\sqrt{\frac{Z_{b1}}{Z_{a1}} + \frac{Z_{b2}}{Z_{a2}}}}$$

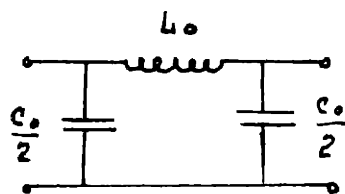
TO GET Z_b MULTIPLY BY $\sqrt{Z_a Z_b}$ AND ITS EQUIVALENTS

$$\text{THEREFORE: } Z_b = \frac{1}{\frac{1}{Z_{b1}} + \frac{1}{Z_{b2}}} + \frac{1}{\frac{1}{Z_{a1}} + \frac{1}{Z_{a2}}}$$

$$\text{LIKEWISE: } \frac{1}{Z_a} = \frac{1}{Z_{a1} + Z_{a2}} + \frac{1}{Z_{b1} + Z_{b2}}$$



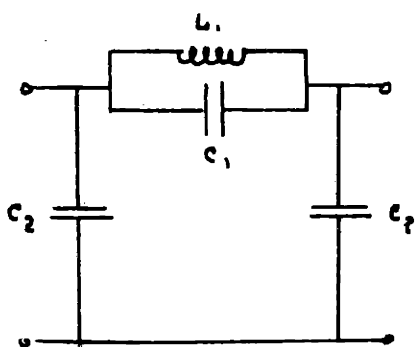
OBTAINING COMPLEX-M LATTICE ON MID-SHUNT BASIS



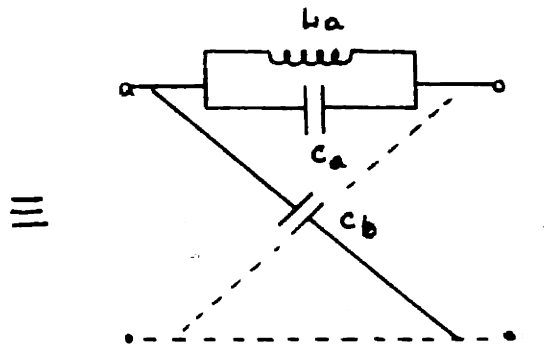
PROTOTYPE π

$$L_0 = \frac{Z_0}{\pi f_c} = Z_1$$

$$C_0 = \frac{1}{\pi f_c Z_0} = \frac{1}{Z_2}$$



SHUNT m -DERIVED π



SHUNT m -DERIVED LATTICE

$$L_1 = m L_0$$

$$C_1 = \left(\frac{1-m^2}{4m} \right) C_0$$

$$C_2 = \frac{C_0 m}{2}$$

VALUES FOR EACH COMPLEX SECTION

$$L_{1a} = \frac{m L_0}{2}$$

$$C_{1a} = \frac{m C_0}{2}$$

$$C_{1b} = \frac{m C_0}{2}$$

$$L_{2a} = \frac{\bar{m} L_0}{2}$$

$$C_{2a} = \frac{\bar{m} C_0}{2}$$

$$C_{2b} = \frac{\bar{m} C_0}{2}$$

DERIVING Z_a AND Z_b FOR LATTICE WHICH IS EQUIVALENT TO TWO CONJUGATE COMPLEX- m SECTIONS IN CASCADE:

FROM FOREGOING:

$$Y_{b1} = \frac{1}{Z_{b1}} = \frac{m}{2} Y_2 = \frac{m C_0}{2}$$

$$Y_{b2} = \frac{1}{Z_{b2}} = \frac{\bar{m}}{2} Y_2 = \frac{\bar{m} C_0}{2}$$

$$y_{a1} = \frac{1}{z_{a1}} = \frac{1}{m} \left(\frac{y_2}{2} + 2y_1 \right)$$

$$= \frac{1}{m} \left(\frac{C_0}{2} + \frac{2}{L_0} \right)$$

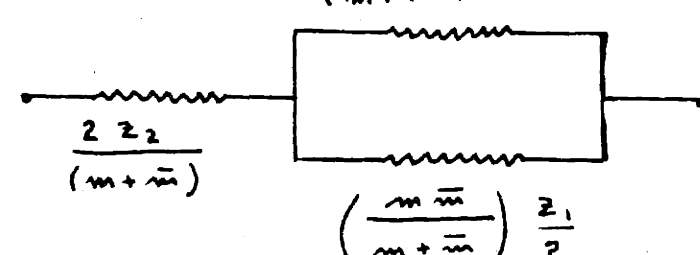
$$y_{a2} = \frac{1}{z_{a2}} = \frac{1}{\bar{m}} \left(\frac{y_2}{2} + 2y_1 \right)$$

$$= \frac{1}{\bar{m}} \left(\frac{C_0}{2} + \frac{2}{L_0} \right)$$

$$z_b = \frac{1}{y_{b2} + y_{b1}} + \frac{1}{y_{a1} + y_{a2}}$$

$$z_b = \frac{1}{\frac{m}{2} y_2 + \frac{\bar{m}}{2} y_2} + \frac{1}{\frac{1}{m} \left(\frac{y_2}{2} + 2y_1 \right) + \frac{1}{\bar{m}} \left(\frac{y_2}{2} + 2y_1 \right)}$$

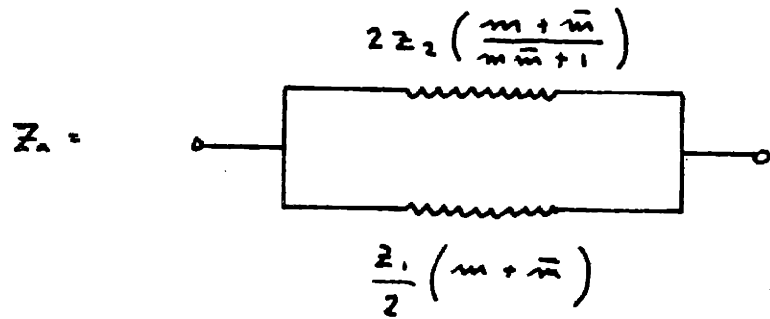
$$= \frac{1}{\frac{y_2}{2} (m + \bar{m})} + \frac{1}{\left(\frac{y_2}{2} + 2y_1 \right) \left(\frac{1}{m} + \frac{1}{\bar{m}} \right)}$$

$$z_b = \frac{\frac{2z_2}{(m + \bar{m})}}{\left(\frac{m\bar{m}}{m + \bar{m}} \right) 2z_2} \parallel \left(\frac{m\bar{m}}{m + \bar{m}} \right) \frac{z_1}{2}$$


$$y_a = \frac{1}{z_{a1} + z_{a2}} + \frac{1}{z_{b1} + z_{b2}}$$

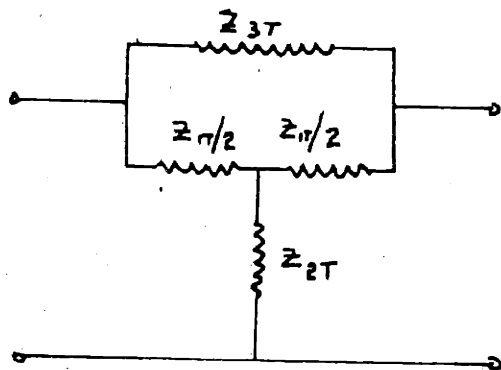
$$\begin{aligned}
 y_a &= \frac{1}{\frac{2z_1}{m} + \frac{2z_2}{\bar{m}}} + \frac{1}{\frac{1}{m} \left(\frac{y_2}{2} + 2y_1 \right) + \frac{1}{\bar{m}} \left(\frac{y_2}{2} + 2y_1 \right)} \\
 &= \frac{1}{2z_2 \left(\frac{m + \bar{m}}{m\bar{m}} \right)} + \frac{\left(\frac{y_2}{2} + 2y_1 \right)}{\left(\frac{m + \bar{m}}{m\bar{m}} \right)} \\
 &= \frac{1}{2(z_2) \left(\frac{m + \bar{m}}{m\bar{m}} \right)} + \frac{1}{(m + \bar{m})} \left\{ \frac{1}{2z_2} + \frac{2}{z_1} \right\}
 \end{aligned}$$

$$y_a = \frac{1}{2z_2} \left\{ \frac{m\bar{m}}{m + \bar{m}} + \frac{1}{m + \bar{m}} \right\} + \frac{2}{z_1} \frac{1}{(m + \bar{m})}$$



CONVERTING COMPLEX-M LATTICE TO BRIDGED-T

(SEE E.A. GUILLEMIN'S, COMMUNICATIONS NETWORKS
 VOLUME 2, P.P. 439-40)



By BARTLETT'S BISECTION THEOREM:

$$Z_a = \frac{1}{\frac{z_{1T}}{2} + \frac{z_{3T}}{2}}$$

$$Z_b = \frac{z_{1T}}{2} + 2z_{2T}$$

BRIDGED-T EQUIVALENT TO LATTICE, IF ABOVE CONDITIONS HOLD.

$$\text{LET: } \frac{Z_{1T}}{2} = 2Z_2 \left(\frac{m + \bar{m}}{m\bar{m} + 1} \right)$$

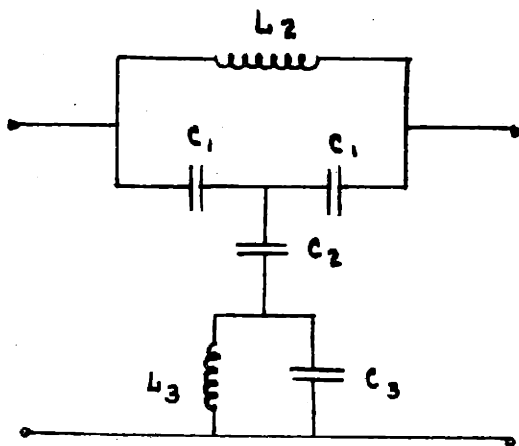
$$\frac{Z_{3T}}{2} = \frac{Z_1}{2} (m + \bar{m})$$

$$\text{THEN: } Z_0 = 2Z_2 \left(\frac{m + \bar{m}}{m\bar{m} + 1} \right) + Z Z_{2T}$$

$$\text{OR } 2Z_{2T} = 2Z_2 \left\{ \frac{1}{m + \bar{m}} - \frac{m + \bar{m}}{m\bar{m} + 1} \right\} +$$

$$\frac{1}{\frac{Z_1}{2} \left(\frac{m\bar{m}}{m + \bar{m}} \right) + 2Z_2 \left(\frac{m\bar{m}}{m + \bar{m}} \right)}$$

EQUIVALENT BRIDGED-T



$$C_1 = \frac{C_0}{2} \frac{(m\bar{m} + 1)}{(m + \bar{m})}$$

$$C_2 = C_0 \frac{1}{\left\{ \frac{1}{(m + \bar{m})} - \frac{(m + \bar{m})}{(m\bar{m} + 1)} \right\}}$$

$$C_3 = C_0 \frac{(m + \bar{m})}{(m\bar{m})}$$

$$L_2 = L_0 (m + \bar{m})$$

$$L_3 = \frac{(m\bar{m})}{(m + \bar{m})} \cdot \frac{L_0}{4}$$

APPENDIX D

SAMPLE CALCULATIONS

USING FORMULA FOR INDUCTANCE ON TOROIDAL CORE:

$$L = 2 \mu b N^2 \ln \left(\frac{r_2}{r_1} \right)$$

FOR CORE P-467585:

$$\text{PERMEABILITY } \mu = 115 \text{ (aemu)} = 115 \times 10^{-7}$$

$$\text{AXIAL HEIGHT } b = 0.35 \text{ INCH} = 0.888 \times 10^{-2} \text{ METERS}$$

$$\text{OUTSIDE DIA. } r_2 = 1.37 \text{ "}$$

$$\text{INSIDE " } r_1 = 0.89 \text{ "}$$

NUMBER OF TURNS REQUIRED TO GIVE AN INDUCTANCE OF
0.956 mh.:

$$L = 2 (115) (0.888) 10^{-9} (N^2) \ln \left(\frac{1.37}{0.89} \right)$$

$$L = 230 (0.888) 10^{-9} (N^2) \ln 1.54$$

$$L = 204 (N^2) 0.432 \times 10^{-9}$$

$$N^2 = \frac{0.956 \times 10^{-3}}{(204)(0.432) \times 10^{-9}}$$

$$N^2 = 1.09 \times 10^4$$

$$N = 105 \text{ TURNS (ANS)}$$

USING FORMULA FOR SATURATION OF TOROIDAL CORE :

$$B = \frac{4\pi N I \mu}{10 \ell} \text{ (GAUSSES)}$$

FOR COIL HAVING 0.956 mh. USING CORE P-467585 :

$$\text{PERMEABILITY } \mu = 115$$

$$\begin{aligned} \text{MEAN CIRCUM. } \ell &= [0.89 + \frac{2}{3}(1.35 - 0.89)] \pi \text{ INCH.} \\ &= 1.197 \times \pi \times 2.54 \text{ cm.} \\ &= 3.03 \times \pi \text{ cm.} \end{aligned}$$

CONSIDER 100 GAUSSES AS MAXIMUM ALLOWABLE SATURATION:

THEN,

$$\begin{aligned} I_{\text{MAX}} &= \frac{100 \times 10 \times 3.03 \pi}{4\pi (105) (115)} \\ &= 62.7 \times 10^{-3} \text{ AMPS.} \end{aligned}$$

ON BASIS OF 1 MILLIWATT INTO 600^w FILTER:

$$I^2 R = .001$$

$$I^2 = \frac{.001}{600} = 1.67 \times 10^{-6}$$

$$I = 1.29 \times 10^{-3} \text{ AMPS.}$$

$$I_{\text{MAX}} = 1.83 \times 10^{-3} \text{ AMPS.}$$

THEREFORE, THIS CORE SHOULD NOT BE SATURATED TO THE POINT OF EFFECTING THE PERMEABILITY AT 1 MILLIWATT LEVELS — THE LEVEL AT WHICH THIS FILTER WAS DESIGNED TO WORK.

ATTENUATION VS $\frac{f}{f_c}$ FOR LOW-PASS NETWORK DERIVED

STRUCTURES HAVING DISPERSION

$$Q = \frac{2\pi fL}{R} = 50$$

$$a = \frac{f_0}{f_c}$$

$$m = \frac{\sqrt{a^2 - 1}}{a}$$

NOTE: THESE CURVES DO NOT INCLUDE REFLECTION EFFECTS, SUCH AS OCCUR IN TERMINAL SECTIONS.

ATTENUATION PER SECTION IN DECIBELS

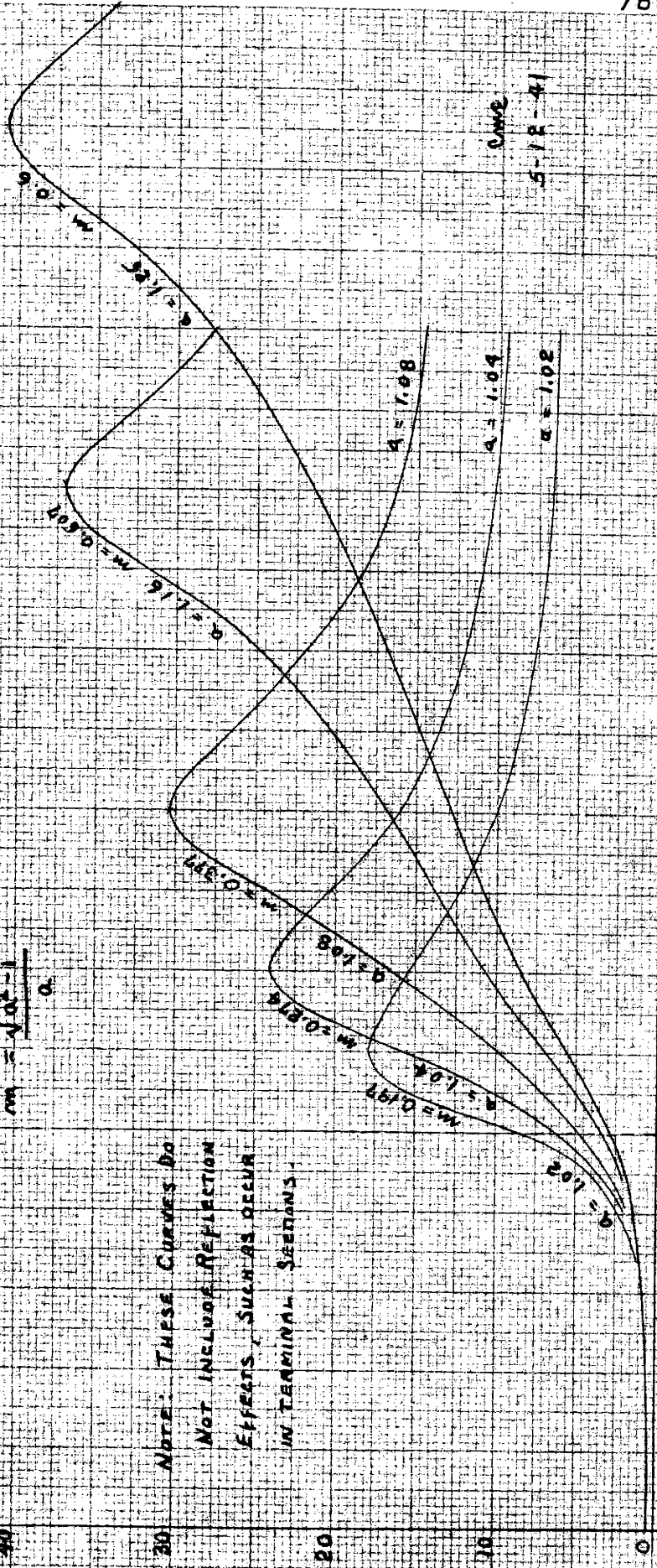
1.20

1.10

1.00

0.90

f/f_c



0.902
5-12-41

ATTENUATION VS $\frac{f}{f_c}$ FOR LOW-PASS M-DERIVED

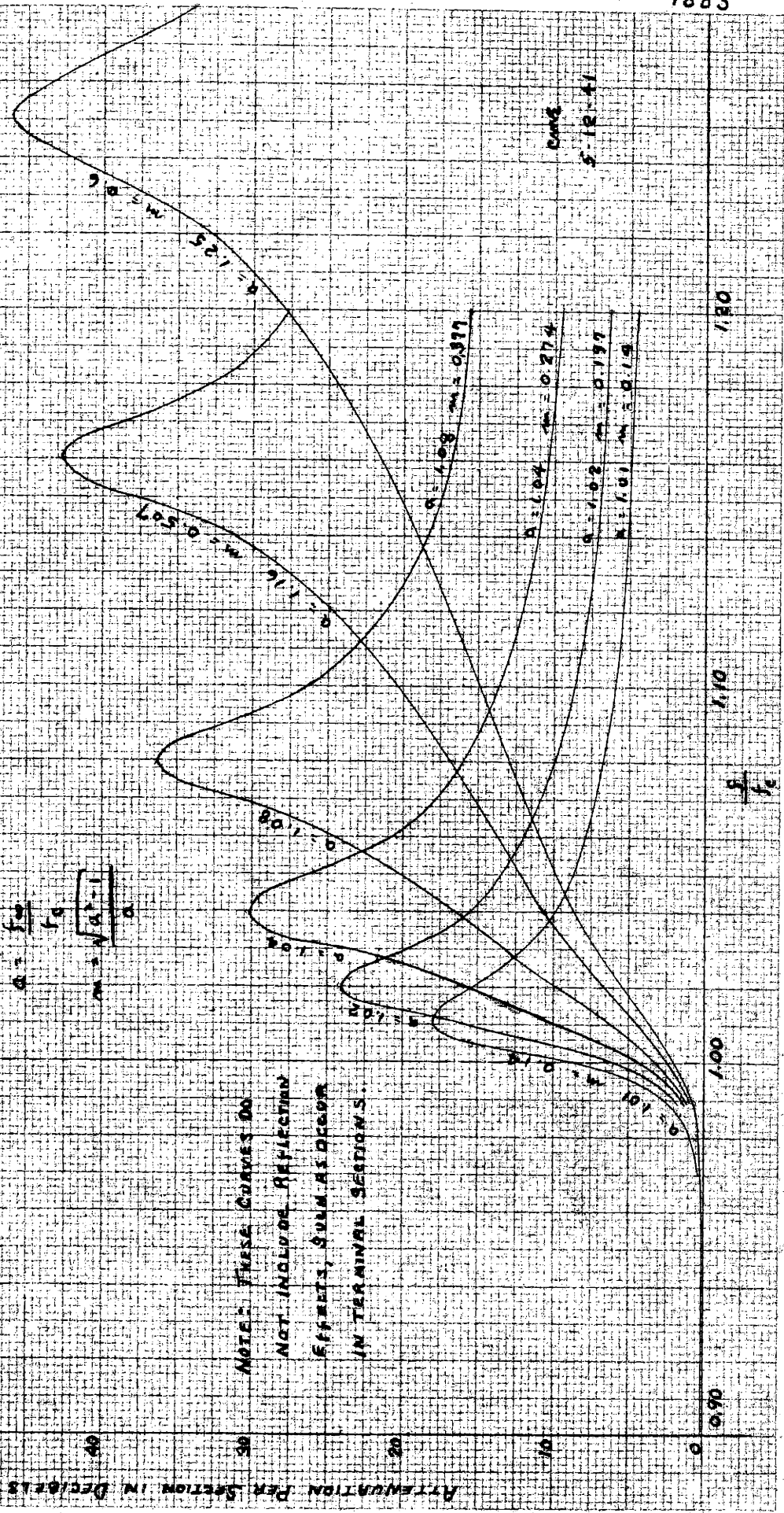
STRUCTURES HAVING DISSIPATION

$Q = 20 \text{ FL} - 100$

$$a = \frac{f_w}{f_c}$$

$$m = \sqrt{\frac{a^2 - 1}{a}}$$

NOTE: THESE CURVES DO NOT INCLUDE REFLECTION EFFECTS, SUCH AS OCCUR IN TERMINAL SECTIONS.



0006
S-12-41

ATTENUATION VS $\frac{f}{f_c}$ FOR LOSSLESS M-DERIVED

STRUCTURES HAVING DISSIPATION

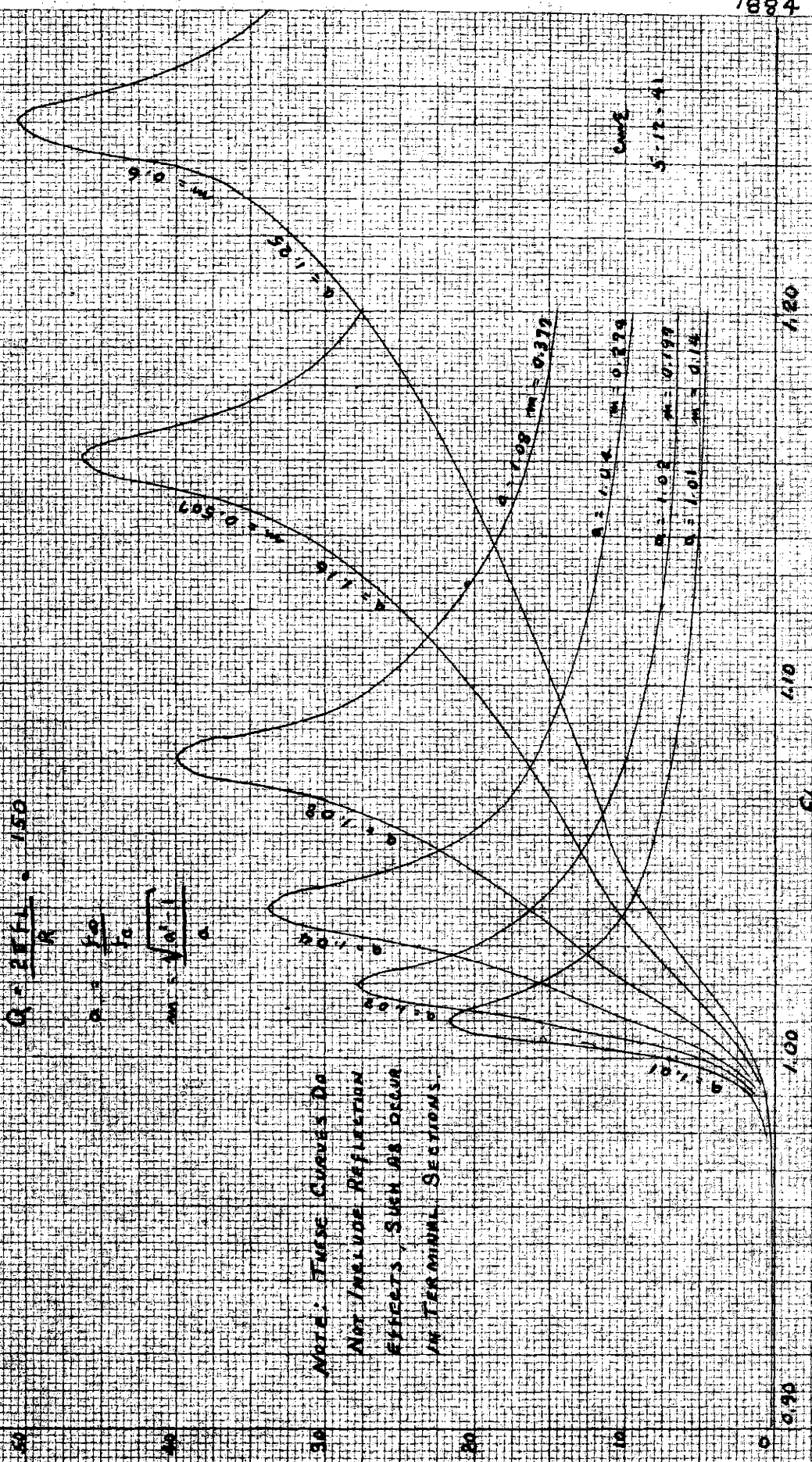
$$Q = \frac{2f_{c1}}{R} \cdot 150$$

$$Q = \frac{f_c}{R}$$

$$m = \frac{\sqrt{1 - \frac{f^2}{f_c^2}}}{Q}$$

ATTENUATION PER SECTION IN DECIBELS

NOTE: THESE CURVES DO NOT INCLUDE REFLECTION EFFECTS, SUCH AS OCCUR IN TERMINAL SECTIONS



CASE 5-12-41

9/5

ATTENUATION VS $\frac{f}{f_c}$ FOR LOW-PASS M-DEVIATED

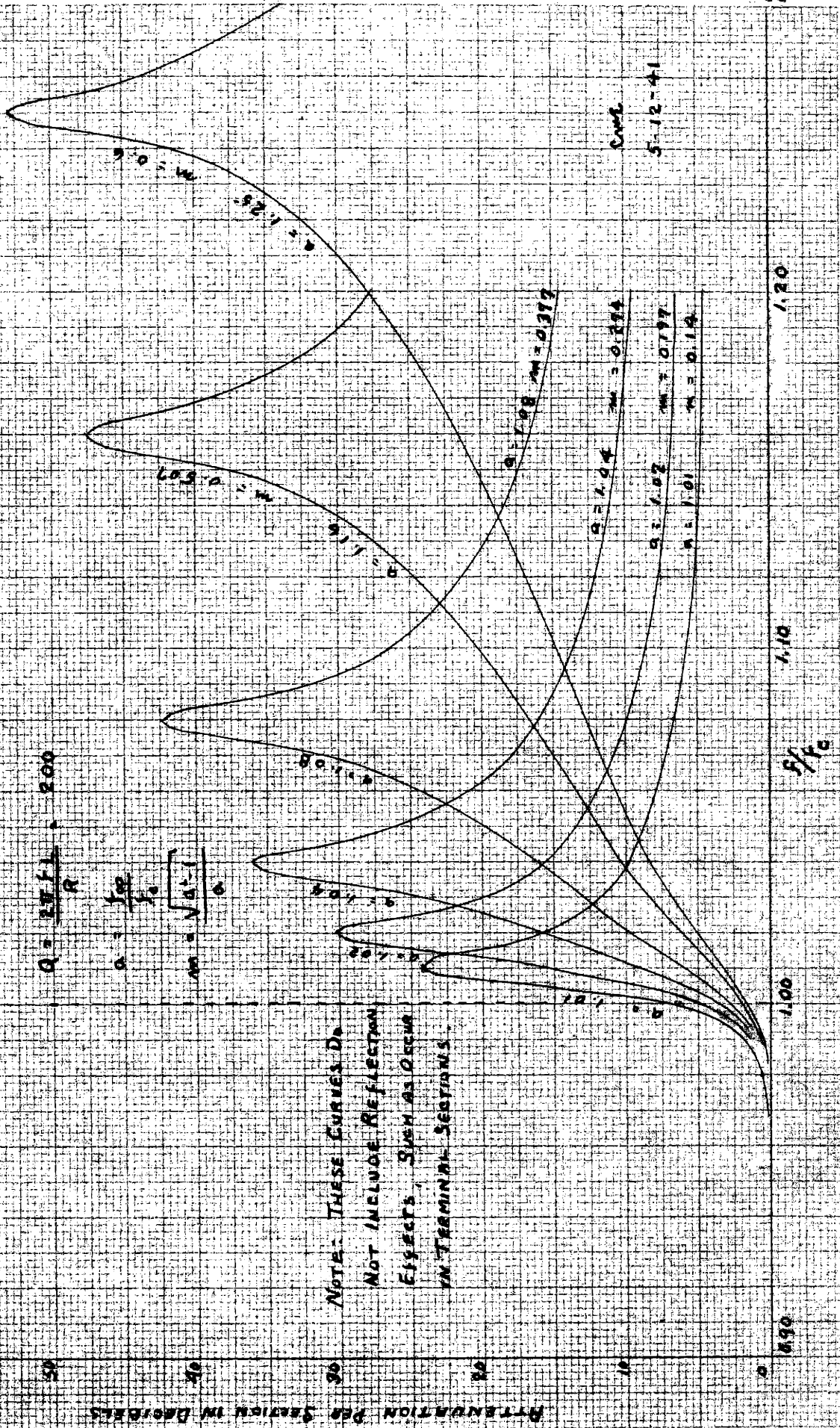
STRUCTURES HAVING DISSIPATION

$$Q = \frac{2\pi f L}{R} = 500$$

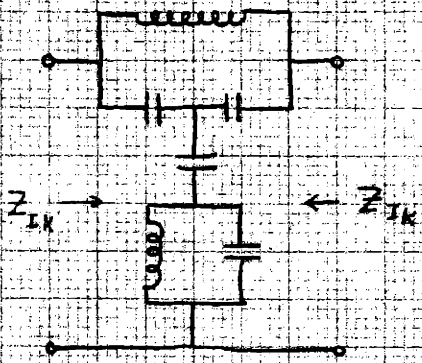
$$a = \frac{f_{02}}{f_c}$$

$$m = \sqrt{a^2 - 1}$$

NOTE: THESE CURVES DO NOT INCLUDE REFLECTION EFFECTS, SUCH AS OCCUR IN TERMINAL SECTIONS.



Low-Pass



ATTENUATION VS $\frac{f}{f_c}$ FOR COMPLEX-M

STRUCTURES HAVING f_{ω} AT f_c

$$\frac{f}{f_c} = 1 + \delta$$

$$\delta = \frac{\Delta}{Q_c}$$

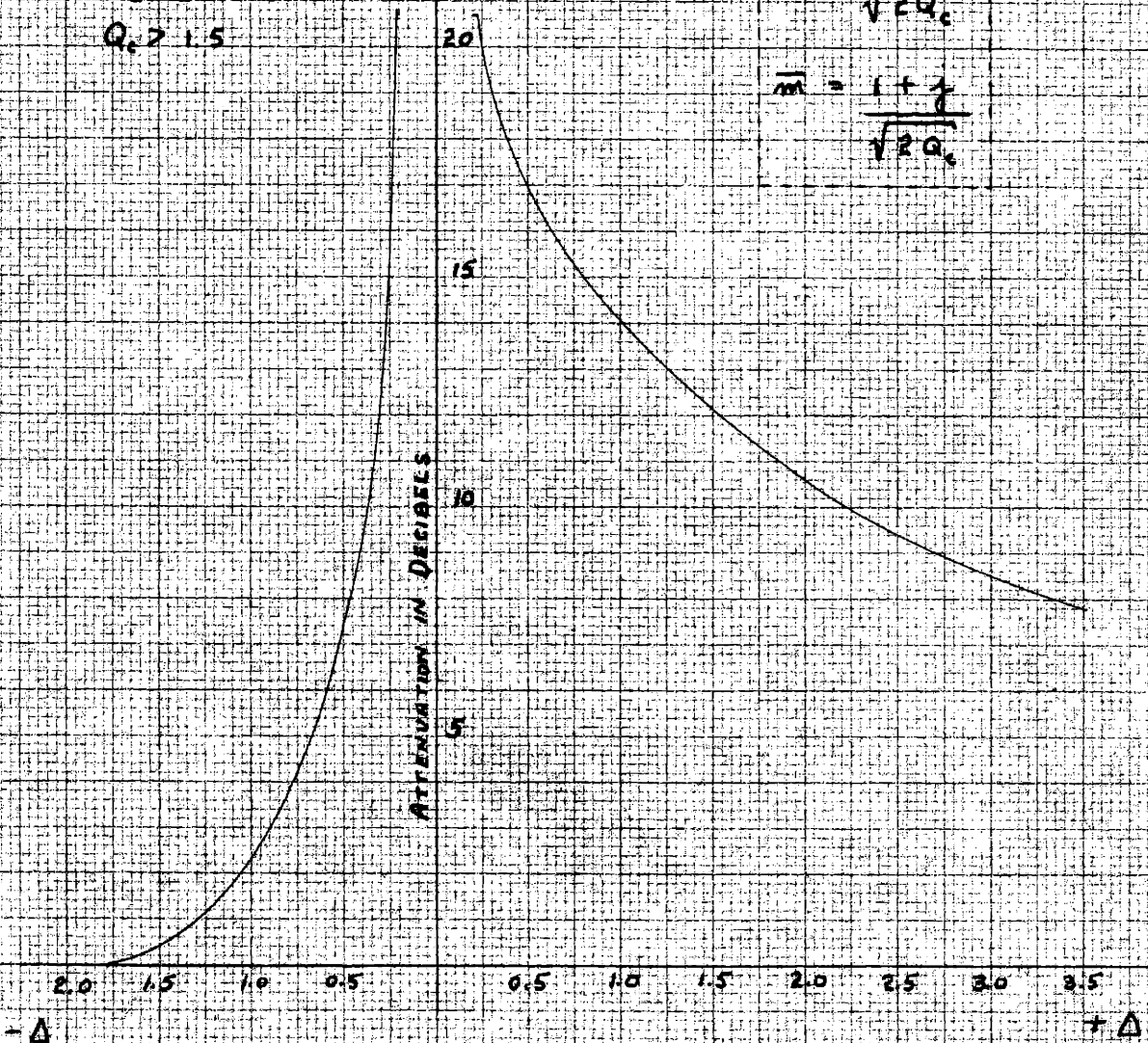
MID-SHUNT DERIVATION

REALIZABLE FOR

$$Q_c > 1.5$$

$$m = \frac{1 - j}{\sqrt{2Q_c}}$$

$$\bar{m} = \frac{1 + j}{\sqrt{2Q_c}}$$



$$\frac{f}{f_c} = 1 + \frac{\Delta}{Q_c}$$

OME

5-13-41

DATA ON COMPLEX M SECTION
TERMINATED IN ITS NOMINAL IMPEDANCE

$Z_0 = 600 \Omega$

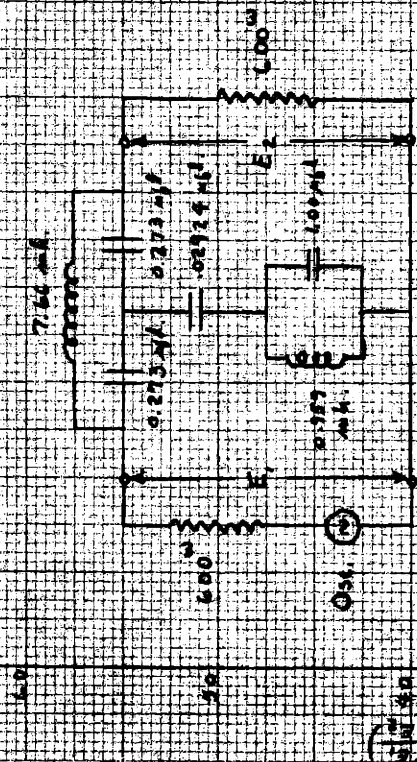
$f_c = f_{\omega} = 5000 \text{ C.P.S.}$

$Q = 50.0$

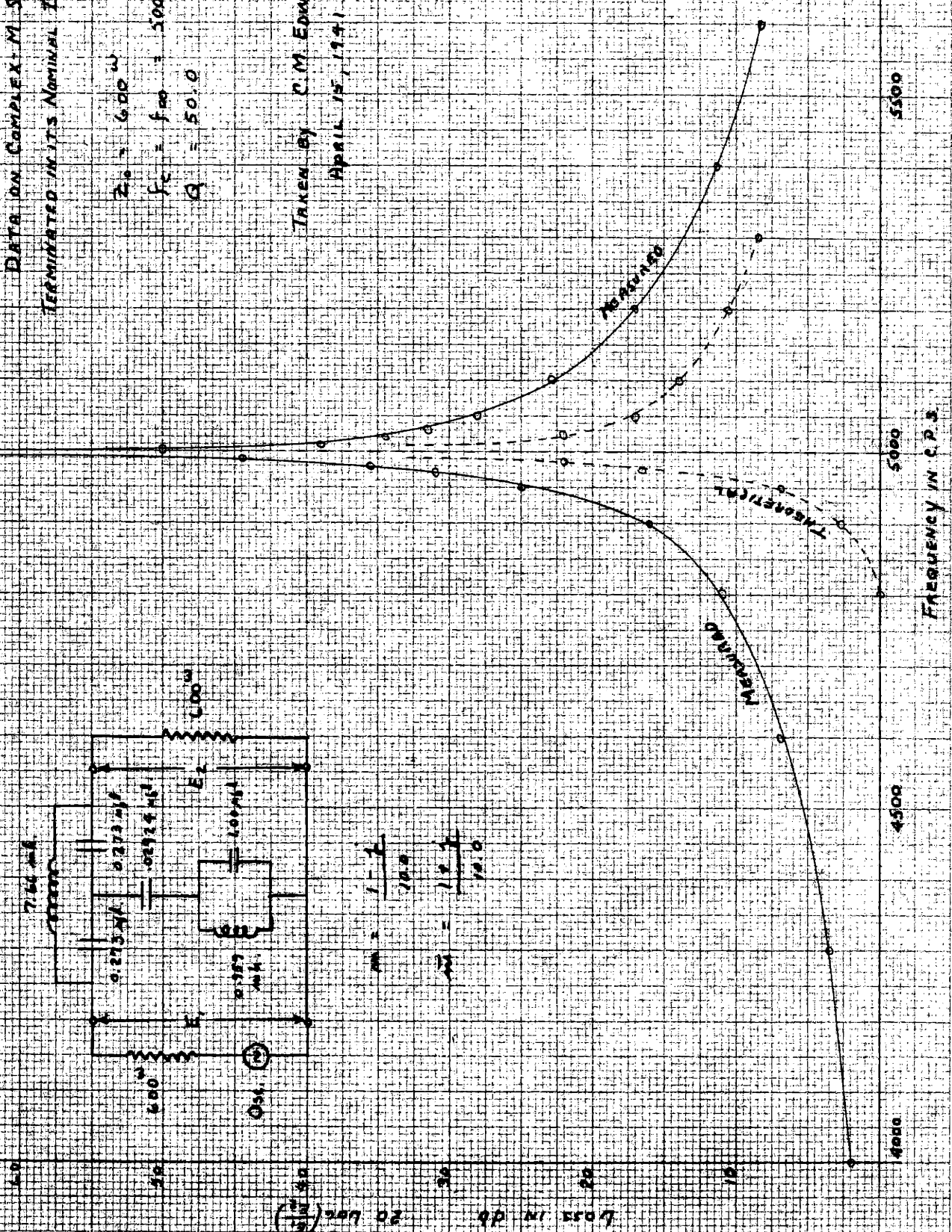
Taken by C. M. EDWARDS

April 15, 1941

C.M.E.
5-13-41



$Q = \frac{1}{\sqrt{1 - \frac{1}{Q^2}}}$
 $Q = \frac{1}{\sqrt{1 - \frac{1}{2500}}}$
 $Q = 50.0$



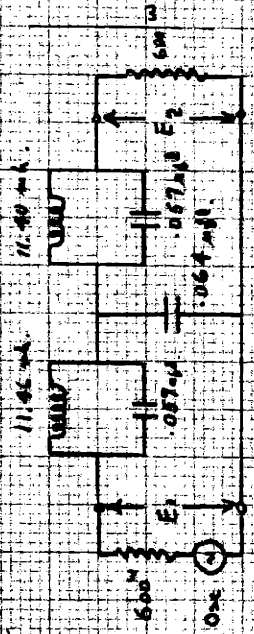
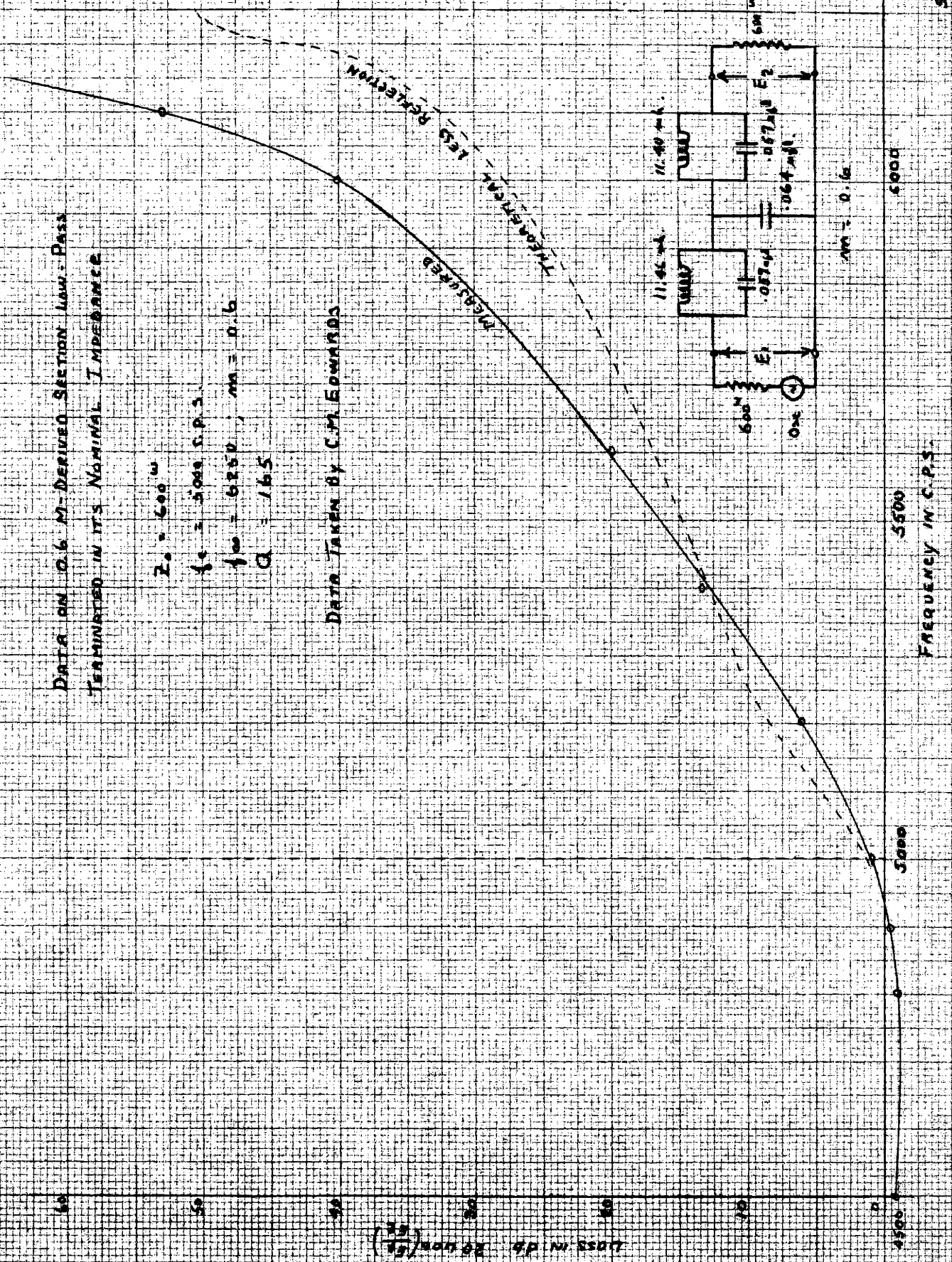
FREQUENCY IN C.P.S.

Loss in db

DATA ON 0.6 M-DERIVED SECTION LOW-PASS
TERMINATED IN ITS NOMINAL IMPEDANCE

$Z_0 = 600 \Omega$
 $f_c = 5000 \text{ C.P.S.}$
 $f_w = 6250, m = 0.6$
 $Q = 16.5$

DATA TAKEN BY C.M. EDWARDS



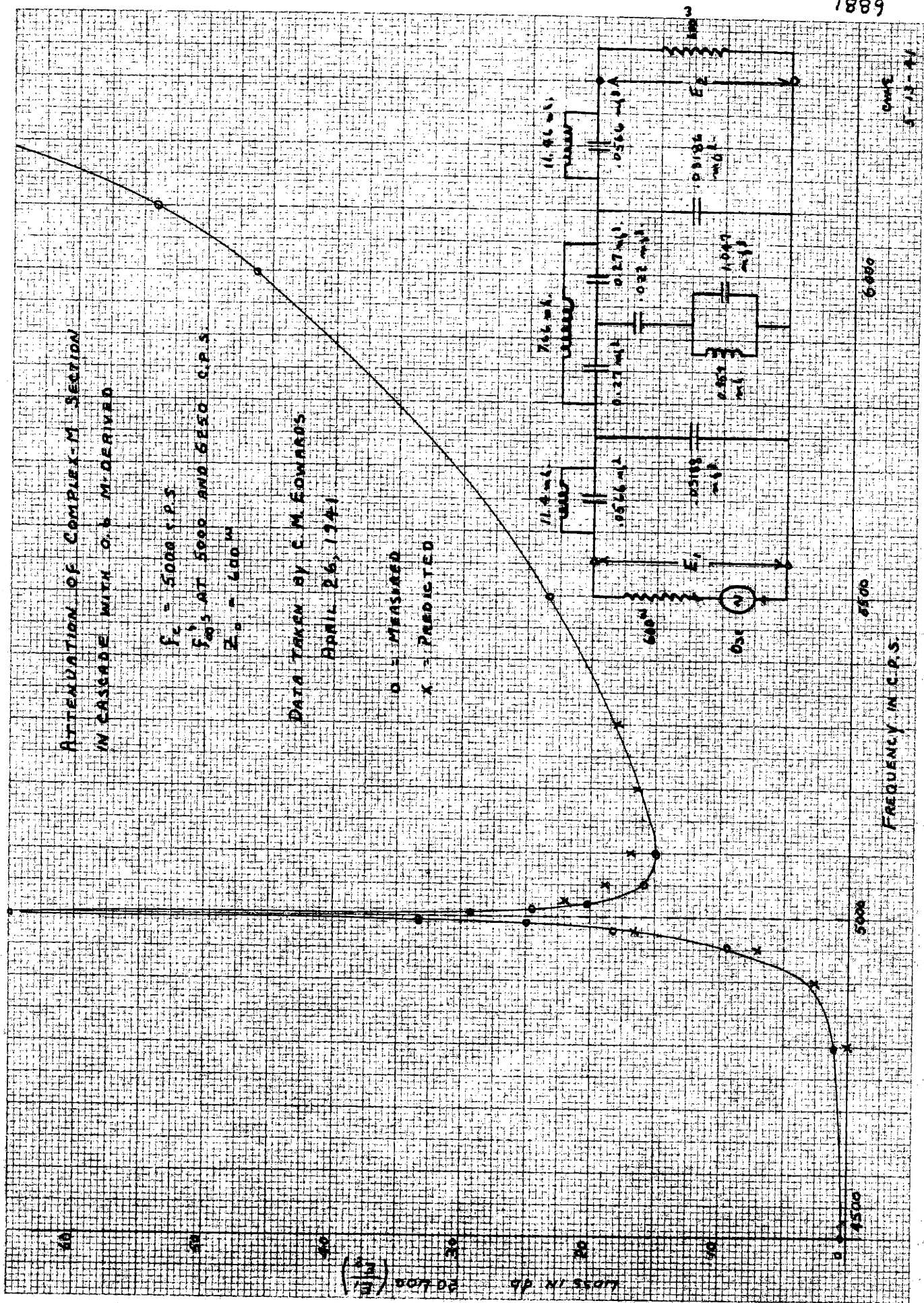
DATE
5/15/41

ATTENUATION OF COMPLEX-M SECTION
IN CASCADE WITH O.6 M. DERIVED

$f_c = 5000$ C.P.S.
 $f_{0.5} \text{ AT } 5000 \text{ AND } 6500 \text{ C.P.S.}$
 $Z_0 = 400 \Omega$

DATA TAKEN BY C. M. EDWARDS
APRIL 26, 1941

O - MEASURED
X - PREDICTED



FREQUENCY IN C.P.S.

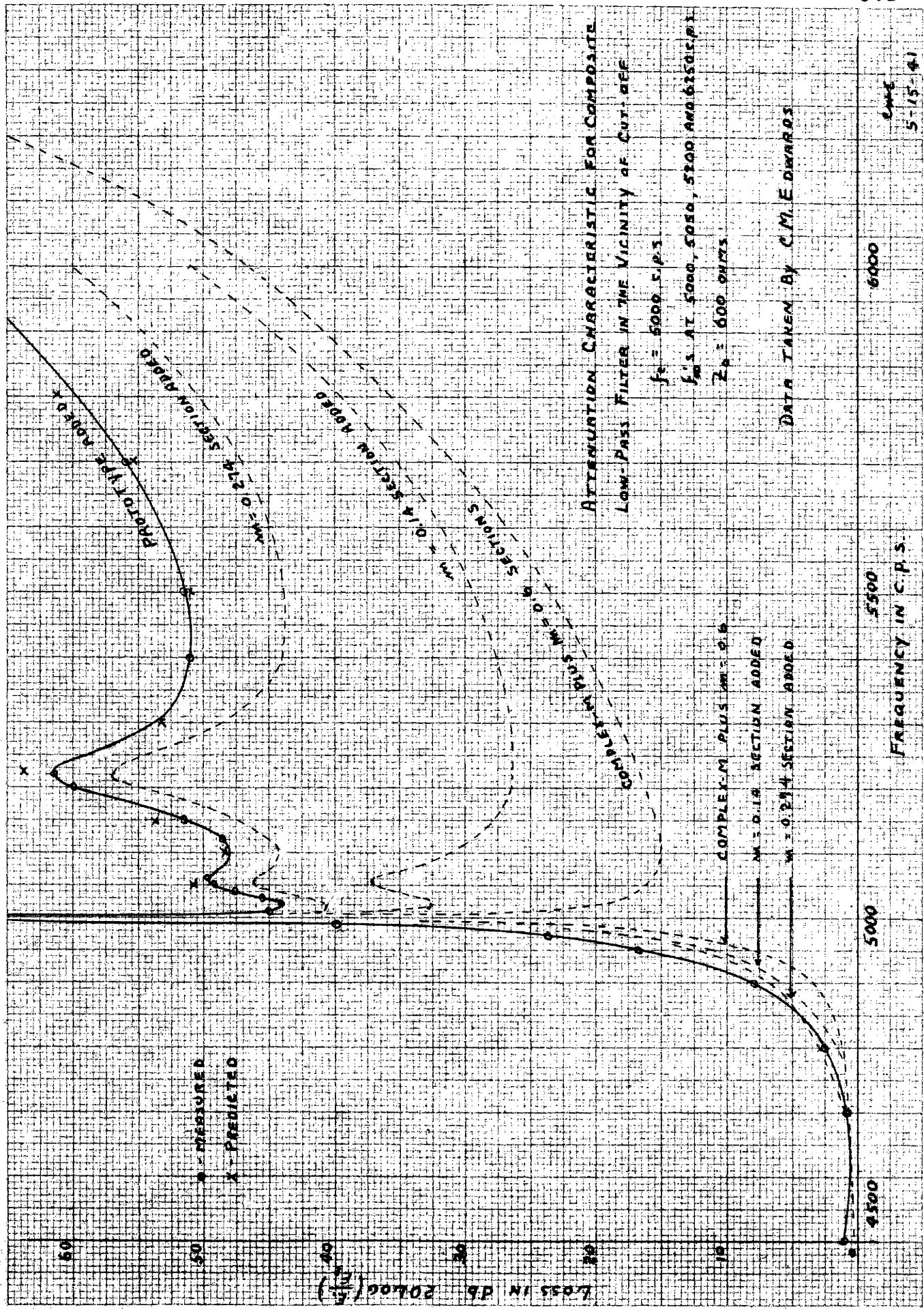
6000

5500

5000

OMEGA

5-13-41



ATTENUATION CHARACTERISTIC FOR COMPOSITE
LOW-PASS FILTER IN THE VICINITY OF CUT-OFF

$f_c = 5000$ S.P.S.
 f_{ms} AT 5000, 5050, 5100 AND 6150 C.P.S.
 $Z_0 = 600$ OHMS

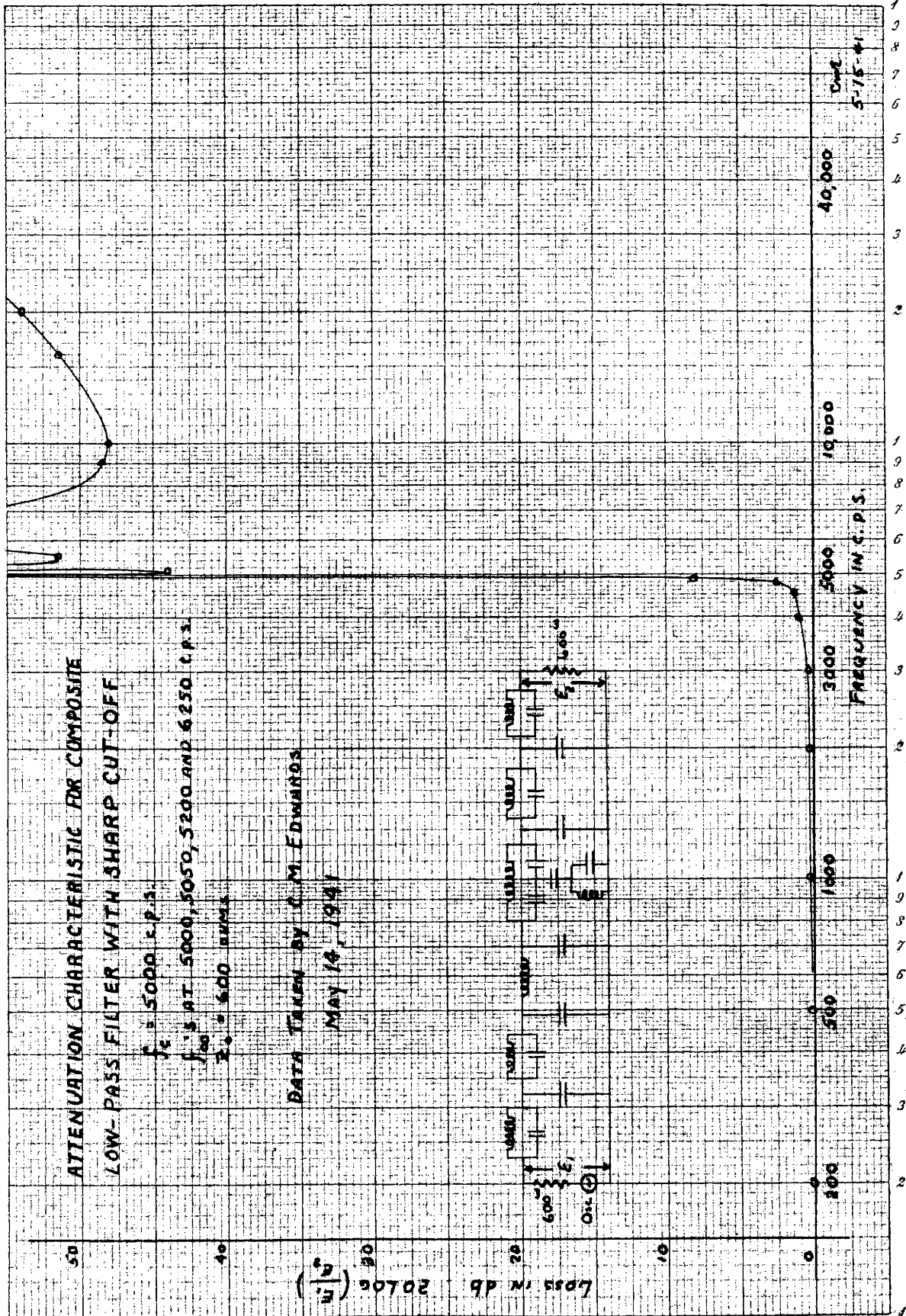
DATA TAKEN BY C.M. EDWARDS

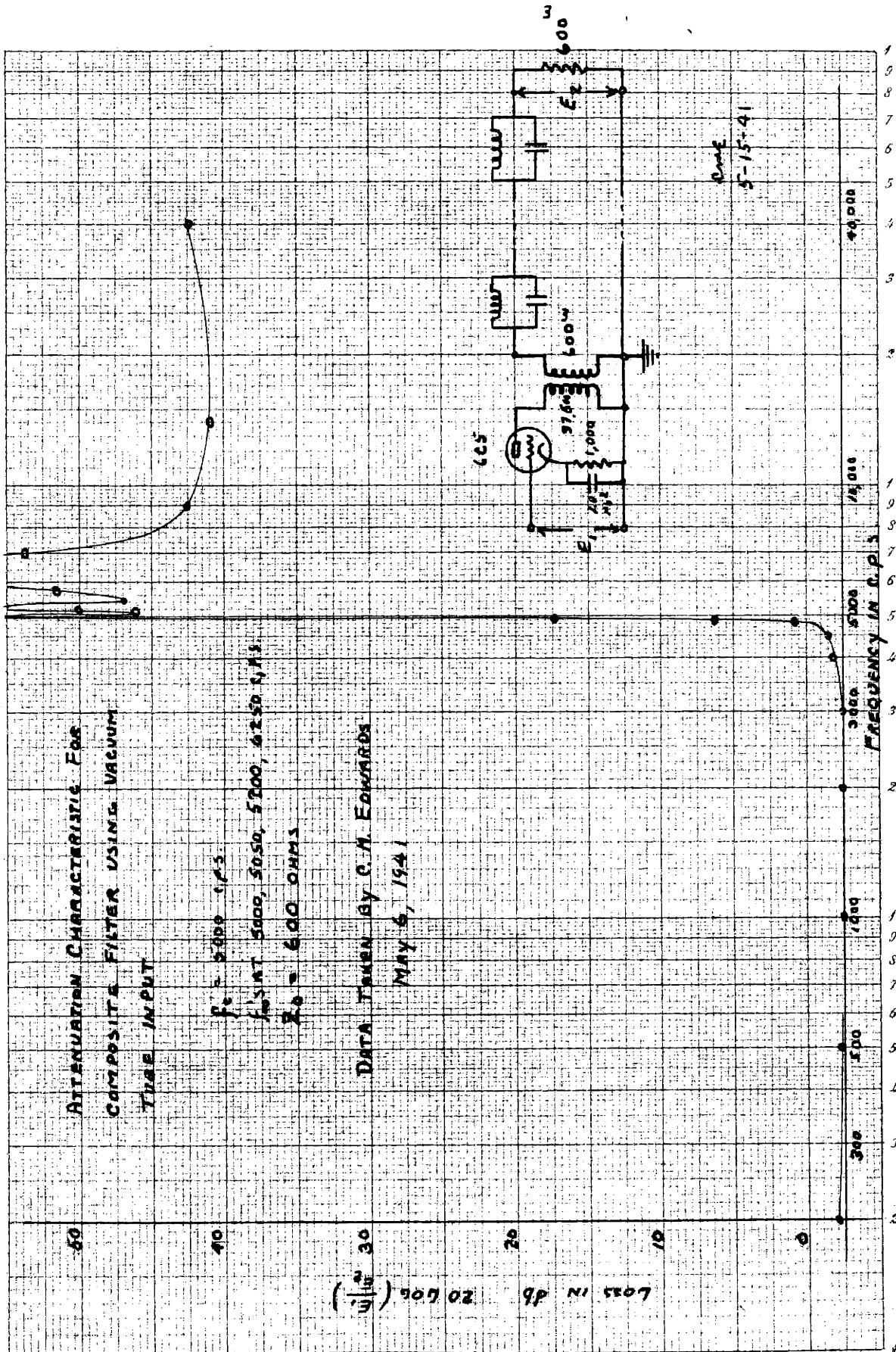
5-15-61

O - MEASURED
X - PREDICTED

Loss in dB $20 \log \left(\frac{E_1}{E_2} \right)$

FREQUENCY IN C.P.S.





CHARACTERISTIC IMPEDANCE FOR COMPOSITE

LOW-PASS FILTER

$f_c = 5000$ C.P.S.

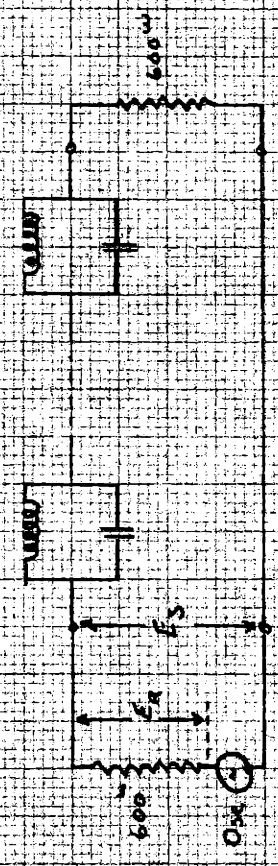
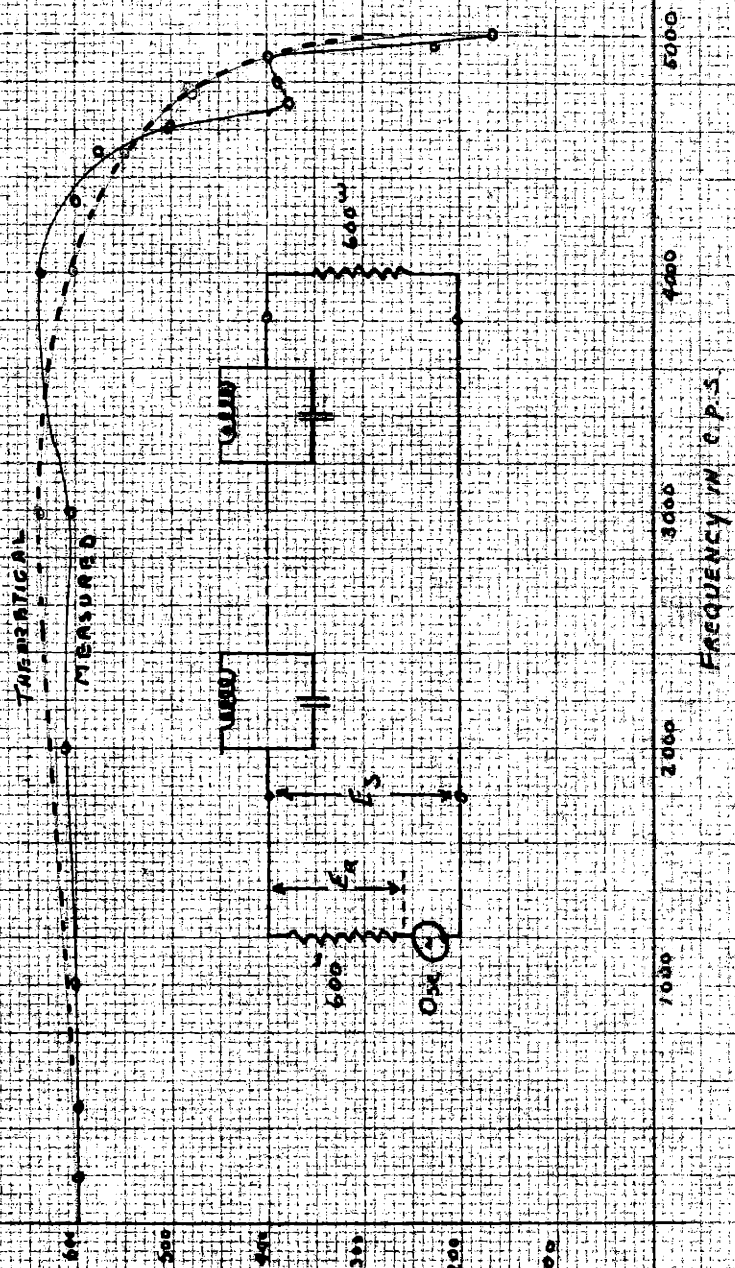
Z_0 AT 5000, 5000, 5000 AND 6250 S.P.S.

$Z_0 = 600$ OHMS

DATA TAKEN BY C.M. EDWARDS

MAY 14, 1941

CHARACTERISTIC IMPEDANCE IN OHMS $Z_0 = 600 \sqrt{\frac{L}{C}}$



2000
5-15-41